The Dissertation Committee for Rebecca E. Symula certifies that this is the approved version of the following dissertation:

Evolutionary and ecological influences on color pattern variation in the Australian common froglet, *Crinia signifera*

Committee:

David C. Cannatella, Co-Supervisor

David M. Hillis, Co-Supervisor

Molly E. Cummings

Lawrence E. Gilbert

Chris J. Bell

Cody W. Edwards

Evolutionary and ecological influences on color pattern variation in the Australian common froglet, *Crinia signifera*

by

Rebecca E. Symula, B.S.; M.S.

Dissertation

Presented to the Faculty of the Graduate School of

The University of Texas at Austin

in Partial Fulfillment

of the Requirements

for the Degree of

Doctor of Philosophy

The University of Texas at Austin

August 2009

Dedication

To my mother and father, for years of support.

Acknowledgements

Over the course of this project, I have received support from numerous sources at the University of Texas at Austin and abroad. The environment in the Hillis-Bull-Cannatella lab has been the source of many research ideas and discussion. I am grateful to all past and present members of the lab for the stimulating discussions and generous ears. Many members of the lab are not only tremendous colleagues, but are incredible friends. Specifically, Jeanine Abrams, Amy Bickham Baird, Jeremy Brown, William Harcombe, Tracy Heath, Shannon Hedtke, Emily and Alan Lemmon, Meredith Mahoney, Matthew Morgan and Santiago Ron. Each provided support, laughter and compassion. I thank my committee for their help and enthusiasm in developing this project, in data analyses and comments on manuscripts: David C. Cannatella, David M. Hillis, Molly E. Cummings, Lawrence E. Gilbert, Christopher J. Bell and Cody W. Edwards.

Performing projects with extensive field components are impossible without the help of local experts and large numbers of volunteers. Murray Littlejohn has provided valuable insight and his love for *Crinia signifera* has been inspirational. Scott Keogh, Steve Donnellan and Dale Roberts first introduced me to *Crinia* and provided lab space for me to perform analyses and examine specimens. Scott acted as my supervisor through the NSF EAPSI program and submitted Animal Ethics permits required for each of the three field seasons. Emma Burns, David Cannatella, Nick Clemann, Darren Crayn, Dan Edwards, Ralph Foster, Ryan and Phillip Garrick , Josh Hale, Hae-Jean Kwon, Ron Luhrs, Michael and Steven Mahony, Dan Rabosky, and Katie Smith helped collect

animals. Ron and Elaine Luhrs provided land for frog collection and for experiments and they remain fantastic friends. LaTrobe University Wildlife Reserve provided space for frog collection and experiments. The Evolutionary Biology Unit at the South Australia Museum, especially Terry Bertozzi and Steve Donnellan, provided specimen access, tissue storage and shipped tissues from South Australia. Museum Victoria provided space for tooth casting, and Brendan and Dean from the Preparations department provided advice on casting materials. Wayne Longmore provided helpful discussion on teeth identification. Diane Bray and Jane Melville stored and shipped tissues. Robert Palmer from the Australia National Wildlife Collection, Craig Reid from the Queen Victoria Museum and Ross Sadlier from the Australian Museum stored and shipped tissues. Amy Baird, Tamara Basham, Jeremy and Erin Brown, David Diers, Will Harcombe and Jean Kwon helped construct clay replicas. The Arthur Rylah Institute for Environmental Research provided consultation and equipment for transect set up. Permits for tissue and voucher collection were issued under New South Wales Parks and Wildlife (Permit Nos. NSWPWS S1119, 12276), Victoria Department of Sustainability and Environment (VIC DSE 10002786, 10004087), Environment ACT (LK20048, LT200488) and Tasmania Department of Primary Industries (TAS FA07096). Institutional Animal Care and Use Committees at the University of Texas at Austin provided IACUC approval (Protocol No. 06051501). Australian animal care and use permits were issued by the New South Wales Animal Care and Ethics Committee (NSW ACEC 04/377, 07/1459) and The Australian National University's Animal Ethics Committee (ANU AEEC Protocol Nos: F.BTZ.68.04, F.BTZ.08.07).

Funding was provided by several sources. NSF EAPSI (OISE-0413386), a grant from the Explorers Club, the University of Texas, Ecology, Evolution and Behavior Program Bennett Account Fellowship, the ASIH Gaige award funded fieldwork. Sequencing was partially funded by a NSF Assembling the Tree of Life grant to D. Cannatella and D. Hillis and the University of Texas, Ecology, Evolution and Behavior (EEB) Program Zoology Scholarship for Excellence. The EEB program at The University of Texas at Austin provided funds for travel to national meetings and living expenses for the last summer of my degree through the Frank and Fern Blair Fellowship and the Hartman Graduate Fellowship.

Data analysis was improved by discussions with lab members and other colleagues in the scientific community. Scott Keogh first suggested population-level analyses of phylogenetic diversity in *C. signifera*. Molly Cummings helped design the clay model experiment and, both she and Butch Brodie suggested additional statistical analyses for data examination. Jeremy Brown, Tracy Heath, Peter Midford, Ted Garland, David Hillis and David Cannatella provided insight for tests of Phylogenetic Signal and Simulations. The University of Texas at Austin Division of Statistics and Scientific Computation Consulting provided advice on statistical analyses for all parts of the dissertation.

My family has been incredibly supportive through the course of my degree. Both my mom and dad have encouraged me to pursue my love of frogs and have always been supportive of my education. They are inspirational in their patience and willingness to accept my need to travel abroad despite the worry it induced over the years.

Several other people have contributed to my career in the study of frogs and biology. Kyle Summers, my master's adviser from East Carolina University, fostered my love for frogs as research systems and taught me the process of research. David Richard, my informal undergraduate adviser at Susquehanna University, reluctantly supported my dream of studying frogs professionally and persuaded my parents to fund my field course to Costa Rica. Karen Beck, my 6th grade teacher, introduced me to the study of Natural History through several weekend bird watching field trips.

Ryan Garrick, has been my best friend throughout this degree. He has served as a sympathetic ear and a critical reviewer of my data analyses, experiments and manuscripts. I would be lost without his support. Steve Donnellan, Michael Mahoney, Matt Morgan and Terry Bertozzi are directly responsible for Ryan and I meeting. Without their encouragement and general good humor and a good forceful shove, I would never have met Ryan.

Evolutionary and ecological influences on color pattern variation in the Australian common froglet, *Crinia signifera*

Rebecca E. Symula, Ph.D.

The University of Texas at Austin, 2009

Supervisors: David C. Cannatella and David M. Hillis

Elucidation of mechanisms that generate and maintain population-level phenotypic variability provides insight into processes that influence within-species genetic divergence. Historically, color pattern polymorphisms were used to infer population-level genetic variability, but recent approaches directly capture genetic variability using molecular markers. Here, I clarify the relationship between genetic variability and color pattern polymorphism within and among populations using the Australian common froglet, *Crinia signifera*. To illustrate genetic variability in *C. signifera*, I used phylogenetic analysis of mitochondrial DNA and uncovered three ancient geographically restricted lineages whose distributions are consistent with other southeastern Australian species. Additional phylogeographic structure was identified within the three ancient lineages and was consistent with geographic variation in male advertisement calls.

Natural selection imposed by predators has been hypothesized to act on black-and-white ventral polymorphisms in *C. signifera*, specifically through mimicry of another

Australian frog, *Pseudophryne*. I used clay replicas of *C. signifera* to test whether predators avoid black-and-white coloration. In fact, black-and-white replicas were preferentially avoided by predators in some habitats, but not in others, indicating that differential selection among habitats plays a role in maintaining color pattern polymorphism. When black-and-white color patterns in a sample of *C. signifera* populations were compared with those in sympatric *Pseudophryne*, several color pattern characteristics were correlated between the species. Furthermore, where *C. signifera* and *Pseudophryne* are sympatric, color patterns are more similar compared to those in allopatry.

Extensive phylogenetic variability suggests that phylogenetic history and genetic drift may also influence *C. signifera* color pattern. Fine-scale phylogenetic analysis uncovered additional genetic diversity within lineages and low levels of introgression among previously identified clades. Measures of color pattern displayed low levels of phylogenetic signal, indicating that relationships among individuals only slightly influence color patterns. Finally, simulations of trait evolution under Brownian motion illustrated that the phylogeny alone cannot generate the pattern of variation observed in *C. signifera* color pattern. Therefore, this indicates a minimal role for genetic drift, but instead supports either the role of stabilizing selection due to mimicry, or diversifying selection due to habitat differences, in color pattern variation in *C. signifera*.

Table of Contents

List of Tables

List of Figures

Chapter 1. Mechanisms of the Evolution of Color Pattern Variation

Understanding mechanisms that generate and maintain naturally occurring phenotypic and genetic variation in nature is fundamental in understanding the formation of new species. The action of microevolutionary forces such as natural and sexual selection on phenotypes often results in genetic divergence among populations within species. Similarly, genetic drift can generate phenotypic and genetic divergence across landscapes of populations. Thus, elucidating the relationship between phenotypic and genetic variation can provide valuable insight into the process of speciation.

Historically, color pattern variability was used as a means to quantify genetic variation within and among populations because it was easily observed and commonly genetically determined (Milstead *et al.* 1974, Straughan and Main 1966, Kettlewell 1961). Quantifying frequencies of multiple forms of color patterns within a single population was used to infer genetic diversity within populations and to hypothesize processes acting differentially among populations. Direct estimation of genetic variability using molecular markers (reviewed in Hedrick 2006) has replaced the use of color pattern-based frequency estimates, leaving the relationship between color patterns variability and genetic diversity unclear. Natural selection (Phifer-Rixey *et al.* 2008), genetic drift (Hoffman *et al.* 2006) and gene flow (Merilaita 2001) have been invoked to explain variation in coloration that occurs within and among populations, but the evolutionary significance of coloration is not always straightforward.

Color patterns are commonly linked with selection through predation (Manríquez *et al.* 2008, Saporito *et al.* 2007). Predator evasion is enhanced by color patterns either by

preventing detection (crypsis) or advertising unpalatability (aposematism). Species that employ crypsis aim to resemble their visual background to avoid detection (Bond 2007, Endler 1978), whereas those that employ aposematism maximize their difference from the visual background to advertise to predators that they are unprofitable or even toxic (Cott 1940). Aposematic species are often associated with protective mimicry, where different species resemble one another to avoid predation. Some authors suggest that mimicry should be viewed as a spectrum rather than discrete categories (Balogh *et al.* 2008, Speed and Turner 1999), but two forms of mimicry are generally recognized: Batesian (Bates, 1862) and Müllerian (Müller 1879). In Batesian mimicry, palatable mimic species resemble aposematic model species in order to deceive predators (Bates 1862). Classical Batesian mimicry predicts that if the non-toxic mimics become too common, predators no longer associate the signal with toxicity, and Batesian mimicry will break down (Ries and Mullen 2008, Pfennig *et al.* 2007). Müllerian mimicry, on the other hand, occurs when two unrelated toxic species converge on a single color pattern, and both species benefit from the reduced cost of training the predator (Müller 1869).

Directional selection imposed by predators is predicted to reduce variability in populations, but unexpectedly, extraordinary color pattern polymorphisms arise in cryptic and aposematic species (e.g., Franks and Oxford 2009, Jiggins *et al.* 2001, Mallet 1993). Poulton (1890) defined color pattern polymorphism as the occurrence of multiple distinctive cryptic pattern variants. Some authors explicitly limit color pattern polymorphisms to refer to observations within populations (e.g., Bond 2007, Gray and McKinnon 2006), but here and by others, the designation is used synonymously with

variability observed within and among populations (e.g., Chapple *et al.* 2008, Mallet and Joron 1999). Originally, Poulton (1890) proposed that populations with color pattern variants decreased the search efficiency of predators. Others have suggested that polymorphisms arise as adaptations to heterogeneous habitats and are maintained through a balance between selection and migration (Bond 2007, Merilaita 2001, Endler 1978). Alone, predation can maintain polymorphisms in prey through frequency-dependent (apostatic) selection when prey is cryptic (e.g., Merilata 2006, Olendorf *et al.* 2006, Bond and Kamil 2002), or number-dependent selection in protective mimicry (e.g., Mallet and Joron 1999, Mallet 1993). In addition, some theoretical studies have proposed that interactions between environmental heterogeneity and predation can maintain and promote the evolution of polymorphic coloration (Forsman and Åberg 2008, Forsman *et al.* 2008).

The possibility that the persistence of a polymorphism is due to neutral processes, such as drift or migration, is often neglected. A few recent studies have attempted to rule out the contribution of neutral factors to phenotypic variation before performing experiments regarding a hypothesized selective mechanism by estimating population structure from genetic markers (Hoffman *et al.* 2006, Nicholls and Austin 2005, Brisson *et al.* 2005, Storz 2002). In these studies, patterns observed in neutral genetic markers are contrasted to patterns of phenotypic differentiation. Neutral evolution is inferred when a correlation between the genetic and phenotypic patterns is strong. The absence of a correlation between phenotypic and genetic differentiation provides motivation to experimentally test for evidence of selection. For example, in a study of *Drosophila*

polymorpha, color pattern was independent of genetic and geographic variation, but was strongly correlated to desiccation resistance. Specific tests for selection in dry habitats showed higher survival in flies with darker coloration (Brisson *et al.* 2005). In the satin bowerbird, similar methods were employed to test hypotheses of advertisement call variation. Calls were independent of genetic variation, but strongly correlated to differences among habitats. Thus, call differences were attributed to differing selective pressures imposed among habitats (Nicholls and Austin 2005). Unlike the former examples, tests for selection in color pattern polymorphisms in leopard frogs (*Rana pipiens*) found no evidence that color pattern polymorphism exceeded the variability expected according to multiple neutral loci (Hoffman *et al.* 2006). Similarly, in the poison frog *Dendrobates tinctorius*, a strong association was found between geographic patterns in polymorphic color pattern and a neutral genetic marker (Wollenberg *et al.* 2008). These results emphasize the importance of testing for evidence of selection before investing in measurements of selection on polymorphisms (Hoffman *et al.* 2006).

In both apostatic selection and mimicry, the perception of the predator is critical for understanding the processes that generate polymorphism (Bond 2007, Mallet and Joron 1999). Prey species use color and pattern to signal to their predators. Effective communication of the signal relies on the predator receiving the appropriate message. Perception of coloration and pattern by a predator depends upon the visual system of the predator (Endler 1990) and the ambient light in natural environments (Endler 1993). For example, non-human predatory mammals are unable to detect colors (e.g., red, yellow) because they lack eye pigments that allow color perception in humans and birds (Endler

1978). To account for these potential issues, two strategies are often employed when exploring the role of color pattern in avoiding predation. First, the ambient light and color reflected by prey species in their natural habitats are quantified relative to the visual background, and compared to the visual system of putative predators (e.g., Darst and Cummings 2006, Endler 1993, 1990). Second, artificial models that resemble prey species are constructed and exposed to predators in their natural environments (e.g., Pfennig *et al.* 2007, Saporito *et al.* 2007, Kuchta, 2005, Brodie 1993).

Much of what is understood about the relationship between color pattern polymorphism and predation has been ascertained using invertebrate prey and avian predators. Invertebrate species often exhibit polymorphisms (e.g., Hanlon *et al.* 2009, Manríquez *et al.* 2008, Phifer-Rixey *et al.* 2008, Chittka and Osorio 2007, Jiggins *et al.* 2001, Cook 1986) and their bird predators perceive and recognize the color to choose their prey (Osorio *et al.* 1999, Endler 1978). Vertebrates also commonly exhibit color pattern polymorphisms (e.g., Chapple *et al.* 2008, Woolbright and Stewart 2008, Galeotti *et al.* 2003, Santos *et al.* 2003, Wente and Phillips 2003, Symula *et al.* 2001, Hoffman and Blouin 2000, Summers *et al.* 1999). Color pattern polymorphisms are extremely common in frogs and havebeen attributed to mimicry (Symula *et al.* 2001), apostatic selection (Hoffman and Blouin 2000, Bull 1975), sexual selection (Maan and Cummings 2008, Summers *et al.* 1999) and genetic drift (Wollenberg *et al.* 2008, Hoffman *et al.* 2006). As in invertebrates, much of what we know about predation on frog color pattern polymorphisms has been assessed based upon avian predators (Darst and Cummings 2006, Saporito *et al.* 2007).

One example of color pattern polymorphism in frogs occurs in the Australian myobatrachid genus *Crinia*. Nearly all *Crinia* exhibit the same dorsal polymorphism (reviewed in Hoffman and Blouin 2000) suggesting that it is a retained ancestral polymorphism in *Crinia* (Bull 1975). Minimally, three different morphs are recognized: lyrate, smooth and ridged (striped). Crosses performed among morphs revealed that the dorsal polymorphism is determined by a single locus with either two co-dominant alleles (Main 1965) or, in some species, two alleles with simple dominance (Bull 1975). In some species, additional morphs resulted from laboratory crosses suggesting that multiple loci may contribute to the polymorphism (Bull 1977, 1975, Main 1968, 1965, 1961). Early field experiments and fitness assays across several different species proposed that polymorphisms are maintained by seasonal variation in selective advantage of the different morphs (Bull 1977, Main 1968, 1961). Alternatively, others observed lower frequencies of putatively more cryptic morphs in some habitats and deduced that polymorphism in dorsal pattern serves as a defense against predation (Odendaal and Bull 1982, Bull 1975, Littlejohn and Martin 1965).

Though the dorsal color and pattern polymorphism is well documented, apparent ventral color pattern polymorphism in *Crinia* has been essentially overlooked. In many early species descriptions, black-and-white ventral coloration was characterized, but multiple subsequent taxonomic reorganizations made it unclear which *Crinia* species exhibit black-and-white ventral coloration (Straughan and Main 1966, Parker 1940). Presently, four species of *Crinia* have been shown to reveal bold ventral coloration when under simulated predator attack (Williams *et al.* 2000). In the remaining species, venters

are pale colored and are either solid in color or bear light gray flecking (Fig. 1.1) (Robinson 2002, Cogger 2000). In contrast, *C. glauerti*, *C. riparia* and *C. signifera* bear bold black-and-white ventral markings (Cogger, 2000), and *C. tasmaniensis* has a similar pattern with red markings instead of black (Parker 1940, Blanchard 1929). In the Western Australia endemic, *C. glauerti*, black-and-white coloration is limited to females (Main 1957, Loveridge 1935), but is found in both sexes in the eastern species *C. riparia* and *C. signifera* (Littlejohn 2003, Cogger 2000, Williams *et al.* 2000). Unlike the other species, ventral coloration in *C. signifera* is polymorphic. Some individuals bear bold black-and-white whereas others have solid gray or white venters (Fig. 1.1).

The black-and-white ventral coloration found among species of *Crinia* is similar to ventral coloration found in another myobatrachid frog genus, *Pseudophryne* (Fig. 1.2). In *Pseudophryne* all species play dead in response to artificial predator attack (Fig. 1.2; Williams *et al.* 2000). Further, all examined species are known to secrete alkaloid skin toxins (Daly *et al.* 1990, 1984). These features combined suggest that ventral coloration and defensive behavior form an aposematic display that warns potential predators of their toxicity. Similarly, some populations of *C. signifera* also bear black-and-white coloration and 'play dead' when under simulated predator attack (Williams *et al.* 2000). Though closely related, phylogenetic analysis indicates that *Crinia* and *Pseudophryne* are not sister taxa (Read *et al.* 2001). Therefore, black-and-white coloration appears to have evolved independently in the two lineages. Finally, skin toxin analysis of *C. signifera* revealed that some peptides are secreted, but it is unknown whether these compounds deter predators (Masseli *et al.* 2004, Erspamer *et al.* 1984). Snakes consume *C. signifera* (Shine 1977),

despite the presence of these compounds (Erspamer *et al.* 1984). Thus, shared behavior and coloration is thought to be a form of defensive mimicry (Williams *et al.* 2000).

Evolutionary relationships among *Crinia* species with bold ventral color pattern were inferred in an effort to resolve conflicting phylogenetic hypotheses of the Australian endemic myobatrachid subfamily, Myobatrachinae (Read *et al.* 2001). Using mitochondrial DNA (mtDNA) markers, phylogenetic analysis uncovered strong support for monophyly in *Crinia*, but individuals that bear bold ventral patterns are not all closely related. *Crinia tasmainiensis* is the sister group to the remainder of the genus. *Crinia glauerti* is more closely related to other western *Crinia* than to the other two black-and-white species. Southern and eastern *C. signifera* and *C. riparia* were parapatric sister taxa, but this relationship was weakly supported. A few individuals of *C. signifera* from different geographic regions were also examined and substantial genetic divergence was found among them (Read *et al.* 2001).

The geographic patterns in *C. signifera* revealed by the molecular phylogeny complemented geographic patterns in *C. signifera* advertisement call (Littlejohn and Wright 1997, Odendaal *et al.* 1986, Littlejohn 1964, 1959). Geographic patterns in advertisement calls have been attributed to dispersal between Tasmania and mainland Australia following Pleistocene glaciation cycles and sea level fluctuations (Littlejohn 2005, 1967, 1964). However, southeastern Australia has been influenced by other drastic changes in habitat and climate since the Tertiary (Markgraf *et al.* 1995). Marine incursions, secondary uplift of the Great Dividing Range, and glaciation at high elevations during the late Miocene and early Pliocene fragmented faunal distributions

(Bowler 1982, Barrows *et al.* 2002, Dickson *et al.* 2002, Gallagher *et al.* 2003). In the Pleistocene, glaciation cycles caused sea level fluctuations (Lambeck and Chappell 2001, Holdgate *et al.* 2003) and repeated contraction and expansion of forest refuges (Williams *et al.* 2006, Hewitt 2004, Hope *et al.* 2004, McKenzie and Kershaw 2004, Desmarchelier *et al.* 2000, Markgraf *et al.* 1995). Sea level changes repeatedly opened and closed a land bridge between Tasmania and mainland Australia (Lambeck and Chappell 2001) and sundered eastern Victoria (East Gippsland) into small patches of terrestrial habitat (Holdgate *et al.* 2003, Bowler 1982).

Apparent color pattern polymorphism, substantial genetic divergence among geographic regions and wide geographic distribution make *C. signifera* an ideal system to investigate processes that generate and maintain phenotypic polymorphisms and assess the relationship between these polymorphisms and genetic variability. In addition, the proposed hypothesis of mimicry suggests a mechanism that may contribute to evolution of color pattern polymorphism. In the following chapters, I use molecular phylogenetixcs to reconstruct population-level phylogeographic relationships among *C. signifera*, assess the role of predation, and contrast the contributions of mimicry and genetic drift in the evolution of color pattern in *C. signifera*.

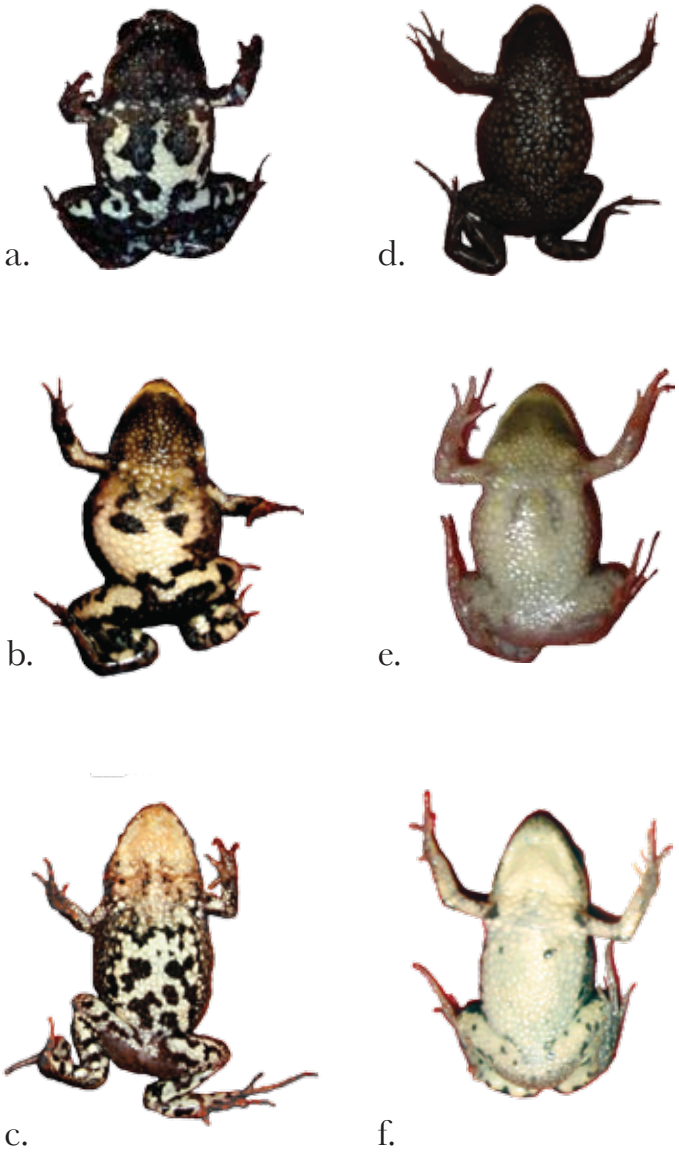

Figure 1.1. A sample of ventral color pattern variation in *C. signifera*. Individuals on the left (a.-c.) are putative mimics of *Pseudophryne*. Individuals with dark throat color are males and those with white throats are females. Individuals on the right (d.-f.) are found in populations either with or without the putative mimics and resemble individuals of other *Crinia* species that lack bold black-and-white coloration.

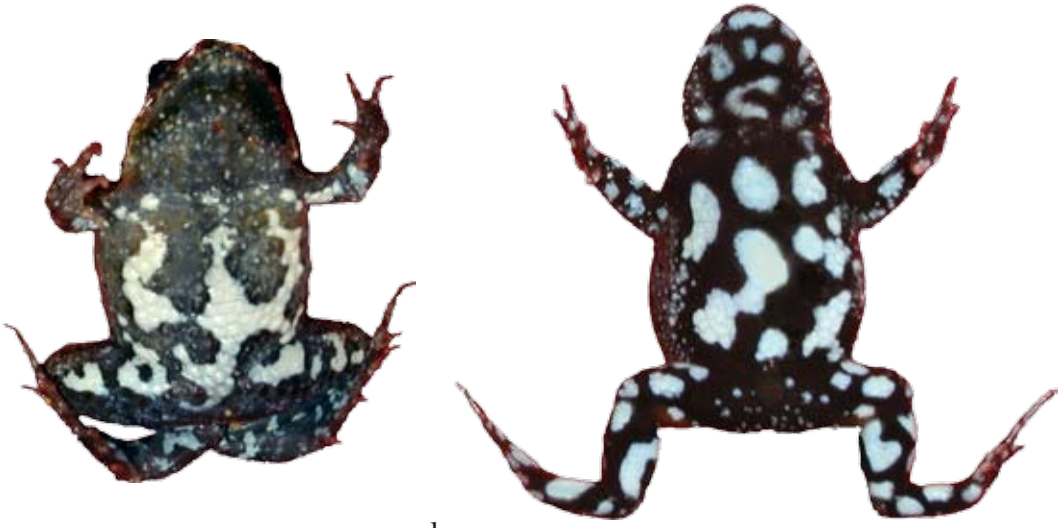

a. b.

Figure 1.2. An example of color patterns associated with the putative mimicry between (a.) *C. signifera* and (b.) *Pseudophryne*. Both species are shown in the posture assumed when under simulated predator attack.

Chapter 2. Ancient phylogeographic divergence in southeastern Australia among populations of the widespread common froglet, *Crinia signifera*.

Summary

Geographic patterns of species diversity in southeast Australia have been attributed to changes in Pleistocene climate, but related phylogeographic patterns and processes are relatively understudied. 12S and 16S mitochondrial DNA sequences in *Crinia signifera* populations were used to infer historical patterns and processes in southeast Australia. Phylogenetic analysis identified three geographically restricted ancient lineages and several geographically restricted sub-clades. Present-day features that may prevent gene flow are absent between these geographic regions. Divergence among the three lineages corresponds to a late-Miocene origin, approximately 9 million years ago (mya). The geographic breaks among the lineages are consistent with Miocene-Pliocene uplift in the Great Dividing Range and elevated sea levels in East Gippsland. Divergence among sub-clades in Victoria and South Australia is estimated to be within the early Pliocene, whereas sub-clades in New South Wales are estimated to have diverged near the Plio-Pleistocene boundary, approximately 2 mya. Geographic limits of sub-clades are consistent with geographic variation in advertisement calls, but are inconsistent with phylogeographic limits previously identified in other southeastern species.

2.1 Introduction

The impact of abiotic factors, such as climate cycles, on the genetic structure of organisms is of great interest in understanding patterns of divergence and speciation. Since the Tertiary, drastic changes in habitat and climate are hypothesized to have influenced genetic patterns in southeast Australia (Markgraf *et al.* 1995). Late Miocene and early Pliocene marine incursions and secondary uplift of the Great Dividing Range, coupled with glaciation at high elevations, fragmented faunal distributions (Gallagher *et al.* 2003, Barrows *et al.* 2002, Dickson *et al.* 2002, Bowler 1982). Pleistocene glaciation cycles caused sea level fluctuations (Holdgate *et al.* 2003, Lambeck and Chappell 2001), repeated contraction and expansion of forest refuges (Williams *et al.* 2006, Hewitt 2004, Hope *et al.* 2004, McKenzie and Kershaw 2004, Desmarchelier *et al.* 2000, Markgraf *et al.* 1995) and, to a lesser extent, glacier formation (Barrows *et al.* 2002, Colhoun *et al.* 1996). Pollen core studies show that habitats fluctuated between temperate wet-forest and more arid heathland throughout the Pleistocene (Williams *et al.* 2006, Hope *et al.* 2004, McKenzie and Kershaw 2004, McKenzie 2002, Hope 1994, Kershaw *et al.* 1991). Sea level changes repeatedly opened and closed a land bridge between Tasmania and mainland Australia (Lambeck and Chappell 2001) and sundered eastern Victoria (East Gippsland) into small patches of terrestrial habitat (Holdgate *et al.* 2003, Bowler 1982).

Numerous fine-scale studies in other Australian regions have shown that genetic variation within species is correlated with climate changes associated with glaciation cycles in the Pliocene (Edwards *et al.* 2007, Schaüble and Moritz 2001, James and Moritz 2000, Schneider *et al.* 1998) and in the Pleistocene (Garrick *et al.* 2007, Dolman and

Moritz 2006, Graham *et al.* 2006, Hugall *et al.* 2002, McGuigan *et al.* 1998). In contrast, the impact of climate fluctuations on southeastern mainland fauna has received little attention. Most such studies have examined patterns among species (e.g., Rockman *et al.* 2001, Donnellan *et al.* 1999) or across smaller geographic scales (e.g., Blacket *et al.* 2006, Nicholls and Austin 2005, Wong *et al.* 2004). These studies predict geographical genetic structuring in the southeast despite the absence of apparent geographic barriers to gene flow. However, large-scale phylogeographic studies of wide-ranging southeastern species are lacking (but see Chapple *et al.* 2005, Chapple and Keogh 2004, Houlden *et al.* 1999).

The southeastern Australia common froglet, *Crinia signifera* (Myobatrachidae), is well suited for testing hypotheses concerning the phylogeographic history of southeastern Australia owing to the wide breadth of its distribution (Fig. 2.1a). However, delimiting the extent of its distribution has been challenging. Morphologically indistinguishable frog populations in southwestern and southeastern Australia were originally assigned to *Crinia signifera sensu lato*. Biochemical data (Heyer *et al.* 1982), advertisement call data (Barker *et al.* 1995, Littlejohn, 1964, 1959, 1958), and experimental crosses resulting in hybrid inviability and gross morphological deformities (Main 1957, Moore 1954) revealed that *C. signifera sensu lato* comprised several species. Identification of these species is supported by phylogenetic analysis of mitochondrial DNA (mtDNA) sequence data (Read *et al.* 2001). Within *C. signifera*, subspecies were described (Parker 1940), but phonotaxis experiments (Straughan and Main 1966, Moore 1954) demonstrated that females do not discriminate among males of different subspecies (Parker 1940) or males from other geographically disparate localities. Thus, *C. signifera sensu stricto* (hereafter *C. signifera*) is limited to

southeast Australia (Fig.1a).

Although these lines of evidence suggest that *C. signifera* is a single species, phylogenetic analysis of mtDNA identified unexpected genetic diversity among four geographically separate populations (Read *et al.* 2001). Also, several studies revealed geographic variation in advertisement calls in the southern portion of its distribution (Fig. 2.1b; Littlejohn 2005, Littlejohn and Wright 1997, Odendaal *et al.* 1986, Littlejohn, 1964, 1959, 1958). Two clear patterns are evident in the advertisement call data. First, there are five distinct call types that vary geographically, primarily in pulse rate (Fig. 2.1b). Call types were designated either by comparing means (Littlejohn 2005, 1959) or by implementing ANOVA (Littlejohn 2005, Littlejohn and Wright 1997, Odendaal *et al.* 1986). Second, frogs from eastern Victoria, southern New South Wales and Tasmania have indistinguishable calls (call type 5; Littlejohn 2005, 1964). Both geographic patterns have been attributed to dispersal between Tasmania and mainland Australia following Pleistocene glaciation cycles and sea level fluctuations (Littlejohn 2005, 1967, 1964). Littlejohn (2005) proposed that populations that share call type 5 are closely related because they were colonized by individuals from Tasmanian populations that dispersed across the Bass Strait land bridge during the Pleistocene.

In this study, we investigate phylogeographic variation in *C. signifera* in southeast Australia. Specifically, we reconstruct the phylogenetic relationships among *C. signifera* populations. Then, divergence times among *C. signifera* clades are estimated and compared to corresponding geological events. Finally, we examine advertisement call variation in light of the phylogenetic relationships and test the hypothesis that *C. signifera*

populations from southern New South Wales, eastern Victoria and Tasmania share similar advertisement calls because they are closely related.

2.2 Methods

Sample collection, DNA sequencing and alignment

Samples of *C. signifera*, *C. riparia* and *C. parinsignifera* were collected between March and August 2004 and in June 2007. *Crinia signifera* were collected at approximately 100 km intervals (Fig. 2.1a; Permit Nos. NSWPWS S1119, VIC DSE 10002786, NSW ACEC 04/377, ANU AEEC Protocol Nos: F.BTZ.68.04, F.BTZ.08.07, Environment ACT LK20048, LT200488, TAS FA07096). Frogs were located using advertisement calls to ensure correct identification. Formalin-fixed voucher specimens were deposited in museums from the state or territory where they were collected (Table 2.1). All tissue samples were stored in 95% ethanol. Additional tissue samples of *C. signifera* were obtained from the South Australia Museum. Localities, GPS coordinates and specimen identification numbers are listed in Table 2.1.

Individuals listed in Table 2.1 were used for DNA sequencing. Total genomic DNA was extracted from toe clips or liver samples using Viogene Blood and Tissue Genomic DNA Extraction Miniprep System (Viogene, Inc., Taipei, Taiwan). Completely overlapping fragments of mitochondrial 12S and 16S rRNA genes were amplified using Failsafe PCR 2X PreMixes Buffer F (Epicentre Biotechnologies, Madison, WI) for polymerase chain reaction (PCR) in order to generate sequences corresponding to

positions 2153-4574 in the complete mitochondrial sequence of *Xenopus laevis* (GenBank Accession No. NC 001573, derived from M10217). Read *et al.* (2001) demonstrated that these genes have sufficient variation for phylogenetic analysis. Primers used for PCR reactions (Table 2.2) were designed to amplify overlapping segments of the complete 12S and 16S genes. All PCR reactions used the following cycle: Initial denaturation 94 ºC for 2 min, 30-35 cycles of 94 ºC for 30 s, 46-55 ºC for 30 s, and 72 ºC for 60 s and a final extension at 72 ºC for 7 min. PCR products were purified from 0.8% agarose using Viogene Gel-M Gel Extraction System (Viogene Inc., Taipei, Taiwan). Purified products were used as templates for sequencing reactions using ABI Prism BigDye Terminator v3.1 chemistry (Applied Biosystems, Foster City, CA). Sequencing reactions were cleaned using 1.5% Sephadex G-50 (S-6022 Sigma, St. Louis, MO) in Centrisep 8-strip columns (Princeton Separations, Adelphia, NJ) and sequenced on an ABI Prism 3100 Genetic Analyzer (Applied Biosystems).

Contiguous sequences of completely overlapping fragments were generated and cleaned using Sequencher v4.6 (Gene Codes Corp., Ann Arbor MI). Sequences were aligned manually in MacClade v4.06 (Maddison and Maddison 2004) using aligned 12S sequences from Read *et al.* (2001) and 12S and 16S *Limnodynastes salminii* sequence (Darst and Cannatella 2004) as references. Alignments were straightforward and did not require the aid of RNA secondary structure models. Single base changes were verified by examining if each peak in the chromatogram was assigned the correct base.

Phylogenetic analysis and genetic divergence

All analyses were run using sequences listed in Table 2.1 and in Read *et al.* (2001) unless otherwise specified. Data from Read *et al.* (2001) included only 691 base pairs (bp) of 12S sequence. Read *et al.* (2001) recovered a potential cryptic species near Coffs Harbour, NSW. To confirm this finding, 12S sequence from additional Coffs Harbour samples are included in the analysis. New sequences of *C. riparia*, the sister taxon to *C. signifera* (Read *et al.* 2001), and *C. parinsignifera* were included in all analyses. These species, which are morphologically similar and sympatric with *C. signifera*, were included to insure correct identification of *C. signifera*. Complete sequences of *C. riparia* and *C. parinsignifera* from this study were used as outgroups based on the Read *et al.* (2001) phylogeny.

Ambiguous regions of sequences were removed before phylogenetic analysis. The beginning and end of some sequences were excluded to minimize regions with missing data. Three regions of ambiguous alignment were excluded (corresponding to positions: 402-409, 967-1038, 1464-1482 in *Xenopus*). Sites for which an individual sequence had a single base insertion were also excluded.

Evolutionary relationships among localities of *C. signifera* were inferred using Maximum Likelihood (ML) and Bayesian inference. The most appropriate model of evolution was determined using the Bayesian Information Criterion in MODELTEST (Posada and Crandall 1998). Three replicate analyses were run using the default parameters in GARLI 0.951 (www.bio.utexas.edu/grad/zwickl/web/garli.html) to estimate the best ML tree. GARLI uses a genetic algorithm to estimate ML topologies and parameters. Nonparametric bootstrapping was performed in GARLI to assess nodal support using 1000 bootstrap replicates.

Bayesian analyses were performed using MRBAYES 3.1.2 (Ronquist and Huelsenbeck 2003). Two runs each with two separate replicates were performed on a NPACI Rocks cluster using four Markov chains per replicate and the temperature parameter set at 0.2. Chains were sampled every 1000 generations for 10 million generations. Analyses ran until the standard deviation of split-frequencies reached 0.01 for the replicates in each run, indicating both runs had converged on the same posterior distribution. Stationarity and burn-in were estimated using MrConverge (www.evotutor.org/MrConverge; Brown and Lemmon 2007). MrConverge defines stationarity as the first sample where the likelihood score is greater than 75% of the previously estimated scores. Burn in is estimated by maximizing the precision of the posterior probability estimates and is calculated as the sum of the standard deviations of the posterior probability estimates for each of the four replicates. The burn-in is then set as the higher of the values determined for stationarity and burn-in. For these runs, burn-in was set as 486,000 generations. Plots of model parameters and likelihood scores versus generations were examined to determine whether the set of post burn-in trees had converged on the same region of tree space in TRACER 1.4 (beast.bio.ed.ac.uk).

To test whether missing 16S rRNA sequence data in Read *et al.* (2001) influences *C. signifera* relationships, two datasets were analyzed (Wiens 2003). First, ML analysis methods described above were run without Read *et al.* (2001) data. Second, a truncated dataset (12S only, 691 bp) was analyzed using all taxa and the same ML methods. When analyzed without Read *et al.* (2001) samples, relationships among *C. signifera* samples are entirely consistent with relationships in the complete dataset. GARLI analyses of the

truncated sequence dataset also recover monophyly of the major clades and sub-clades identified in the complete dataset. However, the relationship among some sub-clades is poorly resolved. Therefore, there does not appear to be an impact of missing data because the relationships among clades and sub-clades remain the same, and the results are presented for the complete dataset.

Frequency-based measures of diversity were not appropriate for this study because all but 10 sequences represent unique haplotypes. Therefore, average pairwise genetic distances were calculated using uncorrected p-distances to assess the diversity among haplotype clades and sub-clades identified by the phylogenetic analyses. Genetic distances were only compared among individuals with complete 12S and 16S sequence.

Estimates of divergence time

To determine whether divergence of the haplotype clades is consistent with known geological events in southeast Australia, divergence times were estimated in r8s 1.71 (Sanderson 2003). Fossil data are typically used to calibrate divergence times, but appropriate fossils are not available for *C. signifera*. Instead, the methods introduced by Leys *et al.* (2004) are implemented for calibration of the nodes. The age of the root node was determined to be the age that matched two independent estimates of substitution rates for 12S and 16S genes in frogs (Evans *et al.* 2004: 0.00249; and Lemmon *et al.* 2007: 0.00277).

The best tree found by GARLI was pruned to remove approximately zero-length branches resulting in a topology with a representative from each sub-clade (Fig. 2.3). In

sub-clades B2 and C4, a single sample from west of the Great Dividing Range and one sample from Kangaroo Island, respectively, were retained because their genetic divergence relative to the remainder of the sub-clade was large. This pruned tree was used to reconstruct divergence times by implementing the semi-parametric penalized likelihood (PL) method in r8s (Sanderson 2003). This method uses a smoothing parameter to estimate times simultaneously with rate change along each branch. Cross-validation procedures were used to determine an optimal smoothing parameter with the root node of *C. signifera* arbitrarily fixed to 23. All estimates of divergence times were performed using the optimal smoothing parameter from the cross-validation procedure, 10 replicates of initial starting conditions and the "check gradient" option to insure correctness of solutions. To identify the age at which the average substitution rate was approximately equal to the rates from the previous studies, multiple iterations were performed by fixing the age of the root of *C. signifera*. In each iteration, the root was fixed to a different age (23, 19, 18.5, 18, 17.5, 17, 16.5, 16, 13, 8, 5, 3 or 1.8 million years ago (mya)).

The root of the tree was fixed to 17.75 mya (determined above) to calculate confidence intervals around the estimated ages of *C. signifera* nodes using nonparametric bootstrapping. Bootstrap replicates were generated using the complete dataset in GARLI with the pruned tree enforced as a topological constraint. This forces the topology to remain the same while estimating different possible branch lengths for the topology. Individuals were subsequently pruned from the bootstrapped trees so that those retained on the replicate trees were identical to those in the pruned tree used above. Confidence

intervals of the estimated ages of the nodes were then calculated in r8s using the 100 bootstrap replicates of the pruned tree.

Hypothesis testing

Hypotheses of diversification in *C. signifera* are based primarily on differences in advertisement calls. Littlejohn (2005) proposed that similarity in advertisement call in populations from Tasmania, East Gippsland, Victoria and southern New South Wales is due to dispersal of Tasmanian populations across the Bass Strait land bridge (Fig. 2.1a) and subsequent colonization along the east coast of mainland Australia during the Pleistocene. Thus, we tested the alternative hypothesis that these localities share a common ancestor.

The Bayesian posterior distribution of trees represents the total set of trees that can be supported by the data. We calculated the proportion of trees in the Bayesian posterior distribution consistent with the alternative hypothesis that samples from Tasmania (Sites 44-47), East Gippsland, Victoria (Sites 20-22) and southern New South Wales (Site 19) are monophyletic. Post-burn-in trees consistent with the alternative hypothesis were filtered in PAUP* 4.0b10 (Swofford 2003). If the proportion of trees consistent with the alternative hypothesis in the posterior distribution is less than 0.05, than the hypothesis of advertisement call similarity due to common ancestry is rejected.

2.3 Results

Phylogenetic analysis and *genetic divergence*

The final analyses were run with an alignment of 2317 bases and included all individuals in Table 2.1 unless otherwise specified. Only ten complete 12S and 16S sequences, two from each of five localities, share identical haplotypes (Fig. 2.2). For the remainder, each sequence represents a unique haplotype. Average pairwise genetic distances are summarized in Table 2.3. Both ML and Bayesian analyses yielded similar relationships among individuals and any differences between ML and Bayesian analyses are reported below. Thus, the ML tree is presented with Bayesian posterior probabilities (bpp) and nonparametric bootstrap support given for each node (Fig. 2.2). MODELTEST chose GTR+I+ Γ as the model of sequence evolution. The best of three ML trees found by GARLI had a -ln likelihood score of 8272.1583 (Fig. 2.2). Base frequencies were estimated as A = 0.330 C = 0.268 G = 0.188 T = 0.214; rate matrix: A-C = 3.714, A-G = 10.816 A-T = 3.007 C-G = 1.005 C-T = 27.483 G-T = 1.000; gamma shape parameter: 0.643; proportion of invariant sites: 0.646. Bayesian analysis recovered a consensus topology identical to the best ML tree.

Crinia riparia is the sister species of *C. signifera* (Fig. 2.2). Two geographically isolated clades are apparent in *C. riparia*, but the divergence is not clearly associated with large geographic distances. Nearly 5% sequence divergence was uncovered between localities less than 100km apart. These results suggest phylogeographic structure in *C. riparia*, but further discussion lies outside the scope of this paper.

Crinia signifera is also monophyletic and comprises the same three clades (A, B, and

C) in both analyses (Fig. 2.2). Average among-clade distances were greater than 2.9% (Table 2.3). Clade A (bpp = 1.00, 100% bootstrap support) comprises samples from East Gippsland, Victoria. Pairwise distances (Table 2.3) in clade A range from 0.0014-0.0063 with a mean of 0.0023. Clade B (bpp = 1.00, 99%) comprises most samples from New South Wales and the Australian Capital Territory. In clade B, pairwise distances range from 0.0022-0.0194 with a mean of 0.0093. Clade C comprises samples from South Australia, Tasmania and Victoria (excluding East Gippsland; bpp = 0.99, 84%). Average pairwise genetic distances are between 0-0.0658 with a mean of 0.0249 within clade C. The relationship among the three clades is poorly resolved. Based on the Bayesian analysis, 56% of the trees in the posterior distribution support clade A as the sister taxon to clade C. For the nonparametric bootstrap replicates, 44% of the trees place clade A as the sister taxon of clades B and C. Only 35% of the nonparametric bootstrap replicates support the most frequent Bayesian topology.

In clades B and C, several resolved sub-clades were also found (Fig. 2.2). Sub-clades are arbitrarily defined as those within major clades that have minimally 2% average among-sub-clade distance. Within clade B, two sub-clades are identifiable; B1 comprises northern New South Wales samples including samples of the potentially cryptic species from Coffs Harbour (bpp = 0.99, 94%) and B2 includes the remainder of central New South Wales and the Australian Capital Territory samples (bpp = 0.91, 74%). There are five sub-clades within clade C (Fig. 2.2). The first, C1 (bpp = 1.00, 99%), includes central Victoria and eastern South Australia. The second, sub-clade C2 (bpp = 0.99, 92%) comprises the remaining locality from New South Wales and those from the

New South Wales border of central Victoria (Fig. 2.2). Sub-clade C3 (bpp = 0.99, 96%) comprises samples from southern Victoria and the Fleurieu Peninsula. Sub-clade C4 (bpp = 0.97, 59%) comprises samples from Kangaroo Island and the westernmost region of South Australia. There are two monophyletic groups in sub-clade C4. One of these clades (bpp=1.0, 99%) comprises the Kangaroo Island samples from Read *et al.* (2001). Average pairwise genetic distances between Kangaroo Island samples and others in sub-clade C4 are greater than 2%, but only have 12S data and may be skewed by missing data. Thus, these were left in sub-clade C4. Finally, sub-clade C5 (bpp = 1.0, 100%) comprises samples from Tasmania.

Divergence time estimates

The best GARLI tree was pruned and converted to an ultrametric tree using PL and the optimal smoothing parameter (32) calculated in r8s (Fig. 2.3b). Multiple iterations of divergence time estimates with different fixed ages of the root node determined that a root age between 16.5-19 mya best approximates the substitution rates of 0.00249 (Evans *et al.* 2004) and 0.00277 (Lemmon *et al.* 2007). Average substitution rates calculated from the different fixed ages are shown in Fig. 2.3a.

Confidence intervals were calculated with the root node fixed to the average of the two best ages (17.75 mya). The estimated age of each node (95% confidence interval) is shown in Fig. 2.3b. Divergence times were not estimated for nodes with short branches and low support. The divergence between the three major clades (A, B, C) was estimated at 8.99 (6.73- 11.87) mya corresponding to a late Miocene divergence. Within clade B,

the sub-clades diverged 2.21 (0.81-3.43) mya, near the Plio-Pleistocene boundary. All divergences between the sub-clades in clade C are Tertiary in origin.

Hypothesis testing

Of the complete set of the post-burn in trees, none of these trees was consistent with the alternative hypothesis. Therefore, we reject that advertisement calls from East Gippsland, Victoria, Tasmania and southern New South Wales populations are similar based on common ancestry.

2.4 Discussion

Phylogenetic analysis, genetic divergence and divergence time estimates

Phylogenetic relationships and genetic divergences have a strong association with geographic location and distance among samples (Fig. 2.2). All clades and nearly all sub-clades are geographically restricted. Only sub-clade C2 contains geographically disjunct samples (central Victoria and the Fleurieu Peninsula, South Australia; Fig. 2.1a). Littlejohn (2005) hypothesized that these areas were connected along coastal regions when the sea level was lower (Lambeck and Chappell 2001). Most large genetic divergences are among geographically disparate locations.

Geographic limits of major clades of *C. signifera* are consistent with geographic limits identified in other studies. The area relationship between clades A and B was initially described in frogs of the *Litoria citropa* species group (Donnellan *et al.* 1999), identified later in open forest frogs, *Limnodynastes* (Schäuble and Moritz 2001), and the

scincid lizard *Egernia whitii* (Chapple *et al.* 2005). The genetic break between clades A and C has also been recovered in *Planipapillus* velvet worms (Rockman *et al.* 2001) and the satin bowerbird, *Ptilonorhynchus violaceus* (Nicholls and Austin 2005). In other studies, the East Gippsland (clade A) region harbors unique haplotypes in koalas (Houlden *et al.* 1999) and chromosomal races in spiders (Rowell 1990). The consistency among studies in these genetic breaks is notable because they do not coincide with conspicuous geographic barriers.

The estimates of divergence time among the major clades and lack of apparent geographic barriers strongly suggest that genetic breaks in *C. signifera* were impacted by geological events in the late Miocene and early Pliocene. Although clade C is isolated from clades A and B by the Eastern Highlands of the Great Dividing Range, the present Great Dividing Range does not seem to act as a barrier to gene flow, as *C. signifera* is found at the tops of mountains (Barker *et al.* 1995). However, during the Miocene and Pliocene, glaciation of the Eastern Highlands (Barrows *et al.* 2002) eliminated suitable habitat and may have led to the isolation of clade C from the remainder of *C. signifera*. Geological evidence also suggests that late Miocene sea level changes in East Gippsland resulted in the formation of isolated patches of suitable habitat that may have isolated clade A from the remainder of the mainland (Gallagher *et al.* 2003, Dickson *et al.* 2002).

In contrast to the major clades, comparative evidence consistent with phylogeographic breaks between sub-clades is lacking. Comparisons between the clade B pattern in *C. signifera* and other organisms is difficult because only two other studies have spanned the break between sub-clades B1 (northern New South Wales) and B2 (central

New South Wales; Fig. 2.2), and in those studies, sampling is sparse. The northern New South Wales and Queensland populations of *Limnodynastes* are distinct from central New South Wales populations (Schäuble and Moritz, 2001). In the tree frog, *Litoria fallax,* the McPherson range at the border of Queensland and New South Wales has acted as a significant barrier to dispersal between Queensland and New South Wales populations (James and Moritz, 2000). This study lacks Queensland *C. signifera* samples and thus, cannot be directly compared to the other studies. Similarly, in clade C there is little comparative support for *C. signifera* sub-clades because few studies include samples that span the range of clade C. Samples from the geographic region of sub-clade C1 also form monophyletic groups in the skink, *Egernia whitii* (Chapple *et al.* 2005) and *Limnodynastes tasmaniensis* (Schäuble and Moritz 2001). However, in these two species and in tiger snakes, *Notechis scutatus* (Keogh *et al.* 2005), relationships among populations differ substantially from the clade C sub-groupings in *C. signifera.*

All of the sub-clades diverged in the Pliocene (Fig. 2.3b). Most sub-clade breaks do not correspond to Holocene or known Pliocene geological events. Only three specific instances potentially can be attributed to geological events. First, geological evidence indicates that Tasmania was last connected to the mainland 17,000 years ago (ya) via the Bass Strait land bridge (Lambeck and Chappell 2001). Tasmanian populations diverged from the mainland 6.02 (4.09-7.83) mya suggesting that the recent separation of Tasmania is not responsible for the divergence between sub-clade C5 and mainland sub-clades. Second, Kangaroo Island populations diverged from mainland Australia populations approximately 3.29 (1.35-5.18) mya in the Pliocene, but Kangaroo Island

was most recently connected to the mainland 25,000 ya (Lambeck and Chappell 2001). Interpretation of this result is limited because sequences from Kangaroo Island have only 12S data. Third, the sister taxon to sub-clade B2 is from the western side of the Great Dividing Range and diverged 2.07 (1.30-3.03) mya at the Plio-Pleistocene boundary. This date is consistent with glaciation of parts of the Great Dividing Range (Dickinson *et al.* 2002). However, this is only a single representative from the western side of the range; this relationship should be tested with additional sampling.

Many studies attribute within-species phylogeographic sub-structure to Pleistocene fluctuations that produced recurring contraction and expansion of suitable habitat (Graham *et al.* 2006, Sunnucks *et al.* 2006, Hugall *et al.* 2002, Schaüble and Moritz 2001). However, *C. signifera* clades and sub-clades appear to have diverged much earlier, during the Miocene and Pliocene. This result is not unprecedented as studies in other species show late Tertiary divergences (Edwards *et al.* 2007, Chapple et al. 2005, James and Moritz 2002).

Phylogenetic and Advertisement call patterns

Advertisement call types (Fig. 2.1b) have been used as the primary evidence to develop hypotheses of genetic differentiation in *C. signifera* (Littlejohn 2005, 1967, Moore 1954). Littlejohn (2005) hypothesized that dispersal from Tasmania to East Gippsland and southern New South Wales resulted in a similar advertisement call (call type 5) among populations from the eastern mainland and Tasmania. Call type 5 is found in Tasmania, East Gippsland and southern New South Wales (Fig. 2.1b) suggesting that

individuals from these regions may be closely related. The Bayesian analysis did not identify any trees consistent with the hypothesis that individuals from these localities are monophyletic. Rejection of Pleistocene dispersal between Tasmania and the eastern mainland is not surprising as the data presented here suggest much older divergences between Tasmania and the mainland. It is more likely that the similarity in advertisement calls in these regions is due to the retention of an ancestral call type rather than an indication of close relationship.

In contrast, phylogenetic relationships within clade C sub-clades reflect advertisement call differences. The geographic regions sampled for call types 1 and 2 (Fig. 2.1b) correspond to sampling sites in clades C1 and C2, respectively (Littlejohn, 1964, 1959, 1958). However, call types 1 and 2 cannot be statistically compared to one another because they were collected and analyzed differently (Littlejohn *et al.* 1993, Odendaal *et al.* 1986, Littlejohn, 1959, 1958). Therefore, whether sub-clades C1 and C2 have distinctive calls is not clear, but they do differ from all other localities (Fig. 2.1b). The disjunct localities in sub-clade C3 share call type 3 (Littlejohn and Wright 1997, Littlejohn 1964). Call type 4 in western South Australia is different from call type 3, and corresponds to the region encompassed by sub-clade C4 (Littlejohn 2005, Littlejohn and Wright 1997). However, like call types 1 and 2, call type 4 has not been compared to all other call types (Littlejohn 2005, Littlejohn *et al.* 1993, Odendaal *et al.* 1986, Littlejohn, 1959, 1958). Thus, differences in advertisement calls appear to be an appropriate predictor of sub-clade membership within clade C, but are apparently much older than proposed by Littlejohn (2005, 1964) and Littlejohn *et al.* (1993).

Taxonomic relationships

High levels of genetic divergence were recovered among samples of *C. signifera* (Table 2.3). Several pairwise comparisons in this 16S rRNA dataset are above 5%, suggesting three cryptic species might be recognized. However, studies of reproductive isolation suggest that *C. signifera* represents a single species. Experimental crosses have been performed among populations from clade B and C (Main 1968, Straughan and Main 1966, Moore 1954). All crosses resulted in normal development and therefore suggest no post-zygotic isolation exists among them. These crosses contrast with those between closely related species of *Crinia* that result in gross abnormalities and incomplete or retarded development of embryos (Main 1968). Further, phonotaxis experiments showed that Queensland females do not discriminate between calls from their own populations and those from Seymour, VIC (Straughan and Main 1966). Though we find historically distinct lineages, the reproductive biology is insufficiently divergent to identify the three lineages as different species. Thus, we argue that it is premature to elevate these three clades to species-level status without detailed studies of morphological variation, intensive phonotaxis experiments (e.g., Kime *et al.* 1998) and analysis of nuclear DNA sequence data.

Table 2.1. Individual identification numbers and sampling localities of individuals used for DNA sequencing. Tissues from the South Australia Museum are indicated by *. Samples and DNA sequence presented from the analysis of Read *et al.* 2002 are marked with †. Localities are arranged from north to south along the east coast and then from east to west. Numbers in the left column correspond to localities on the map and tree in Fig. 2.2. Latitude and longitude are in decimal degrees. States are abbreviated as follows: NSW, New South Wales; VIC, Victoria; SA, South Australia; TAS, Tasmania. Museums used for voucher deposition are abbreviated as follows: South Australia Museum, SAM; Museum Victoria, MV; Australian National Wildlife Collection, ANWC; Australian Museum, AM; Queen Victoria Museum, QVM.

Site	Individual	Species	Locality	State	Region	Latitude Longitude	Museum	GenBank
1	BS054	*C. signifera*	Evans Head	NSW	Northern NSW	-29.09 153.59	AM	EU443860
2	ABTC25425*	*C. signifera*	Glenn Innes	NSW	NSW	-29.71 151.75	--	EU443863
3	ABTC12334*	*C. signifera*	Armidale	NSW	NSW	-30.22 151.67	--	EU443873
4	BS040, Cr50060, Cr50062-64, Cr50066-68†	*C. signifera*	Coffs Harbour	NSW	Northern NSW	-30.30 153.11	--	EU443861, EU448122-EU448128
5	BS035	*C. signifera*	Port Macquarie	NSW	NSW	-31.50 152.90	AM	EU443872
6	BS033	*C. signifera*	Clarencetown	NSW	NSW	-32.57 153.44	AM	EU443874
7	BS011	*C. signifera*	Cooranbong	NSW	NSW	-33.13 151.33	AM	EU443875
8	BS154	*C. signifera*	Macquarie Woods	NSW	NSW	-33.41 149.31	AM	EU443862
9	BS022	*C. signifera*	Coogee	NSW	NSW	-33.93 151.26	AM	EU443866
10	ABTC17627*	*C. signifera*	Heathcote	NSW	NSW	-34.07 151.02	AM	EU443867
11	BS162	*C. signifera*	Kangaroo Valley	NSW	NSW	-34.74 150.54	AM	EU443870
12	ABTC12884-85*	*C. signifera*	Wagga Wagga	NSW	VICSA	-35.13 148.23	--	EU443883, EU443880
13	87-88†	*C. signifera*	Mullingans Flat	ACT	NSW	-35.17 149.17	--	EU448130-EU448131
14	BS240-241	*C. signifera*	Canberra	ACT	NSW	-35.24 149.11	ANWC	EU443864-EU443865
15	BS060	*C. signifera*	Ulladulla	NSW	NSW	-35.35 150.45	AM	EU443871
16	ANWC 2048†	*C. signifera*	Jerrabombera	ACT	NSW	-35.35 149.15	--	EU448132
17	86†	*C. signifera*	Braidwood	NSW	NSW	-35.43 149.80	AM	EU448129
18	BS164	*C. signifera*	Kianga	NSW	NSW	-36.20 150.13	AM	EU443869
19	BS067	*C. signifera*	Eden	NSW	NSW	-37.05 149.90	AM	EU443868
20	99†	*C. signifera*	Noorinbee	VIC	East Gippsland	-35.17 149.15	MV	EU448133
21	BS175, BS180	*C. signifera*	Cann River	VIC	East Gippsland	-37.56 149.15	MV	EU443876, EU443878
22	BS183-184	*C. signifera*	Bairnsdale	VIC	East Gippsland	-37.67 147.56	MV	EU443877, EU443879
23	ABTC12882-83*	*C. signifera*	0.5k E Granya	VIC	VIC-SA	-36.10 147.32	--	EU443881-EU443882
24	BS088, BS093	*C. signifera*	Lilydale	VIC	Central VIC	-37.78 145.36	MV	EU443900, EU443898
25	BS185, BS189	*C. signifera*	Seymour	VIC	Central VIC	-37.01 145.14	MV	EU443901-EU443902
26	BS001	*C. signifera*	Bundoora	VIC	Central VIC	-37.72 145.05	MV	EU443899
27	BS195-196	*C. signifera*	Maryborough	VIC	VIC-SA	-37.31 143.98	--	EU443891-EU443892

Table 2.1. *Continued*

Site	Individual	Species	Locality	State	Region	Latitude Longitude	Museum	GenBank
28	BS197-198	*C. signifera*	Stawell	VIC	VIC-SA	-37.07 142.76	MV	EU443893-EU443894
29	BS141	*C. signifera*	Hamilton	VIC	Central VIC	-37.70 141.91	MV	EU443897
30	BS131	*C. signifera*	Portland	VIC	VIC-SA	-38.37 141.61	MV	EU443884
31	ABTC37438*	*C. signifera*	Mount Gambier	SA	VIC-SA	-38.05 140.94	SAM	EU443888
32	ABTC14924†	*C. signifera*	Penola	SA	VIC-SA	-37.37 140.83	SAM	EU448134
33	BS212-213	*C. signifera*	Naracoorte	SA	VIC-SA	-37.10 140.79	SAM	EU443895-EU443896
34	BS227	*C. signifera*	Mary Seymour Conservation Park	SA	VIC-SA	-37.16 140.62	SAM	EU443886
35	ABTC37700-01*	*C. signifera*	Padathaway	SA	VIC-SA	-36.69 140.48	--	EU443889-EU443890
36	ABTC58307*	*C. signifera*	Gum Lagoon Conservation Park	SA	VIC-SA	-36.27 140.02	--	EU443885
37	ABTC58814*	*C. signifera*	Milang	SA	Fleurieu Peninsula	-35.40 139.97	--	EU443904
38	ABTC36237*	*C. signifera*	Kingston	SA	VIC-SA	-36.82 139.85	--	EU443887
39	BS096-98	*C. signifera*	Adelaide Hills	SA	Western SA	-35.06 138.75	SAM	EU443918-EU443920
40	BS116-118, BS127-129	*C. signifera*	Clare	SA	Western SA	-33.84 138.62	SAM	EU443921-EU443926
41	BS106-108	*C. signifera*	Crystal Brook	SA	Western SA	-33.33 138.24	SAM	EU443915-EU443917
42	ABTC33253*	*C. signifera*	Second Valley	SA	Fleurieu Peninsula	-35.52 138.22	--	EU443903
43	ANWC1706, ANWC1708-10†	*C. signifera*	Kangaroo Island	SA	Western SA	-35.75 137.62	SAM	EU448136, EU448138, EU448139, EU448137
44	BS433-435	*C. signifera*	Sheffield	TAS	TAS	-41.39 146.33	QVM	EU443909-EU443911
45	BS423-425	*C. signifera*	Epping Forest	TAS	TAS	-41.78 147.32	QVM	EU443912-EU443914
46	BS413-416	*C. signifera*	Wielangta Forest	TAS	TAS	-42.65 147.90	QVM	EU443905-EU443908
47	ABTC17180†	*C. signifera*	Nugent	TAS	TAS	-42.70 147.75	--	EU448135
--	ABTC26421, Cr50061, Cr50065†	*C. sp*	Coffs Harbour	NSW	--	--	--	EU448118-EU448120
--	ABTC14772*	*C. riparia*	Mambray Creek	SA	Flinders Ranges	--	--	EU443858
--	BS207	*C. riparia*	Warren Gorge	SA	Flinders Ranges	--	SAM	EU443856
--	BS222-223	*C. riparia*	Telowie Gorge	SA	Flinders Ranges	--	SAM	EU443859, EU443857
--	BS153	*C. parinsignifera*	Macquarie Woods	NSW	--	-33.41 149.31	AM	EU443855
--	ABTC17569†	*C. parinsignifera*	Wagga Wagga	NSW	--	--	SAM	EU448117

Table 2.2. Primers used for PCR and DNA sequencing. Positions are in reference to *Xenopus* (GenBank Accession No. NC001573, derived from M10217). Primers designed specifically to amplify difficult regions in *Crinia* species are designated as: This paper. All other primers were designed in the labs of D.M. Hillis and D.C. Cannatella.

Primer Name	Sequence (5'-3')	Position	Reference
MVZ59	ATAGCACTGAAAAYGCTDAGATG	2153-2180	Goebel *et al.* 1999
tRNA-VAL	GGTGTAAGCGARAGCTTTKGTTAAG	3034-3059	Goebel *et al.* 1999
12SM	GGCAAGTCGTAACATGGTAAG	2968-2988	Cannatella *et al.* 1998
16SA	ATGTTTTTGGTAAACAGGCG	3956-3975	Goebel *et al.* 1999
12L1	AAAAAGCTTCAAACTGGGATTAGATACCCCACTAT	2475-2509	Goebel *et al.* 1999
16SH	GCTAGACCATKATGCAAAAGGTA	3282-3304	Goebel *et al.* 1999
16SC	GTRGGCCTAAAAGCAGCCAC	3623-3642	--
16SD	CTCCGGTCTGAACTCAGATCACGTAG	4549-4574	--
12Sb-H	GAGGGTGACGGGCGGTGTGT	2897-2916	Goebel *et al.* 1999
PC3000r	CGGTGGTTTAGTGTGGGGGTGT	3000-3022	This paper
PC3000f	CCCACACTAAACCACCGCCACT	3000-3022	This paper
PC3800r	DGGGTGTATTACCCGGGGGCTG	3800-3822	This paper
PC3800f	CCGACAAAGTGGGCCTAAAAGC	3800-3822	This paper
SBC16Sc-50down	ATHATGCTAGAACTAGTAACAAGAA	3673-3698	This paper
BS223R	TCGCCTGTACTAGATTGTTAGAATG	3050-3075	This paper
BS223F	CATTCTAACAATCTAGTACAGGCGA	3050-3075	This paper
12S1R	CCACCTAGAGGAGCCTGTCC	2601-2620	This paper

Table 2.3. Summary of pairwise uncorrected p-distance within and among clades. Clades refer to major clades in Fig. 2.2.

	Uncorrected p-distance		
	Mean	Standard Deviation	Range
All samples	0.0026	0.0097	0-0.0459
Among clades			
A-B	0.0330	0.0027	0.0072-0.0282
A-C	0.0302	0.0037	0.0256-0.0375
B-C	0.0314	0.0057	0.0148-0.0244
Within Clades			
Clade A	0.0036	0.0023	0.0014-0.0063
Clade B	0.0093	0.0047	0.0022-0.0194
Clade C	0.0249	0.0118	0-0.0658

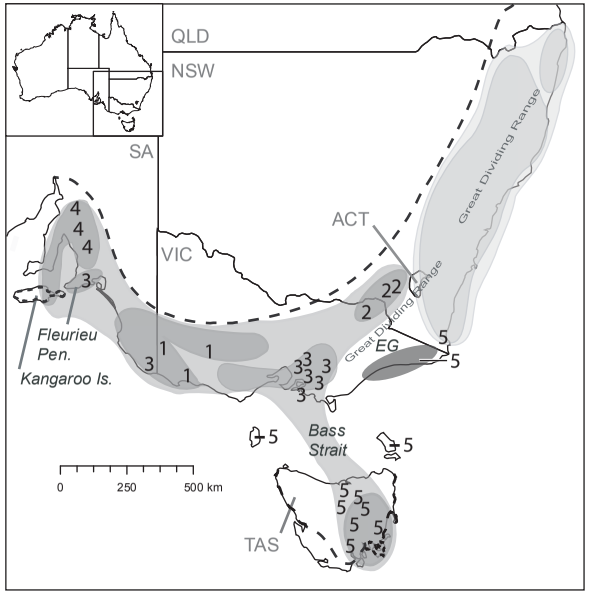

a.

Call Type	Site Location	Pulses Per Call	Call Duration (ms)	Pulse Rate (pulses/s)
Call Type 1	Mainland Western, VIC, SA[c]			
Call Type 2	North East, VIC[d] Tocumwal, NSW[e]			
Call Type 3	Victor Harbour, SA[b] Millicent, SA[b] Mainland Central, VIC[c]			
Call Type 4	Adelaide, SA[d]			
Call Type 5	Mallacoota, VIC[a] Boydtown, NSW[a] Lune River, TAS[a] Tasmania, TAS[c]			

b.

Figure 2.1. Summary of advertisement call differences in *C. signifera*. (a.) The distribution of *C. signifera* is shown below the dotted line on the mainland and above the dotted line in Tasmania. The advertisement call sampling sites are indicated by call type number. Shading on the map represents the clades and sub-clades. State and territory names are abbreviated: ACT, Australian Capital Territory; NSW, New South Wales; QLD, Queensland; SA, South Australia; TAS, Tasmania; VIC, Victoria. Regions of geographic interest are abbreviated: EG, East Gippsland; FP, Fleurieu Peninsula; KI, Kangaroo Island. (b.) The table summarizes boxplots adapted from each of the original studies of advertisement calls (a. Littlejohn, 2005, b. Littlejohn and Wright, 1997, c. Littlejohn, 1964, d. Littlejohn, 1959, e. Littlejohn, 1958). Delineation of call types is based on statistical tests of the original studies. For simplicity, all sites examined in the original studies are not shown. Two types of boxplots are shown. First the open boxes in call types 3 and 5 are whisker plots. The box represents the interquartile ranges, the horizontal lines indicate values that fall within1.5 times the interquartile range, and the line within the box is the median. Second, for all other call types, the solid boxes show two standard errors on either side of the mean, the open box indicates one standard deviation, the horizontal line shows the range, and the vertical line is the mean.

Figure 2.2. (Next page) Relationships among populations of *C. signifera* and the geographic distribution of clades and sub-clades. The best ML tree estimated using GARLI (-lnL=8372.1583) is shown. Solid black dots represent Bayesian posterior probabilities above 0.95 and nonparametric bootstrap support >85%. White dots represent Bayesian posterior probabilities >0.95 and nonparametric bootstrap support <85%. Branches without dots indicate support <0.95 Bayesian posterior probability and <75% nonparametric bootstrap support. Individuals with identical haplotypes are indicated on the tree by *. The scale on the tree is in substitutions per site. Shading behind the clades corresponds to shading on the map. Numbers next to localities on the tree correspond to numbers in Table 2.1 and on the map to the left of the tree. Dots and numbers on the map show sampling localities listed in Table 2.1. Abbreviations on the map are: ACT, Australian Capital Territory; NSW, New South Wales; QLD, Queensland; SA, South Australia; TAS, Tasmania; VIC, Victoria.

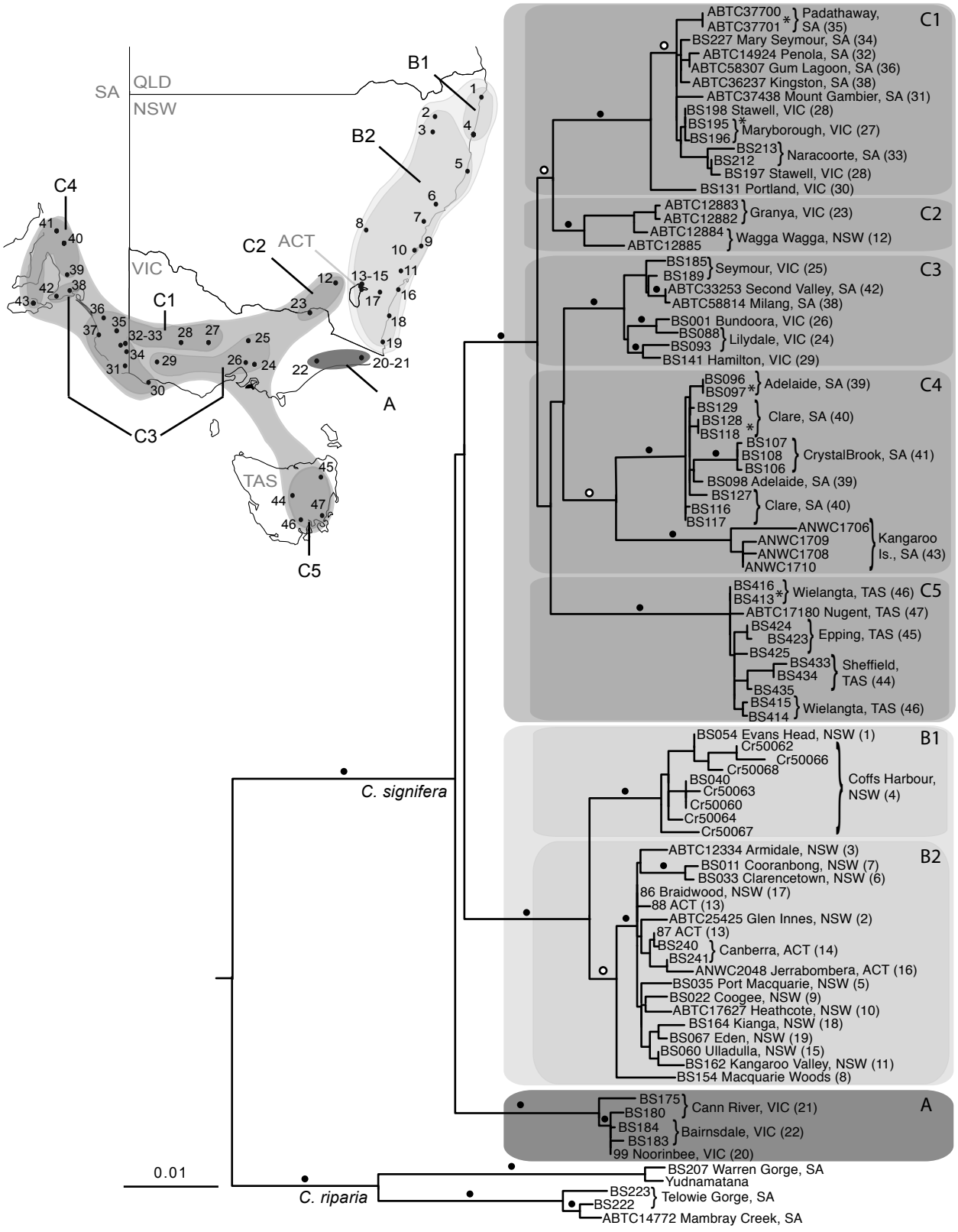
SA
QLD
NSW
VIC
ACT
TAS
B1
B2
C1
C2
C3
C4
C5
A
1
2
3
4
5
6
7
8
9
10
11
12
13-15
16
17
18
19
20-21
22
23
24
25
26
27
28
29
30
31
32-33
34
35
36
37
38
39
40
41
42
43
44
45
46
47
ABTC37700 * Padathaway, ABTC37701 * SA (35)
BS227 Mary Seymour, SA (34)
ABTC14924 Penola, SA (32)
ABTC58307 Gum Lagoon, SA (36)
ABTC36237 Kingston, SA (38)
ABTC37438 Mount Gambier, SA (31)
BS198 Stawell, VIC (28)
BS195 * BS196 Maryborough, VIC (27)
BS213 BS212 Naracoorte, SA (33)
BS197 Stawell, VIC (28)
BS131 Portland, VIC (30)
ABTC12883 ABTC12882 Granya, VIC (23)
ABTC12884 ABTC12885 Wagga Wagga, NSW (12)
BS185 BS189 Seymour, VIC (25)
ABTC33253 Second Valley, SA (42)
ABTC58814 Milang, SA (38)
BS001 Bundoora, VIC (26)
BS088 BS093 Lilydale, VIC (24)
BS141 Hamilton, VIC (29)
BS096 BS097 * Adelaide, SA (39)
BS129 BS128 * BS118 Clare, SA (40)
BS107 BS108 BS106 CrystalBrook, SA (41)
BS098 Adelaide, SA (39)
BS127 BS116 BS117 Clare, SA (40)
ANWC1706 ANWC1709 ANWC1708 ANWC1710 Kangaroo Is., SA (43)
BS416 BS413 * Wielangta, TAS (46)
ABTC17180 Nugent, TAS (47)
BS424 BS423 Epping, TAS (45)
BS425
BS433 BS434 Sheffield, TAS (44)
BS435
BS415 BS414 Wielangta, TAS (46)
BS054 Evans Head, NSW (1)
Cr50062 Cr50066 Cr50068 BS040 Cr50063 Cr50060 Cr50064 Cr50067 Coffs Harbour, NSW (4)
ABTC12334 Armidale, NSW (3)
BS011 Cooranbong, NSW (7)
BS033 Clarencetown, NSW (6)
86 Braidwood, NSW (17)
88 ACT (13)
ABTC25425 Glen Innes, NSW (2)
87 ACT (13)
BS240 BS241 Canberra, ACT (14)
ANWC2048 Jerrabombera, ACT (16)
BS035 Port Macquarie, NSW (5)
BS022 Coogee, NSW (9)
ABTC17627 Heathcote, NSW (10)
BS164 Kianga, NSW (18)
BS067 Eden, NSW (19)
BS060 Ulladulla, NSW (15)
BS162 Kangaroo Valley, NSW (11)
BS154 Macquarie Woods (8)
BS175 BS180 BS184 BS183 Cann River, VIC (21) Bairnsdale, VIC (22)
99 Noorinbee, VIC (20)
C. signifera
C. riparia
0.01
BS207 Warren Gorge, SA Yudnamatana
BS223 BS222 Telowie Gorge, SA
ABTC14772 Mambray Creek, SA

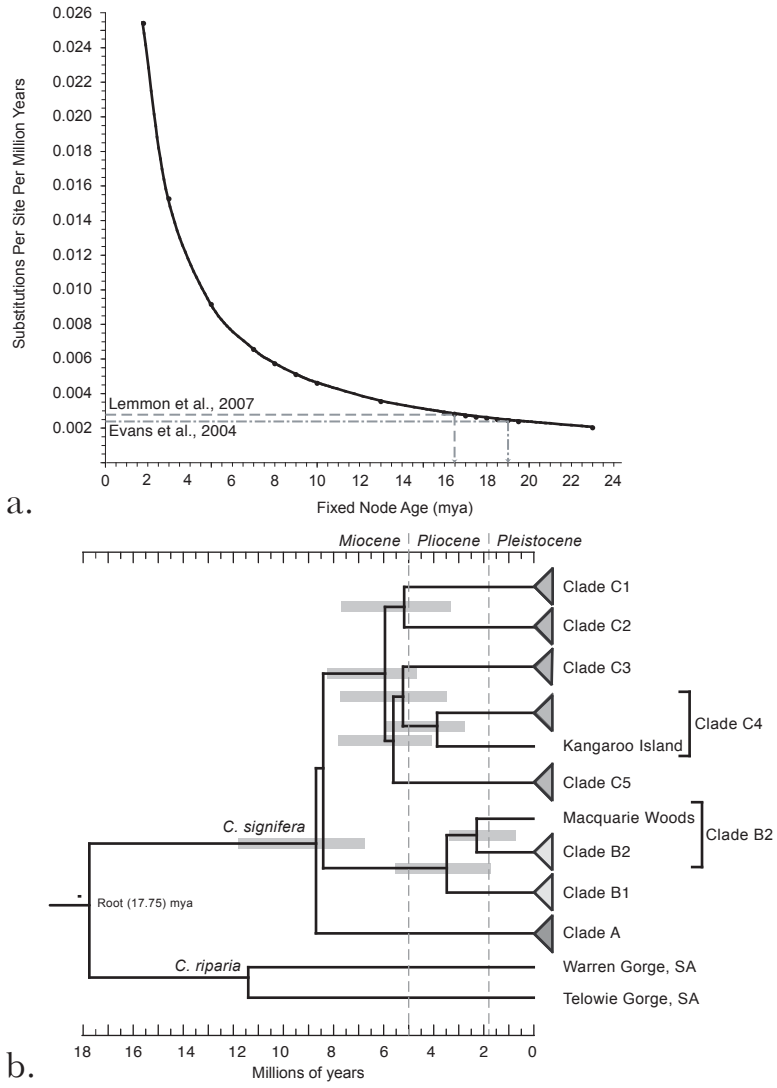

Figure 2.3. Calibration of the divergence time estimates and chronogram indicating estimated divergence times. (a.) Calibration of the *C. signifera* tree. Multiple iterations were performed with the root node fixed to different ages. Each iteration produced a substitution rate. The plot shows the fixed age of the node and the corresponding substitution rate estimated by r8s. The best estimate of the root age is approximately equal to the substitution rates determined from two independent studies. The estimates from the previous studies are based on fossil calibrations, and are shown on the graph as a dashed and dotted line and a dashed line. (b.) Chronogram of the best GARLI tree resulting from fixing the age of the root to17.75 mya. Clades and sub-clades (shaded triangles) are labeled based on the inclusion of a single representative from that clade. Shading of the triangle corresponds to shading in Fig. 2.2. Two individuals were included from B2 and C4 because the divergence between the individuals was higher than most others in the sub-clade. The extra individual remains outside of the sub-clade triangle. Gray boxes behind the nodes are confidence intervals calculated from 100 nonparametric bootstraps of the best GARLI tree topology.

Chapter 3. Differential predation on color pattern variants of the Australian common froglet, *Crinia signifera*.

Summary

Color pattern polymorphisms, the presence of multiple color patterns in a single population, are commonly associated with predation through mechanisms such as frequency-dependent selection or differential selection among heterogeneous habitats. Understanding how predation influences vertebrate color pattern polymorphisms is enhanced by using predators in their natural habitats. However, identification of predators that prey upon vertebrates is challenging. In this study, I used attack markings on clay replicas of the polymorphic Australian common froglet, *Crinia signifera*, to identify natural predators and to test whether predators discriminate between two different color patterns (black-and-white and white). Transects were established in two habitat types (woodland and vineyard) in order to evaluate potential predator composition differences between habitats. Predation rates were unexpectedly high in both transects (woodland = 43.96%, vineyard = 20.21%). Both attack rates and the proportion of attacks on different color patterns were significantly different between transects ($G_{H\,Rate} = 10.85$, $p = 0.0099$; $G_{H\,Color} = 5.23$, $p = 0.02$) suggesting a correlation between habitat differences and predation on different color patterns. Mammals were identified as the primary attackers of the replicas, as has been demonstrated by similar studies in Australia. Binomial tests of predator choice indicated no difference between incidence of attacks on black-and-white and white replicas in the woodland ($p = 0.676$), but demonstrated that black-and-white replicas were attacked significantly less frequently in the vineyard ($p = 0.0021$). Binary

logistic regression indicates that black-and-white coloration is attacked significantly less often in the vineyard habitat (Wald's $\chi 2 = 4.59$, $p = 0.032$) suggesting that black-and-white coloration is advantageous in the vineyard. The combination of differences in attack rate and avoidance of black-and white coloration among habitats suggest that predation contributes to the evolution and maintenance of color pattern polymorphism in *C. signifera*.

3.1 Introduction

Color pattern polymorphism is defined as the simultaneous occurrence of multiple different variants or morphs in the same population at frequencies too high to be a result of mutation (Ford 1975, Poulton 1890). Animals that exhibit color pattern polymorphisms provide an opportunity to investigate the origin and maintenance of natural variation within and among populations. Color polymorphisms are commonly linked with selection either through predation or adaptation to heterogeneous habitats (e.g., Manríquez *et al.* 2008, Phifer-Rixey *et al.* 2008). Often, coloration is used as a signal to escape predation either by avoiding detection (crypsis) or advertising noxiousness (aposematism). Cryptic species (Cott 1940, Poulton 1890) minimize their detectability by resembling their visual background (Bond 2007, Endler 1978), while aposematic species maximize their conspicuousness to warn predators that they are unpalatable or toxic (Cott 1940).

Directional selection imposed by predators is predicted to reduce variability in populations, but unexpectedly, phenotypic polymorphisms are apparent within both

cryptic and aposematic species. Predation can maintain polymorphisms in prey through frequency-dependent (apostatic) selection when prey is cryptic (e.g., Merilata 2006, Olendorf *et al.* 2006, Bond and Kamil 2002), or number-dependent selection (Mallet and Joron 1999) when one prey species mimics another aposematic species (e.g., Mallet 1993). Alternatively, polymorphisms can arise as adaptations to heterogeneous habitats (or microhabitats) and can be maintained through a balance between selection and gene flow (Bond 2007, Endler 1978). In addition, theoretical studies have proposed that interactions between environmental heterogeneity and predation maintain and promote the evolution of polymorphic coloration (Forsman and Åberg 2008, Forsman *et al.* 2008).

To examine the contribution of predation and habitat differences to color polymorphism, it is critical to identify natural predators. Many studies of predation on phenotypically polymorphic species focus on invertebrate prey species. These studies benefit from the ability to identify natural predators and quantify their impact (e.g., Hanlon *et al.* 2009, Manríquez *et al.* 2008, Phifer-Rixey *et al.* 2008, Cook 1986). Identifying predators of vertebrates is more challenging because it relies on rare observations of predation events or gut content analyses. Experiments that test whether predators avoid vertebrate prey often use hypothetical or unnatural model predators, such as chickens (e.g., Svádová *et al.* 2009, Darst and Cummings 2006). While these studies are crucial for understanding predation dynamics, the outcomes of some studies using model predators conflict with outcomes of similar studies that use natural predators (reviewed by Speed 2000). Therefore, addressing questions relating to natural

evolutionary processes that maintain color pattern polymorphism in the wild is difficult in the absence of known predators.

Clay replicas have been successfully used as a means to identify natural predators and quantify predation pressure (e.g., Pfennig *et al.* 2007, Kuchta, 2005). Furthermore, soft clay can be used to identify natural predators because beak and tooth impressions are left following a predatory attack (Berry and Lil 2003, Boulton and Clarke 2003, Brodie 1993). Even in small vertebrates, like frogs, clay replicas have been used successfully to assess predator discrimination among color patterns (Saporito *et al.* 2007, Kuchta 2005).

In Australia, several myobatrachid frogs are polymorphic in color pattern (Hoffman and Blouin 2000) and many exhibit putative anti-predator defenses (Williams *et al.* 2000). However, a relationship between color patterns and predator evasion strategies has not been demonstrated. Specifically, *Crinia signifera*, the common froglet, is an example of a widely distributed taxon with relatively well-understood ecology, life history and reproductive biology, but for which mechanisms driving geographic patterns of phenotypic polymorphisms have not been investigated in the context of predation (Lemckert 2005a, b, Lauck 2005, Williamson and Bull 1996). Among potentially interbreeding populations, individual members of each population vary in the proportion of black on the ventral surface (Cogger 2000). Within populations, black-and-white individuals co-exist with individuals that have solid white, gray or black ventral surfaces (Fig. 3.1). When attacked by a predator, *C. signifera* "plays dead" (thanatosis), exposing its ventral surface (Williams *et al.* 2000). All *C. signifera* individuals play dead regardless of ventral coloration (Symula *unpubl. data*) and individuals from some populations secrete

peptides that have been shown to result in smooth muscle contraction *in vitro* (Maselli *et al.* 2004, Erspamer *et al.* 1984). The combination of a defensive behavior, bold coloration and potentially noxious skin secretions may function to deter predators. However, whether the signal is aposematic remains untested partially because records of predation on *C. signifera* are limited to rare predation by a few elapid snake species (Shine 1977).

One hypothesis suggests that the exposure of black-and-white ventral coloration by *C. signifera* is due to mimicry of frogs in the genus *Pseudophryne* (Williams *et al.* 2000). All *Pseudophryne* species play dead and have black-and-white mottled venters (Cogger 2000), but the *Pseudophryne* display is accompanied by secretion of the skin alkaloid, pseudophrynamine (Daly *et al.* 1990). Some similar alkaloids are known to cause paralysis and death in mice (Smith *et al.* 2002, Daly 1995, Daly *et al.*1990, 1984). When brightly colored, dendrobatid poison frogs that secrete alkaloids are avoided by predators (Darst and Cummings 2006). Therefore, by sharing coloration and defensive behavior with *Pseudophryne*, *C. signifera* may be afforded protection from predators.

No tests have been conducted to evaluate whether the black-and-white coloration (or the playing dead behavior) deters predators in either *C. signifera* or *Pseudophryne*. Elucidation of the effect of natural predators can provide insight into how polymorphism is maintained in populations of *C. signifera*. However, natural predators of *C. signifera* or *Pseudophryne* are unknown. Diet composition and foraging behavior suggest that reptiles, birds and mammals are potential predators of frogs. Gut content analyses of birds, though they reveal small frogs in the diet, do not conclusively identify *C. signifera* or *Pseudophryne* as part of the diet (Higgins and Davies 1996, Marchant and Higgins 1990a,

b, 1993, Barker and Vestjens 1979, Lowe 1978). Likewise, small frogs have been found in gut contents of native mammals that frequently forage among vegetation along freshwater shorelines (e.g., *Antechinus*, water rats), but the frogs consumed can only be confidently assigned to the family (Strahan 1995). In a survey of gut contents, only a single species of snake contained either *C. signifera* or *Pseudophryne bibronii*, but these frogs made up less than 0.6% of the diet of the snake (Shine 1977).

In this study, I used soft clay replicas to test the response of predators to polymorphic coloration of *C. signifera*. Though *C. signifera* is variable in black-and-white color pattern among populations, I focus on within-population polymorphism in this study by using clay replicas of two different *C. signifera* morphs (black-and-white and white; Fig. 3.1). I specifically aimed to test whether the black-and-white coloration in *C. signifera* affords protection from predators, and to identify putative predators of *C. signifera* in different habitats.

3.2 Methods

Replica construction

Plaster molds were made from a plastic frog that was approximately the size of *C. signifera* (snout-vent-length = 25mm). From the molds, 448 replicas were constructed using white Original Sculpey® Modeling Compound (Polyform Products Co., Elk Grove Village, IL). All replicas were painted on the dorsal surface with brown acrylic paint to resemble the dorsal coloration of *C. signifera*. Half of the replicas (224) were painted on the ventral side to resemble black-and-white (putatively mimetic) individuals previously

captured at the site. The remaining 224 replicas were left white to represent non-mimetic individuals from the experimental site (Fig. 3.1).

Transect set-up

The experiment was performed at Noorinbee Selection Vineyards and Winery in Cann River, Victoria, Australia between 26 May-7 June 2007. Transects were established over a 48 h period in two habitat types. One transect was set up in a woodland area and a second transect was set up along drainage ditches in a vineyard. Both sites were observed to have natural populations of *C. signifera*.

Pairs of a mimetic (black-and-white) and a non-mimetic (white) replica were placed along both transects with spacing of 5 m between pairs. A small green marker was placed approximately 1 foot from each pair to ensure that missing pairs could be identified. Pairs of clay replicas were set on the ground, ventral side up, with approximately 3-5 cm between each replica. Thus, although the color pattern normally is displayed along with a defensive behavior, this experiment specifically emphasized the effect of the color pattern without the potentially confounding effects of the behavior. Transects were left for 24 h before observations.

Data collection and scoring of attacks

Observations began on 28 May 2007. Both transects were observed in late morning and early afternoon to avoid interfering with peak bird activity. Due to an unexpectedly high predation rate, the woodland was observed daily. The vineyard

transects were observed every second day. If replicas were damaged, bitten or otherwise irreparable, both members of the pair were removed. Disturbances, bite marks or other damages were recorded. For each observation of recent predator activity on a pair (i.e., attacked or damaged), pair number, color pattern of the affected individuals and type of activity were scored. Each activity was categorized as activity on both replicas, activity on only white replicas or only black-and-white replicas. Type of activity on replicas was then categorized as attacked or damaged. Pairs were categorized as "attacked" if they were disturbed (replicas were moved away from original positions or were flipped without damage), bitten (replicas bore obvious teeth or beak marks and were intact), destroyed (replicas no longer resembled frogs or were in tiny pieces) or missing (replicas were absent from original site). Individuals that were bitten or destroyed were categorized into different types of bites based on putative predator. Replicas were scored as "damaged" when the damage incurred was not caused by a predator (e.g., weathering of paint).

To account for damaged replicas and non-independent attacks, an adjusted dataset was created removing some observations from statistical analyses. First, on each transect the total number of pairs was reduced by the number of damaged pairs and then by the number of pairs attacked by animals that were unlikely predators (e.g., wallabies). Second, adjacent pairs that were attacked on the same day were categorized as pseudo-replicates unless it was determined that different predators were responsible for the attack. Each pseudo-replicate was counted as a single attack and these pairs were scored based on the color of the replica that was attacked. For example, if white members of each of two pairs were attacked, the disturbance was categorized as a single attack on a white

replica. However, if a black-and-white replica was attacked in one pair and a white in the second pair, the attack was scored as a single attack on both replicas. Then, the total number of pairs was reduced to account for the number of pseudo-replicates.

Statistical analyses

All statistical analyses were performed on the adjusted dataset. The two transects represented two experimental replicates. If the two replicates meet the null expectation that attack frequencies are equivalent, results from the two transects can be pooled as a single statistical population (Sokal and Rohlf 1995). To determine whether results from the different habitats could be pooled, G-tests were performed in two ways. First, G-tests of heterogeneity were used to test whether the total number of attacks differed among sites. Second, to test the hypothesis that the color attack frequency differed among habitats, G-tests of independence were performed (Sokal and Rohlf 1995). Then, binary logistic regression was used to test whether the probability of attack on black-and-white replicas was significantly different among habitats. Finally, to test whether white replicas were attacked more frequently than black-and-white replicas, a binomial test was performed. This test includes only data where a clear choice was made between the two different color patterns and disregards pairs where both replicas were attacked. The binomial test was chosen over the G-test of independence because the experiment was designed as a predator choice test where each pair represents a single trial.

Bite mark identification

To identify mammal predators that left bite marks in the clay replicas, I used a two-step method. First, to generate a set of prints to compare to those in experimental replicas, skulls from the Museum Victoria (Melbourne, Australia) collection were used to make teeth prints in fresh clay. Second, clear bite impressions on replicas were cast using Easycast® Very fast cure polyurethane resin (Barnes Products Pty. Ltd.). Tooth casts were then compared to teeth from skulls of predatory mammals, and to images on Museum Victoria's Bioinformatics website (http://museumvictoria.com.au/bioinformatics/mammals/images/thumbindex.htm), and identified using a key that characterizes traces left behind by Australian mammals (Triggs 2004). Many observed bite marks did not leave marks of the entire jaw or even complete individual teeth. As a result, predator identification was limited to when a clear incisor, premolar or partial jaw was left, in isolation, or when a replica retained key jaw or tooth features (Triggs 2004). Also, because clay was chewed or bitten multiple times, prints were often longer than the actual tooth, distorting the resulting casts. Finally, many replicas were destroyed, and left in tiny pieces from which no tooth casts could be made.

3.3 Results

Data collection and scoring of attacks

Adjusted totals for both transects are shown in Table 3.1. In the woodland transect, of the total 101 pairs 91 pairs met the criteria for including data. Eight pairs were excluded due to pseudoreplication, one pair due to a bite by a Swamp Wallaby

(*Wallabia bicolor*) and one pair due to human induced damage. Swamp Wallabies are primarily herbivorous, so the attack was removed because it is unlikely to represent a major predator of *C. signifera*. Data collected after 4 June were discarded because 30 pairs of replicas disappeared, over a 24-hour period on 4 June. It is likely that a predator discovered the transect and removed these pairs. Thus, to avoid artificially inflating estimated predation rates these data were not included.

Of the 123 pairs on the vineyard transect, 94 met the inclusion criteria. One pair was excluded due to pseudoreplication and 27 pairs were excluded due to environmental damage. In these 27 pairs, clay was often scraped off by something other than a predator, potentially a slug. Pairs with this type of damage were removed as they were found.

In the woodland, there were 16 instances where both members of the pairs were attacked. In these, there were only five cases where the attack category (Disturbed, Bitten, Destroyed, Missing) differed between the color patterns. These attacks were scored as events in which both replicas were attacked by a single predator to avoid arbitrary differentiation of attack severity.

Attack rates and predator preferences

Attack rates are the ratio of the total number of attacks to the adjusted total number of replicas on the transect. In the woodland, 43.96% of the pairs were disturbed, bitten or destroyed compared to 20.21% in the vineyard. The G-test of heterogeneity on attack rates indicated that total attack rates were significantly different between the

vineyard and woodland transects ($G_H = 10.85$, $p = 0.0099$). Therefore, data on attack rate could not be pooled and each transect was considered separately. Figure 2 illustrates the attack rate based on color morph for each transect. The G-test of independence on color morph indicated that the proportion of attacks on only black-and-white replicas and only white replicas were significantly different ($G_H = 5.23$, $p = 0.02$) between the vineyard and woodland, so predator choice tests were examined for each transect separately. Similarly, binary logistic regression indicated that the probability of attack on black-and-white replicas was significantly higher in the woodland (Wald's $\chi^2 = 4.59$, $p = 0.032$).

By using pairs of clay replicas on each transect, each pair represented a single replicate of a predator choice test. Thus, for statistical analyses, attacks on both individuals were not included because choice could not be assessed. On the woodland transect, the binomial test indicated no difference between attacks on black-and-white and white replicas (Binomial test $p = 0.676$). In the vineyard, white replicas were attacked significantly more often than black-and-white replicas (Binomial test, $p = 0.0021$).

Bite mark identification

Casting of teeth from clay replicas revealed that only mammalian teeth prints were observed, and all but one bite mark was made by potential frog predators. The single exception was left by the herbivorous Swamp Wallaby (*Wallabia bicolor*). Three other disturbances were potentially attributable to birds (peck marks). It was not possible to positively confirm birds as predators based on these instances because none of the

attacked replicas had distinctive marks seen in comparable studies (e.g., Pfennig *et al.* 2007, 2001, Brodie 1993).

The primary predator in the woodland was the common Brushtail possum (*Trichosurus vulpecula*), identified by marks left by the incisors from the lower jaw (Fig. 3.3a), and in some replicas, claw marks. Several other replicas contained remnants of sharp canine impressions. Though some bore similarity to canines of Spot-tail quolls (*Dasyurus maculatus*), these replicas lacked the key feature of four incisors beside the canine (Triggs 2004). Without any incisors, these attacks could not be conclusively confirmed as quoll bites. Similarly, most of the destroyed replicas were not identifiable (Fig. 3.3c).

In the vineyard, though many teeth prints yielded clear casts, most replicas did not have sufficient tooth detail to conclusively identify a predator. However, there were obvious differences in predator composition between the vineyard and the woodland. First, none of the replicas in the vineyard were bitten by common Brushtail possums. Second, one vineyard replica (Fig. 3.3b.) bore a strong canine tooth and three of the four incisors indicative of a Spot-tail quoll (Triggs 2004). Third, one replica had bite marks that could be tentatively confirmed as a rat (*Hydromys chrysogaster*), but tooth casts were too elongated and misshapen to confirm that identification. Fourth, some markings suggest that birds may have pecked at least three replicas (Table 3.1). Marks similar to the putative rat and birds were absent in the woodland.

3.4 Discussion

In this experiment, clay replicas of *C. signifera* were attacked frequently (20-45% of pairs attacked), with mammals imposing the greatest pressure (58.4% of all bites). Black-and-white replicas were preyed upon less frequently in the vineyard habitat (Wald's $\chi 2 = 4.59$, $p = 0.032$). Between experimental sites, there were significant differences in attack rates and in the proportion of black-and-white and white individuals attacked ($p = 0.02$, Fig. 3.2). Testing for heterogeneity in predation was not possible owing to only a few conclusively identified predators on either transect. However, the results suggest that the predator composition differed between habitats.

Attack rates

The attack rate in the woodland habitat was notably high. In clay replica studies performed in North America, attack rates range between 6.8% (Pfennig *et al.* 2001) and 16.5% (Pfennig *et al.* 2007). Similarly, in a clay replica study of aposematic frogs in Costa Rica, attack rates were 15.4% (Saporito *et al.* 2007). In contrast, attack rates up to 86% were observed on clay egg replicas used to estimate nest predation levels in Australian (Berry and Lil 2003, Fulton and Ford 2003, Matthews *et al.* 1999). In the woodland transect of this study, 45% of the pairs had suffered some sort of disturbance in less than one week. This suggests that *C. signifera*, and potentially other similar-sized frogs, are under high predation risk. Thus, developing defensive strategies may be particularly advantageous in these frogs. Defensive strategies in frogs are common (Williams *et al.* 2000). Both *C. signifera* and *Pseudophryne* species play dead and expose a putatively

aposematic (warning) coloration to avoid predation. Strategies of defense in other Australian frogs include noxious secretions and bright coloration on the dorsum (e.g., *Notaden*, *Pseudophryne*), inflation and elevation of the body (e.g., *Limnodynastes*, *Neobatrachus*) and defensive vocalizations (e.g., *Litoria*, *Cyclorana*; Cogger 2000, Williams *et al.* 2000). Further, other myobatrachid frog species bear black-and-white coloration that may be directed at avoiding similar predators (e.g., *Pseudophyrne*, *Adelotus brevis*; Barker *et al.* 1995). The results presented here suggest that the diversity of apparent defensive mechanisms in Australian frogs may have evolved in response to the apparent high risk of predation.

Relative to attack rates on white replicas, low rates on the black-and-white replicas in the vineyard suggest that display of the black-and-white coloration is advantageous in some habitats. These results imply that *Pseudophryne* species that bear similar coloration are also afforded protection from predators. *Pseudophyrne* were not found in either experimental site because the experiment was performed just before the breeding season, but were found later in the season. This experiment does not directly provide evidence that *C. signifera* is a mimic of *Pseudophryne*, but only that color pattern is beneficial in some habitats. Furthermore, I do not address whether the ventral coloration is aposematic in this study. It is possible that black-and-white replicas were more difficult to detect in the high light environment of the vineyard. When on dark soil backgrounds or in shaded areas, white replicas (and *C. signifera* with white venters) were easier to find than those that are black-and-white (R. Symula, *pers. obs.*). Data demonstrating that one color is more easily detected might be obtained by constructing transects of replicas with some individuals on white paper (i.e., Wüster *et al.* 2004, Brodie 1993) or by illustrating

with digital photographs that the two different forms differ in the degree to which they resemble the background (i.e., Villafuerte and Negro 1998, Endler 1990). In addition, aposematic prey species should indicate to predators that the prey is unprofitable (e.g., toxic or distasteful). In *C. signifera*, peptide compounds secreted from the skin cause elevated heart rates in cell culture and may be detrimental to predators (Maselli *et al.* 2004, Erspamer *et al.* 1984). Experiments have not been performed with real predators to demonstrate that these compounds deter predators, partially because predators were previously unknown.

Mammals were identified as the primary group of predators (58.4% of attacks). Certainly, frogs have been identified in the diet of Brushtail possums and Spot-tail quolls (Wells 2007, Strahan 1995). In many studies, mammalian attacks on clay replicas are discarded because mammals tend to rely on olfactory cues and often cannot perceive color (Endler 1978). Thus, non-human mammals are not considered visual predators. However, in studies of egg and nest predation where clay is used for model eggs, mammals frequently mistake models for food items (Piper and Catterall 2004, Boulton and Clarke 2003, Matthews *et al.* 1999). In this study, differential attacks between color morphs suggest that visual cues rather than olfactory cues are used in the vineyard. In many of the studies in which mammalian predation is disregarded, the visual signals are often composed of colors that reflect outside the mammalian visual spectrum (e.g., Brodie 1993, Endler 1978). Though reflectance data are lacking for *C. signifera*, neither the black nor white in *Pseudophryne* reflect outside of the human visual spectrum (R. Symula, *unpubl.*

data). Thus, black-and-white color patterns of *C. signifera* and *Pseudophryne* are likely to be detectable by mammals.

Heterogeneity in overall attack rate between transects ($G_H = 10.85$, $p = 0.001$), attack rate differences between white and black-and-white replicas ($G_H = 5.23$, $p = 0.02$) and significant differences in the probability of attack on black-and-white replicas between habitats (Wald's $\chi^2 = 4.59$, $p = 0.032$) is surprising because the transects were less than five km apart. Several factors could contribute to these small-scale differences. First, predator composition between habitats may differ as supported by the examination of tooth prints. Small teeth marks similar to rat (*Hydromys chrysogaster*) incisors were found on replicas from the vineyard, but not in the woodland. Also, several replicas found in the woodland were destroyed, but that type of attack was not found in the vineyard. Bites by Brushtail possums were common in the woodland (13 pairs confirmed by prints from incisors; Fig. 3.3, Table 3.1), but absent in the vineyard. Lack of available possum habitat may explain the absence of bite marks on the vineyard transect. Second, light conditions differ between habitats. Though measurements of available light were not obtained, the woodland habitat had substantially more canopy cover than the vineyard. As a result, the ability to detect the replicas between habitats may have differed. Alternatively, predators may have been able to discern that these replicas were not real food items in the vineyard. Third, it is possible that heterogeneity is due to stochastic differences between transects. All replicas were constructed with identical plaster molds, clay and paint in an effort to minimize these differences, but other stochastic differences could contribute to the

differences among sites. For example, during the weeks of observations, putative predators may not have been actively foraging in the vineyard.

Habitat heterogeneity is thought to generate phenotypic polymorphisms when the selective advantage of each morphotype depends on the location where it occurs (Bond 2007). Gene flow between these habitats is posited to maintain the polymorphisms (Merilata 2001, Endler 1978). For instance, when there is variation among habitats occupied by a single species, different color morphs may be more advantageous in some habitats. If there is then gene flow among habitats, then polymorphisms may appear within each of the different habitats (Merilata 2001, Endler 1978). Because the probability of being preyed upon is influenced by the ability of a predator to detect prey items, the characteristics of the habitat (e.g., amount of light, color of substrate, predator composition) may influence the strength of predation. When habitats are heterogeneous at small scales, predation pressure may vary similarly among habitats.

Crinia signifera is a habitat generalist that occurs naturally in open or forested areas where there is pooling water (Cogger 2000, MacNally 1985) and may therefore be exposed to dramatic differences in habitat and predation. The scale at which the differences occurred in this study was very small (<5 km among sites). Dispersal distances have not been directly estimated in *C. signifera*, but frogs of similar size are capable of dispersing over 200m in a single breeding season (Williamson and Bull 1996) supporting the hypothesis that dispersal or gene flow could contribute to the polymorphisms found within populations or habitats. The two study areas used here do not represent the extent of habitat variability found across the *C. signifera* distribution. Therefore, given the

apparent differences in attack rate and the frequency of attacks on different color patterns found in this study, predation differences could be more pronounced across the distribution and contribute more substantially to the evolution of color polymorphism in *C. signifera*.

Table 3.1. Summary of attack rates on individual clay replicas and potential predators of *C. signifera*. Numbers shown in parentheses () indicate the number of pairs that were attacked in each category (Bitten, Flipped, Moved or Missing). Numbers in brackets [] indicate number of instances where both members of a pair were attacked. Question marks indicate uncertainty in identification of predators. For the total, the number of individuals within a pair is represented.

Woodland				Vineyard			
Type of Disturbance		Replica		Type of Disturbance		Replica	
Bitten (24) [10]	*Putative predator*	Black & white	White	Bitten (15)	*Putative predator*	Black & white	White
	Common Brush-tail Possum (13)	3 [9]	1 [9]		Bird (3?)	0	3
	Spot-tail quoll (4?)	2 [1]	0 [2]		Spot-tail Quolls (1)	0 [1]	0 [1]
	Unknown (7)	1 [2]	4 [2]		Rat (2)	0 [1]	1 [1]
					Unknown (9)	1 [1]	7 [1]
Flipped (3) [0]	--	1 [1]	1 [0]	Flipped (2)	--	1	1
Moved (2) [0]	--	1 [0]	1 [2]	Moved (2)	--	0	2
Missing (11) [5]	--	3 [7]	2 [6]				
	Total	30	30		Total	5	17
	Attack Rate (by color)	38.5%	38.5%		Attack Rate (by color)	5.3%	18.1%

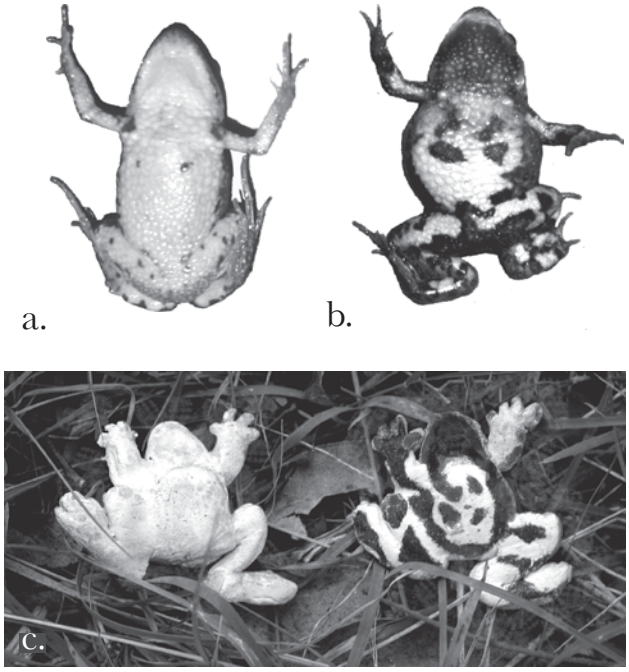

Figure 3.1. Representative *C. signifera* and clay replicas. (a.) Example of an individual with white ventral coloration. (b.) Example of an individual with black-and-white ventral coloration. Both individuals are from the experimental site. (c.) Pair of clay replicas and pair set-up used in experiment.

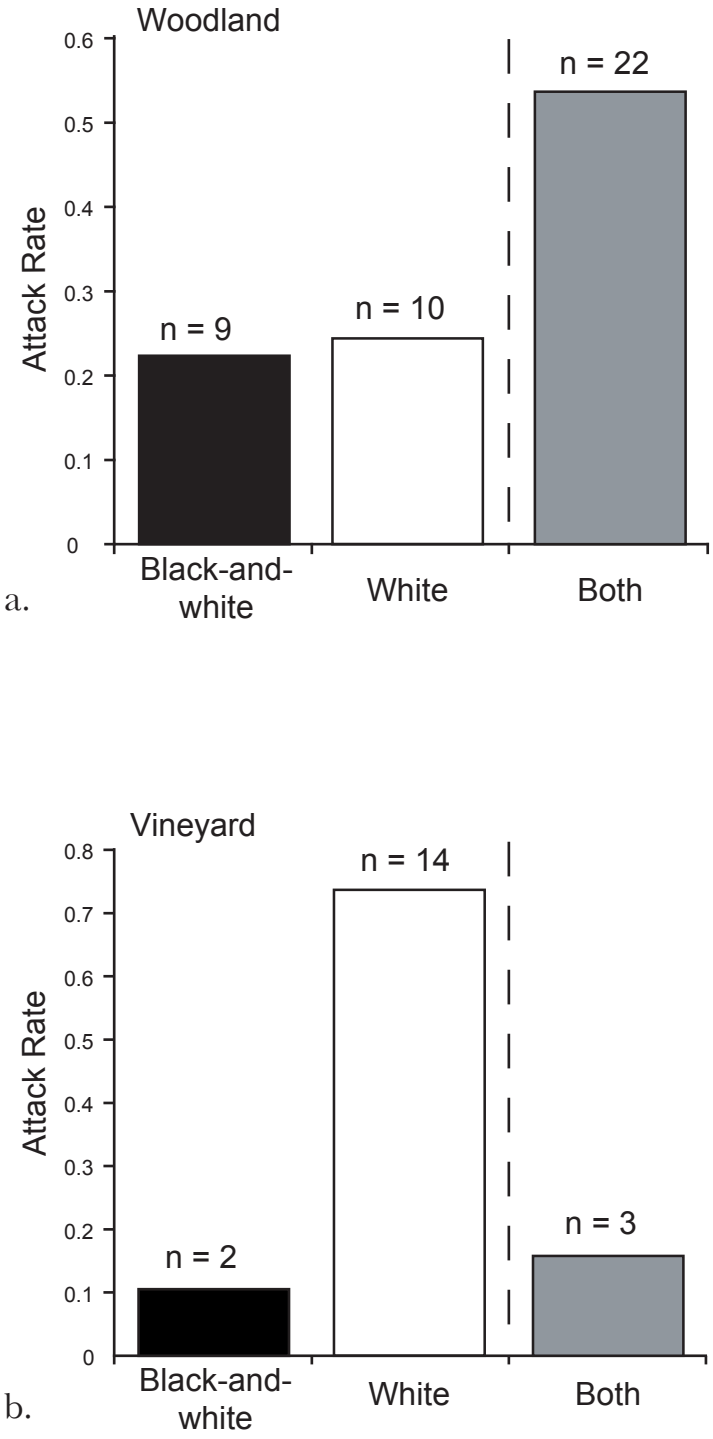

Figure 3.2. Proportions of attacked replicas in (a.) Woodland and (b.) Vineyard. Black bars indicate the attacked black-and-white replicas. White bars indicate attacked white replicas and gray bars indicate instances where both replicas were attacked. Numbers of attacked individuals (n) are shown above each bar.

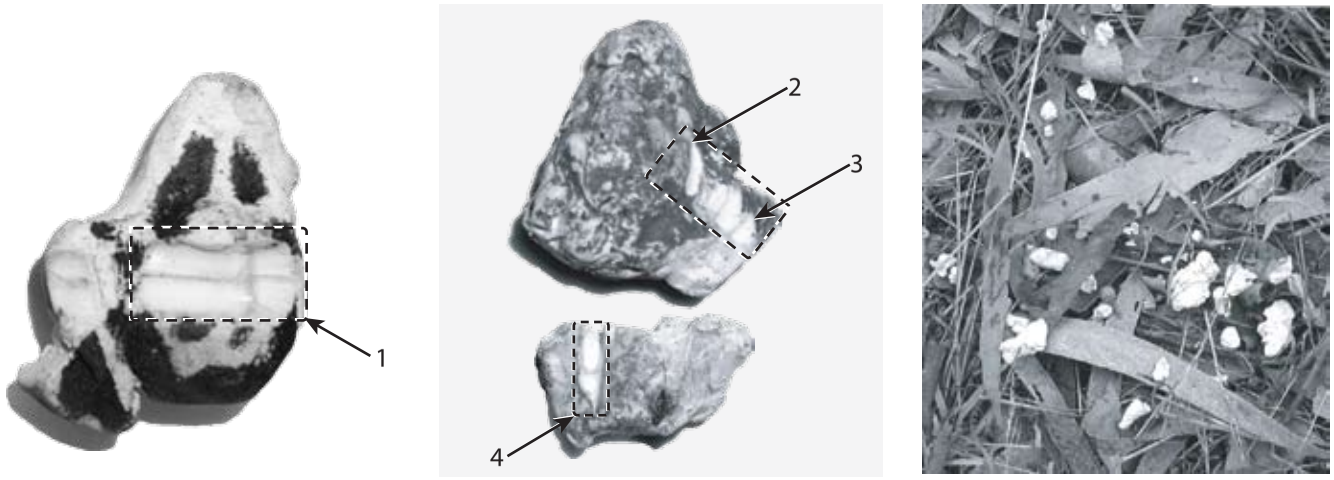

a. b. c.

Figure 3.3. Representative examples of bite marks found in clay replicas. (a.) Common Brushtail Possum with the incisors indicated at 1. (b.) Spot-tail Quoll tooth marks on both black-and-white and white replicas. At 2, the dorsal side of the black-and-white replica showing lower canine and at 3, three of the four incisors described by Triggs (2004). At 4, another canine from piece of the white replica. This part of the replica has been enlarged to show detail. The width of the bite mark is approximately equal to the width of the tooth at arrow 2. (c.) Remnants of a destroyed replica where the smallest piece is approximately 1/10 the size of the full replica shown in A. These pieces bore tooth marks, but the pieces were too fragile and too small to cast.

Chapter 4. Phylogenetically independent evolution of color pattern variation in the Australian common froglet, *Crinia signifera*, and the implications for mimicry.

Summary

Elucidation of mechanisms that generate and maintain color pattern variation can provide insight into processes that influence genetic divergence within and among populations. In Australia, the common froglet, *Crinia signifera*, is polymorphic in ventral coloration and is hypothesized to be a mimic of sympatric *Pseudophryne*. Previous phylogenetic analyses revealed several deeply diverged cryptic lineages that, in turn, have high levels of genetic diversity within them. Therefore, the combination of diversity in color pattern and molecular markers suggest a potential role for neutral processes, such as genetic drift, as non-selective alternatives for generating color pattern polymorphism. In this study, I quantified color pattern variability in *C. signifera* in order to examine the roles of mimicry and phylogeny in maintaining phenotypic variability. I compared color pattern between *C. signifera* and sympatric populations of *Pseudophryne* to test the hypothesis of mimicry. Then, I used phylogenetic simulations to examine whether phylogenetic relationships alone can generate the observed pattern of variability in color pattern. Phylogenetic analysis revealed additional genetic diversity within lineages and identified low levels of introgression among previously identified clades and sub-clades. Significant correlation between color pattern in *C. signifera* and *Pseudophryne* was found in two whole frog measures, Number of Black Patches ($r = 0.819$, $p = 0.045$) and Total White Perimeter ($r = 0.812$, $p = 0.047$) and several measures of patch shape. Furthermore,

randomization tests indicate that sympatric *C. signifera* are more similar to *Pseudophryne* than those in allopatric populations for Proportion of White ($U' = 4.77$, $p < 0.005$) and Number of Black Patches ($U' = 5.34$, $p < 0.005$). Despite the phylogenetic variation exhibited within and among lineages, simulations of trait evolution under Brownian motion illustrated that the phylogeny alone cannot generate the pattern of variation observed in *C. signifera* color pattern. Therefore, it is unlikely that genetic drift along the phylogeny is responsible for the variability observed in *C. signifera*. Combined, these results suggest a role for mimicry in shaping among-population variability in *C. signifera* color pattern.

4.1 Introduction

A primary goal in evolutionary biology is to understand the mechanisms that generate and maintain phenotypic and genetic variation within species. Historically, color pattern polymorphisms, the occurrence of distinct color pattern variants within populations (Hoffman and Blouin 2000, Poulton 1890), were used to infer population-level processes that led to genetic variation. The popularity of these markers arose from the ease of quantification and commonly simple mechanisms of genetic inheritance of color patterns. Presently, molecular markers are used as an alternative means to infer evolutionary processes acting on populations (Hedrick 2006). These molecular estimates of variation are often left decoupled from estimates generated from color patterns. An array of mechanisms has been proposed to explain color pattern polymorphisms such as frequency-dependent selection (Allen and Weale 2005), natural selection (Pfennig *et al.*

2007), sexual selection (Maan and Cummings 2008), gene flow (Merilaita 2001) and genetic drift (Hoffman *et al.* 2006). Similarly, these mechanisms can enhance or eliminate genetic divergence within and among populations. Therefore, elucidating processes that simultaneously facilitate or limit both color pattern and genetic divergence can provide valuable insight into the process of speciation.

Natural selection through predator avoidance is often invoked as a means to generate and maintain color pattern polymorphism specifically. Often, color patterns serve as protective defenses that enhance predator avoidance either through crypsis, where prey resemble their habitat to minimize the probability of predator detection (Bond 2007), or through aposematism, where conspicuous prey maximize the probability of detection to warn predators of their toxicity (Servedio 2000, Mallet and Joron 1999). Directional selection through crypsis or aposematism should result in fewer color pattern variants, but counterintuitively, polymorphisms arise in both cryptic and aposematic species (See below).

Cryptic polymorphisms are often attributed to apostatic (frequency-dependent) selection (Allen and Weale 2005) and, less commonly, to habitat heterogeneity (Punzalan 2005, Merilaita 2001). Under apostatic selection, the presence of multiple color pattern variants hinders the ability of a predator to associate a particular variant with profitable prey (Poulton 1890). Predators readily recognize the most common variant and it suffers the highest predation rate. As a result, the frequency of this color pattern declines, and a different color pattern becomes relatively more common in a population. Thus, when apostatic selection acts on polymorphic color patterns, fluctuations occur in color pattern

variant frequencies (e.g., Olendorf *et al.* 2006). Habitat heterogeneity generates polymorphisms when cryptic color patterns vary in effectiveness within or among particular habitats. This is best illustrated by the well-studied color pattern polymorphism in *Cepaea* snails where predation is highest on the most conspicuous color pattern (*reviewed in* Jones *et al.* 1977, Cain 1973). If habitats are uniform and selection acts on the most conspicuous form, gene flow among habitat types can maintain the polymorphism, whereas in heterogeneous habitats, polymorphisms can be maintained within a single habitat because relative conspicuousness varies within the habitat (Phifer-Rixey *et al.* 2008, Bond 2007).

Aposematic polymorphisms commonly arise from protective mimicry (Mallet and Joron 1999). In protective mimicry (Pasteur 1982), species share similar color pattern in order to avoid predation (Müller 1879, Bates 1862). In Batesian mimicry, non-toxic (mimic) species share color pattern with toxic (model) species and mimics are under negative frequency-dependent selection (Brower 1960, Fisher 1927). When a mimic becomes common, predators no longer associate the shared color pattern with toxicity and the advantage of the color pattern decreases (Pfennig *et al.* 2007, Charlesworth and Charlesworth 1975). Through diversifying selection, Batesian mimics can avoid the cost of becoming common by mimicking a novel model or by no longer bearing a mimetic signal. In Müllerian mimicry (Müllerian convergence), toxic species share color patterns to reduce the cost of training a predator that a color pattern is distasteful. Positive frequency-dependent selection predicts that Müllerian co-models will converge on a single color pattern (Mallet and Joron 1999, Müller 1879), but polymorphism is common

(e.g., Symula *et al.* 2001, Brower 1996, Brown and Benson 1974). Experimental studies in *Heliconius* butterflies demonstrated higher survival rates in butterflies that match local co-model species, and found divergent selection when models are geographically variable (Kapan 2001). Simulations support the formation of polymorphic co-models under at least two scenarios, when predation is low or when gene flow is high (Sherratt 2006, Joron and Iwasa 2005). Müllerian mimetic polymorphisms have been linked to the process of speciation when assortative mating results in genetic divergence among forms (e.g., Jiggins *et al.* 2001).

The contribution of neutral processes, such as genetic drift or gene flow, to the generation and maintenance of color pattern variation is often neglected. However, neutral processes have been addressed in a few studies (Wollenberg *et al.* 2008, Hoffman *et al.* 2006, Nicholls and Austin 2005, Brisson *et al.* 2005, Storz 2002). In these studies, patterns observed in neutral genetic markers are compared to patterns of phenotypic differentiation. Neutral evolution is inferred when a correlation between genetic and phenotypic patterns is strong. In contrast, the absence of a correlation between phenotypic and genetic differentiation provides motivation to experimentally test for signatures of selection. For example, in *Drosophila polymorpha*, color pattern was independent of genetic and geographic variation, but strongly correlated to desiccation resistance. Specific tests for selection in dry habitats showed higher survival in flies with darker coloration (Brisson *et al.* 2005). In the satin bowerbird similar methods were employed to test hypotheses of advertisement call variation. Calls were independent of genetic variation, but strongly correlated to habitat differences. Thus, call differences

were attributed to selective pressures imposed in different habitats (Nicholls and Austin 2005). Unlike the former examples, in leopard frogs (*Rana pipiens*) and in the poison frog, *Dendrobates tinctorius*, evidence was found that color pattern variability did not exceed the variation expected according to neutral loci and was attributed to genetic drift (Wollenberg *et al.* 2008, Hoffman *et al.* 2006).

Most often, color pattern polymorphisms are examined in invertebrates (e.g., Hanlon *et al.* 2009, Manríquez *et al.* 2008, Phifer-Rixey *et al.* 2008, Jiggins *et al.*, 2001, Cook 1986), but color pattern polymorphisms are also common in vertebrates, especially in frogs (e.g., Wollenberg *et al.* 2008, Hoffman *et al.* 2006, Croshaw 2005, Hoffman and Blouin 2000, Summers *et al.* 1999). Cryptic dorsal color pattern polymorphisms in frogs have been attributed to drift (Hoffman *et al.* 2006) and selection (Bull 1975, Milstead *et al.* 1974, Main 1965). Aposematic color polymorphisms in frogs have most often been attributed to mimicry (Darst and Cummings 2006, Santos *et al.* 2003, Schaefer *et al.* 2002, Symula *et al.* 2001, Lamar & Wild 1995), but also to sexual selection (Maan and Cummings 2008, Summers *et al.* 1999) and genetic drift (Wollenberg *et al.* 2008).

Another example of polymorphic coloration in frogs occurs in the Australian common froglet, *C. signifera*. Like others in the genus, *C. signifera* dorsal color pattern polymorphism is attributed to crypsis (Bull 1975, Straughan and Main 1966, Main 1965), but *C. signifera* ventral coloration is a putatively aposematic warning signal. In some descriptions of *C. signifera*, a diagnostic feature is bold black-and-white ventral coloration (Cogger 2000). Unexpectedly, field observations of *C. signifera* revealed that bold black-and-white coloration varies in proportion of black among populations (Symula, *unpubl.*

data). Furthermore, some populations lack black-and-white coloration altogether (Fig. 1.1). In addition, individuals that lack the black-and-white pattern are commonly found syntopically with black-and-white individuals. Therefore, *C. signifera* apparently bears polymorphic ventral color pattern within and among populations.

The black-and-white ventral coloration found in *C. signifera* is similar to that in another sympatric myobatrachid frog genus, *Pseudophryne* (Fig. 1.2). Relative to *C. signifera*, *Pseudophryne* is rare and is limited by their breeding biology because they require terrestrial nesting sites (Mitchell 2005, Cogger 2000). Thus, even though the species are co-distributed, they are not always found syntopically. In *Pseudophryne,* all species exhibit thanatosis (play dead) in response to artificial predator attack (Williams *et al.* 2000). Further, all examined species are known to secrete alkaloid skin toxins (Smith *et al.* 2002, Daly *et al.* 1990, 1984). Combined, these features suggest that defensive behavior and ventral coloration form an aposematic display that warns potential predators of their toxicity. Similarly, *C. signifera* 'play dead' under simulated predator attack (Williams *et al.* 2000). *Crinia signifera* secretes a variety of peptides, but the role of these compounds in deterring predators is unknown (Masseli *et al.* 2004, Erspamer *et al.* 1984). Elapid snakes infrequently consume *C. signifera* (Shine 1977), despite the presence of these compounds (Erspamer *et al.* 1984). However, predators avoid black-and-white coloration of *C. signifera* in the absence of chemical compounds (Chapter 3). Thus, shared behavior and coloration is thought to be a form of defensive mimicry (Williams *et al.* 2000).

Although the presence of the black-and-white color pattern may play a role in predator avoidance, within- and among-population color pattern variation may be a

product of neutral processes, such as genetic drift. Phylogenetic analysis using mtDNA revealed several deeply diverged, phenotypically indistinguishable lineages among populations of *C. signifera* (Symula *et al.* 2008). Within lineages, genetic divergence was also unexpectedly high. Thus, high levels of genetic divergence and color pattern variation may indicate an association between color pattern variation and phylogenetic relationships within and among populations.

In this study, I used ventral color pattern variation to examine the putative mimicry of *Pseudophryne* and investigate the potential role of genetic drift in generating phenotypic variation in *C. signifera*. Specifically, I collected, measured and quantified *C. signifera* color pattern variation. Then, from sites where *C. signifera* was observed to share the putative mimetic color patterns, I collected and measured color patterns from *Pseudophryne*, and tested for a correlation in color pattern between the species and for whether sympatric *C. signifera* populations were more similar to *Pseudophyrne* than allopatric populations. Next, using randomization tests, I tested for a relationship between *C. signifera* color pattern and phylogeny. Finally, to test whether genetic drift could generate the observed color pattern polymorphism, I compared the observed dataset to datasets generated by phylogenetic simulations under neutral models of trait evolution.

4.2 Methods

Sample collection

Crinia signifera samples were collected between March and August 2004 and between May and August 2007. Frogs were located using advertisement calls to ensure

correct species identification. From each site, between three and ten *C. signifera* were captured by hand, photographed and toe-clipped. When present, two to ten *Pseudophryne* individuals were collected at each site. For both species, individuals not retained as voucher specimens were released at the site of capture. A complete list of all sampled localities, GPS coordinates, specimen identification numbers and total number of individuals collected per site are listed in Table 4.1 (*C. signifera*) and Table 4.2 (*Pseudophryne*). Geographic distribution of sampling sites is illustrated in Fig. 4.1.

Specimen preparation and tissue collection

After all frogs at a site had been photographed (see below), tissues were harvested from each individual. Toes were clipped from all *C. signifera*. At all sites, three individual *C. signifera* and no more than two *Pseudophryne* were euthanized and fixed in formalin as voucher specimens. Livers were removed from vouchers before formalin fixation. In order to prevent disruption of ventral color pattern on vouchers, livers were extracted through incisions made along the side of the frog. All tissues were stored in 95% ethanol. Both tissues and voucher specimens of *C. signifera* were deposited in museums from the state or territory where they were collected (Table 2, 5). *Pseudophryne* tissues were deposited in the Australian Biological Tissue Collection at the South Australian Museum and vouchers were deposited in the museums from the state or territory where they were collected (Table 4.2).

DNA sequencing and alignment

To examine relationships among sites and samples of *C. signifera*, a truncated region of the 12S and 16S mtDNA gene was amplified and sequenced for phylogenetic analysis following methods used in Symula et al. (2008). The mtDNA gene region was chosen for by examining a subset of samples. First, up to two individuals from each site (Fig. 4.1) were sequenced for the entire 12S/16S gene. Phylogenetic analysis using GARLI 0.951 (www.bio.utexas.edu/grad/zwickl/web/garli.html) was performed on this new dataset to assess relationships among newly added sample sites and those in Symula *et al.* (2008). Second, the DNA sequence alignment was split into four truncated datasets. Each dataset included sequence data that spanned the region between one of each of the four overlapping primer pairs (mvz59-12Sb, 12L1-16Sh, 12Sm-16Sa, 16Sc-16Sd; Table 2.1). Third, each of the four truncated datasets were used to reconstruct phylogenies using maximum likelihood in GARLI 0.951 and maximum parsimony with 100 bootstraps in PAUP* 4.0b10 (Swofford 2003). Topologies and retention indices were compared among the four datasets. The approximately 800 base pair fragment that amplified between the 12Sm and 16Sa primers recovered the topology most similar to that found in Symula *et al.* (2008) and had the second highest retention index of 0.896. The 16Sc-16Sd dataset had the highest retention index, 0.905, but did not recover monophyly of the three major clades identified in Symula *et al.* (2008). Therefore, the region between the 12Sm and 16Sa primers was used to examine relationships among all samples and sites.

Individuals from Table 4.1 were used for DNA sequencing. Total genomic DNA

was extracted from toe clips or liver samples using Viogene Blood and Tissue Genomic DNA Extraction Miniprep System (Viogene, Inc., Taipei, Taiwan). All polymerase chain reactions (PCR) were performed using the Failsafe PCR 2X PreMixes Buffer F (Epicentre Biotechnologies, Madison, WI) and the following cycle: Initial denaturation 94 ºC for 2 min, 30-35 cycles of 94 ºC for 30 s, 46-55 ºC for 30 s, and 72 ºC for 60 s and a final extension at 72 ºC for 7 min. Primers used for PCR reactions include those listed in Table 2 that amplify positions between 12Sm and 16Sa. PCR products were purified from 0.8% agarose using Viogene Gel-M Gel Extraction System (Viogene Inc., Taipei, Taiwan). Approximately 40ng of purified PCR products were sequenced at the University of Texas at Austin Institute for Cellular and Molecular Biology DNA Sequencing Core Facility using an ABI Prism 3730 DNA Analyzer (Applied Biosystems).

Consensus sequences were generated and edited using Sequencher v4.6 (Gene Codes Corp., Ann Arbor MI). Sequences were aligned manually in MacClade v4.06 (Maddison and Maddison 2004) using previously aligned 12S and 16S *C. signifera* sequences as references (Symula *et al.* 2008). Single base changes were verified by examining if each peak in the chromatogram was assigned the correct base.

Phylogenetic analysis

Phylogenetic analyses were performed using individuals listed in Table 4.1. Individuals from Read *et al.* (2001) were excluded from all phylogenetic analyses because they did not contain overlapping base pairs with the fragment used in this study. Previously obtained sequences of *C. riparia* (n=4) were used as outgroups based on Read *et*

al. (2001) and Symula *et al.* (2008).

Samples from Symula *et al.* (2008) were trimmed to exclude any characters not present in the new sequences to avoid potential issues with missing data. Ambiguous regions of sequences were excluded from phylogenetic analysis. The beginning and end of some sequences were excluded to minimize regions with missing data. Sites for which an individual sequence or a few sequences had a single base insertion were also excluded.

Evolutionary relationships among localities of *C. signifera* were inferred using Maximum Likelihood (ML) and Bayesian inference. The most appropriate model of sequence evolution was determined using the Bayesian Information Criterion in MODELTEST (Posada and Crandall 1998). ML analyses were performed using GARLI 0.951. All redundant sequences were removed from ML analyses. When using a random starting tree, initial searches repeatedly converged on a topology where major clades identified in Symula *et al.* (2008) were non-monophyletic. To address this, 100 independent runs were performed with the Neighbor-Joining (NJ) tree as the starting tree. In all 100 runs, major clades were monophyletic and all trees had significantly higher likelihoods than runs performed with a random starting tree. Therefore, final analyses were performed with the pre-defined NJ starting tree.

Bayesian analyses were performed using MRBAYES 3.1.2 (Ronquist and Huelsenbeck 2003). Two separate replicates were performed on a NPACI Rocks cluster using four Markov chains per replicate and the temperature parameter set at 0.2. Chains were sampled every 1000 generations for 50 million generations. Plots of model parameters and likelihood scores versus generations were examined to determine whether

the set of post burn-in trees had converged on the same region of tree space in TRACER 1.4 (beast.bio.ed.ac.uk). For these runs, burn-in was set as 24,661,000 generations leaving 2,000 trees in the posterior distribution.

Digital Photography

At each site, the dorsal and ventral surfaces of each individual were photographed with an Olympus C-3020 Optical zoom 3.2 Megapixel digital camera (Olympus America, Inc. Center Valley, PA). For each photo, frogs were placed in a small plastic container with a 2.5 cm square 18% gray card (Delta 1, Dallas, TX) used to calibrate internal camera light meters. Though gray cards can be used to optimize color printing, they cannot be used to standardized color within an image because the absolute neutral gray is not reproduced in digital photographs (Stevens *et al.* 2007). Instead, they are used here to optimize contrast of white and black on the ventral surface. All images were taken with the built-in flash to ensure that lighting conditions were identical among individuals and sites. Images were composed such that the height of each image was the same as the gray card length and were stored as both .JPG and .TIF digital files.

Image standardization

All image manipulation was performed in the Image Processing Toolbox in MatLab v7.1 (The Mathworks, Inc., Natick, MA). Color images were first converted to grayscale based on the gray card in each image. Images were then rotated so that the edge of the gray card was perpendicular to the image edge. Gray card length, in pixels,

was obtained using the "imtool" function. The image was rotated a second time so that forelimb insertions of the frog were parallel to the top of the image. Then, the gray card and background were cropped out of the image. Due to characteristics of frog skin, flash reflection generates areas with saturated pixels scattered across an image. Saturated pixels were removed from the image by implementing two different MatLab functions, "imextendedmax" and "roifill". The first (imextendedmax) identifies saturated regions by finding pixels that have high values compared to neighboring pixels. The second (roifill) fills saturated regions according to values of neighboring pixels. Neighbors used to fill saturated regions are found at a user-specified distance from the center of the saturated area. In the first function, detection of saturated areas depends upon whether the pixel is next to white or black pixels. For example, when flash reflection occurs among a group of white pixels, the difference between saturated areas and neighboring pixels is much less than when saturated areas are among darker pixels. Necessarily, values used to identify flash saturation were set separately for each image. In some instances, small regions of flash reflection were removed manually from the binary image because automated commands filled in naturally occurring white patches in grayscale images.

Color pattern in *C. signifera* and *Pseudophryne* covers the belly, hind limbs, forelimbs and, on females, the throat (Fig. 1.1, 1.2). Though all members of *C. signifera* and *Pseudophryne* play dead, individuals often vary in limb position or posture and therefore, the areas of black-and-white coloration that are displayed. In addition, vocal sacs on the throats of male frogs tend to be solid black whereas females have lighter throat colors. To ensure images were comparable among individuals, the following steps were taken to

eliminate differences. All limbs were manually trimmed from the image at the point of limb insertion, leaving behind only the image of the head and torso. *Crinia signifera*, regardless of pattern or color, bear two small, raised white spots at the base of the throat at forelimb insertions (Fig. 3.2). These mark the end of male-limited vocal sacs, so the throat region anterior to arm insertion spots was cropped out of the image. Then, all images were rotated so that these spots were parallel to the top edge of the image. *Pseudophryne* lack comparable spots, so to make images directly comparable to *C. signifera* all *Pseudophryne* were cropped at the top of the forelimb insertion and rotated so that the top of the cropped image was horizontal.

Pattern measurement

Measurements of ventral patterns were taken only if the images met the following conditions. All images contained a complete gray card standard and the entire frog. In all measured images, no part of the belly was obscured by limbs, toes, debris, posture or folded skin. Images were discarded if male frogs had vocal sacs inflated, if individuals had apparent internal parasites that distorted the shape or area of the ventral surface, or if flash saturation could not be adequately removed.

Grayscale, cropped images were converted to binary images to facilitate measurement of pattern characteristics. Conversion of a grayscale image renders white and lighter grays to white in the binary image, so this analysis does not allow identification of subtle differences between white and gray. White pixels of binary images are scored with a value of one and black pixels are scored with a value of zero. All white

measures were based on pixels with a value of one in the original binary image. To measure black pattern characteristics, the binary image was inverted so that all black areas were scored with a value of one.

Ventral surfaces of *C. signifera* or *Pseudophryne* are either solid in color or are comprised of black patches and white patches (Fig. 1.1, 1.2). Two categories of measurements were collected from each frog (Table 4.3). First, nine measurements that describe characteristics of the whole-frog ventral pattern were calculated (e.g., Proportion of White). Second, 20 measurements were taken to describe the shape and size of individual patches on each frog (e.g., White Patch Area). To avoid arbitrary identification of patches, MatLab algorithms that identify patches based on connectivity between white pixels in the binary image delimited each patch ("bwlabel"). Then, measurements were taken on each identified patch using the "region properties" function. Measurements for all patches with an area smaller than 10 pixels were discarded. Where appropriate, the length of the gray card (2.5 cm) was used to convert all measures from pixels to length or area. Then, individual patch measures were summarized for each frog by taking the mean of each measure. These means were used along with whole-frog measures in subsequent analyses. All measures are listed and described in Table 4.3 and MatLab Image Analysis Toolbox commands are provided following each description. Elaboration on how patches are defined and how each measure is calculated is describe in the Image Processing Toolbox documentation (The MathWorks, Natick, MA).

Statistical analyses of pattern measures

To identify pattern characteristics that contribute to the observed variation among individuals and sites, pattern measures were examined using Principal Components Analysis (PCA) in SPSS v16.0.2 (SPSS, Inc. 2007 Chicago, IL). All factors with eigenvalues greater than one were extracted, and the slope of the scree plot was examined to determine the number of factors that contribute significant variance. The initial solution was rotated to identify simple structure using Varimax and Oblimin rotations. Oblimin rotation revealed no correlation between factors, so the Varimax solution was used in subsequent analyses (Tabachnick and Fidell 2007). Rotated factor scores were calculated for each individual using the correlation matrix so that variance was appropriately scaled.

Mimicry between C. signifera *and* Pseudophryne

Pseudophryne color patterns were collected from five sites where *C. signifera* were observed to bear black-and-white patterns. In the geographic region where *Pseudophryne* were compared, there are two putative sympatric species, *P. bibronii* and *P. dendyi* that are distinguished by the length of the hind limb (Robinson 2002, Cogger 2000, Barker *et al.* 1995). Both species were collected for this study, but were not explicitly considered when measuring patterns. No published phylogeny for *Pseudophryne* exists, however preliminary phylogenetic analysis suggests that east coast Australia *Pseudophryne* are composed of multiple cryptic species that are not geographically limited (T. Bertozzi, S. Donnellan *pers. comm.*). Thus, the measures presented here are likely composite measures for at least two

Pseudophryne species.

The hypothesis of mimicry predicts that model and mimic share similar color patterns. Strong comparative evidence for mimicry is found when populations of a single species resemble different sympatric models. *Crinia signifera* is sympatric with several species of *Pseudophryne* that bear different color patterns. Therefore, under the hypothesis of mimicry, color pattern differences in *C. signifera* should be correlated to differences in *Pseudophryne*. To test this hypothesis, means of each of the 29 measures were calculated at each of five sympatric sites for both *C. signifera* and *Pseudophryne*. Table 4.1 (*C. signifera*) and Table 4.2 (*Pseudophryne*) indicate the number of individuals measured at each of the five sites. Bivariate correlations were performed between each color pattern measure in SPSS. The Bonferroni correction was applied to calculate experiment-wise alpha associated with performing multiple tests (Zar 1999).

The hypothesis of mimicry also predicts that *C. signifera* should be more similar to *Pseudophryne* when they occur in sympatry. To test whether the difference between color pattern in *C. signifera* and *Pseudophyrne* is significantly less in sympatry than in allopatry, a randomization test was performed. The color pattern in both species is made up of black and white features, so one measure of black and one measure of white were examined. PCA factor scores were not used because the composition of these factors differed between *C. signifera* and *Pseudophryne*. Instead, two raw measures, Proportion of White and Number of Black Patches, were used because the interpretation of aspects of color pattern quantified by these measures is straightforward. Furthermore, Proportion of White did not load on any of the rotated factors and Number of Black Patches represented a

measure that was significant in bivariate correlations. Means were calculated for each of 48 *C. signifera* sites (Fig. 4.1, Table 4.1) and each of five *Pseudophryne* sites (Fig. 4.1, Table 4.2) for both measures. For both traits, 1000 pairs of *C. signifera* sites were paired randomly with the five *Pseudophryne* sites. Pairs were designated as either sympatric (collected from the same site) or allopatric. For each pair, the absolute difference between means of the two species was calculated. Then, differences between all pairs were ranked from low to high, and a one-tailed Mann-Whitney test was performed to test whether the differences in sympatric means was significantly lower than allopatric means (Zar 1999).

Phylogenetic correction for non-independence of data points was not performed for two reasons. First, the majority of sampled sites are taken from clade B and individuals from these sites are not more closely related to sympatric individuals. Second, tests for phylogenetic signal (below) indicate very low contribution of the phylogeny to the color pattern.

Phylogenetic signal in C. signifera *color pattern measures*

Phylogenetic analyses of mtDNA uncovered multiple cryptic lineages in *C. signifera* and high genetic variation within and among sites (Symula *et al.* 2008). Therefore, it is possible that color pattern variation is influenced by phylogenetic relationships among sampling sites. To test whether closely related individuals resemble one another, detection of phylogenetic signal was performed using randomization tests in the MatLab-based PHYSIG_LL (Blomberg *et al.* 2003). The PHYSIG program randomly permutes tip data and, for each permutation, calculates the mean squared error (MSE) using

Generalized Least Squares (GLS). When there is strong phylogenetic signal, the variance (MSE) among relatives is low, and randomly permuted tip data should generate higher variance than the observed data. When 95% of randomly permuted datasets show greater variance than the observed data, then the null hypothesis of no phylogenetic signal can be rejected (Blomberg *et al.* 2003).

Before the tests of phylogenetic signal were performed, the best GARLI tree was edited such that missing data was removed. *Crinia riparia*, the sister group to *C. signifera*, was pruned from the tree using the PDTREE module of PDAP v 6.0 (Garland *et al.* 1993). Tips of *C. signifera* individuals that lacked color pattern data were pruned using PAUP* 4.0b10 (Table 4.1). Overall tree length was scaled by a factor of two in the PDTREE module of the DOS version of PDAP to facilitate calculations of MSE. Then, the tree was converted to phylogenetic covariance matrix in the PDDIST module of PDAP (Garland *et al.* 1993). For each measure, multiple individuals were represented as the mean of all individuals with identical DNA sequences.

Two of the original measures (Proportion of White and Number of White Patches) and the first three rotated factor scores obtained from PCA of color pattern measures were used to perform tests of phylogenetic signal. The raw measures were chosen because they were not correlated with any of the Principal Components factors and because these measures quantify visually interpretable aspects of color pattern. For each measure, 1000 permutations were performed on the scaled tree with no branch length transformations in PHYSIG_LL. The following statistics were calculated: a descriptive statistic, K, that compares the observed pattern of tip data using the best ML tree to the

expected pattern under strict Brownian Motion on the same phylogeny; the likelihood scores of the trait evolving along the best ML tree and along a star phylogeny; the p-value for the randomization test.

Phylogenetic simulations

To test whether color pattern polymorphism in *C. signifera* could be attributed to genetic drift, phylogenetic simulations using the Brownian motion (BM) model of trait evolution were performed as implemented in the PDSIMUL module of PDAP (Garland *et al.* 1993, Martins and Garland 1991). BM models are reasonable approximations for trait evolution due to genetic drift (Felsenstein 1985). Specifically, these simulations aim to test whether the combination of tree topology and branch lengths of the best ML tree could have generated the observed pattern of variance in color pattern found within and among populations of *C. signifera*. Each simulation was performed with two traits and the correlation between the two traits set to zero. Two combinations of traits were used. The first used the raw measures Proportion of White and Number of White Patches and the second used the first two PCA factors (Black Patch Size and Shape and White Patch Size and Shape).

Two classes of simulations were performed. The PDSIMUL module specifies two classes of BM, gradual and speciational. In gradual BM (BMg), change is proportional to the branch lengths of the tree whereas in speciational BM (BMs), change is proportional to branching (speciation) events. In both classes of BM, the probability of change is drawn from a bivariate normal distribution with mean of zero and variance of one

(Felsenstein 1988). For both BMg and BMs simulations, the final means parameter was set to the observed mean and variance of the tip data. Setting the final means parameter results in stochastically constant rates of trait change in BMg, but changing rates of trait evolution determined by the number of speciation events in BMs (Garland *et al.* 1993). Both classes of BM models were run under unbounded and bounded conditions. Unbounded simulations were performed first and examined to assess whether simulated trait values exceeded biologically realistic values. In all cases, simulated trait values exceeded realistic values in unbounded simulations, so bounds were set as the observed minimum and maximum of each trait using the "soft-bounce" algorithm. When simulated traits reach a specified bound, the simulated value is reflected away from the boundary approximately the same amount that it would have exceeded the boundary. For all simulations, 1000 new color pattern datasets were generated and a null distribution for each trait for each class or model of evolution was calculated in SPSS. Then, to test whether the phylogeny explained the pattern of variance, the simulated and observed datasets were compared.

To test whether the pattern of variance in the color pattern data is explained by the pattern of variance in the phylogeny, the MSE_0/MSE ratio was used as a test statistic. This statistic is calculated as the ratio of the mean squared error of the trait values (MSE_0) to the phylogenetic variance-covariance matrix (MSE). MSE_0 measures the mean squared error of the data using the phylogenetically corrected mean (ancestral trait value). When the phylogeny explains the pattern of variance in the observed data, then MSE_0/MSE values are large, and closely related individuals resemble one another more

than distant relatives (Blomberg *et al.* 2003). Therefore, if the observed MSE_0/MSE is less than 95% of the simulated datasets then the null hypothesis can be rejected indicating that the observed data has more variability among close relatives than expected under the model of genetic drift.

4.3 Results

Sample collection

A total of 443 *Crinia signifera* samples were collected from 27 sites in 2004 and 22 sites in 2007 (Table 4.1, Fig. 4.1). For *Pseudophryne*, 24 individuals were collected from five localities. A complete list of localities, GPS coordinates, specimen identification numbers and total number of individuals collected per site are listed in Table 4.1 (*C. signifera*) and Table 4.2 (*Pseudophryne*) and localities are illustrated in Fig. 4.1.

DNA sequencing and alignment

The final mtDNA dataset comprised 852 base pairs of sequence data from 374 *C. signifera* individuals (Table 4.1). In total, 57 redundant haplotypes were identified (n=174), and only eight of these were shared by more than four individuals. The high degree of redundancy relative to Symula *et al.* (2008) is likely a combination of the increased sampling density at each site and the shortening of overall sequence length. For example, seven sequences (accounting for 3 redundant haplotypes) that were unique in Symula *et al.* (2008) were identical in the new dataset. In all but 16 haplotypes, individuals that share haplotypes were from the same sampling locality. In 15 of the 16,

all redundant haplotypes are from geographically neighboring site localities. In one instance, an individual from the region encompassed by the mainland Victorian clade C3 was identical to sequences from the Tasmanian clade C5. The most common haplotype (n=18) was shared among four geographically proximate sampling sites (Fig.10: Kalaru (Site 50), Eden (Site 19), Boydtown (Site 51), Mallacoota (Site 53)) from clade B2. Thus, the short fragment only slightly underestimates variability in this mtDNA locus among individuals in *C. signifera*.

Phylogenetic analysis

MODELTEST chose the general time reversible (GTR+I+Γ) model of sequence evolution and the parameters estimated for this model are shown below. The best of 100 ML trees found by GARLI had a -ln likelihood score of 5558.435728 (Fig. 4.2). Base frequencies were estimated as A = 0.365 C = 0.285 G = 0.147 T = 0.203; rate matrix: A-C = 1.977, A-G = 13.951 A-T = 1.301 C-G = 0.869 C-T = 13.234 G-T = 1.000; gamma shape parameter (Γ): 0.557; proportion of invariant sites (I): 0.537. Bayesian analysis recovered a consensus topology identical to the best ML tree. Thus, the best of 100 GARLI trees is illustrated in Fig. 4.2 with Bayesian posterior probabilities shown for nodal support. For tips that represented multiple haplotypes, all individuals that shared the same mtDNA sequence are listed at that tip. Clade and sub-clade labels are retained from Symula *et al.* (2008) for consistency.

Both ML and Bayesian analyses identified *C. signifera* as a well-supported monophyletic group (bpp = 1.00) that comprised three geographically restricted clades

(A-bpp = 1.00; B-bpp = 1.00; C-bpp = 1.00; Fig. 4.2). However, relationships among A, B and C are not strongly supported (bpp = 0.84). These results are consistent with the phylogeny recovered in Symula *et al.* (2008; Fig. 2.2). Adding additional sites extended the range of clade A to include samples to the south and west of the Great Dividing Range (see Fig. 2.1) and extended the range of clade C to the east (Fig. 4.2a, b). Additional sites and increased sampling density uncovered evidence of introgression among the major clades and some sub-clades. Between clades A and B, haplotypes from Mallacoota (Site 53) were found in both clades A and B1 (Fig. 4.2b, c, d). Between clades A and C, haplotypes from Drouin (Site 58) were found in clades A and C3 (Fig. 4.1, 10b, c, e).

The shorter mtDNA 16S sequence revealed most of the same sub-clades as Symula *et al.* (2008). Sub-clade B1 (bpp = 0.95) was composed of samples from Coffs Harbour (Site 4) and Evans Head (Site 1, Fig. 4.2b, d). Sub-clade B2 was not recovered as a monophyletic group, but all newly collected samples from New South Wales belong to clade B. Non-monophyly of sub-clade B2 was anticipated from preliminary, primer-based analyses and was attributed to the use of fewer informative characters. Some samples from Mallacoota, Victoria (Site 53; Fig. 4.1, 4.2b, c, d) are found within clade B. Within clade C, all of the sub-clades found in Symula *et al.* (2008) were recovered with strong support except for sub-clade C2 (Fig. 4.2a) as was anticipated based on the primer-based analyses. Most Victoria sites collected in 2007 fall within sub-clade C3. Sub-clade C3 is the sister clade to C4 (bpp = 0.99; Fig. 4.2a, e), but relationships among other sub-clades are not supported. Samples on the western side of the Great Dividing Range from

Mansfield, Victoria (Site 57, Fig. 4.2b, f) formed a new sub-clade C6 (bpp = 0.99) along with two individuals from Seymour, Victoria (Site 25, Fig. 4.2b, f). Unlike Symula *et al.* 2008, sub-clades also had evidence of introgression among sites. Individuals from Hamilton (Site 29, Fig. 4.1) and Portland, Victoria (Site 30, Fig. 4.1) were found in sub-clades C1 and C3 (Fig. 4.2). One individual from Warnambool, Victoria (Site 66) had the same haplotype as several individuals from Sheffield, Tasmania (Site 47, Fig. 4.2b, f). Individuals from Seymour (Site 25) are found in sub-clade C3 and C6. Clade membership of localities was otherwise identical to those identified in Symula *et al.* (2008).

Pattern measurement and Principal Components Analysis

Of the 443 *C. signifera*, 351 individuals were measured for pattern characteristics (Table 4.1). PCA of all 29 measures identified eight components with eigenvalues greater than one that explained 83.76% of the variance in the *C. signifera* dataset (Table 4.4, 4.5). Based on the slope of the scree plot, only three of eight factors were shown to contribute significant variance (59.14%). Each of the first three factors was composed of three or more variables with factor loadings above 0.7 (Table 4.5). In addition, the remainder of the factors comprised two or fewer measures suggesting that those contribute more to the dataset when considered alone (Table 4.5; Tabachnick and Fidell 2007). Following rotation in PCA, only three of the whole frog measures were not correlated with any other measure, Proportion of White, Total Black Area and White Patch Eccentricity. The measures Proportion of White and Number of White Patches were strongly correlated to other elements of the first principal component, but this correlation was

removed following rotation. These two measures represent color pattern features that are easy to interpret (Fig. 4.3). Thus, these two raw measures and the first three PC factors are considered in subsequent analyses.

For *Pseudophryne,* 26 individuals from five sites were analyzed (Table 4.2). Only six components with eigenvalues greater than one were extracted with PCA. These six components explained 91.33% of the variance in *Pseudophryne*. Based on the slope of the scree plot, three of the six components contributed significant variance. Variables that were correlated with each factor are listed in Table 4.5. Total White Perimeter, Proportion of White, White Euler Number and White Patch Squareness were not correlated with any of the rotated factors.

The majority of measures correlated with Factors 1-3 were the same in *C. signifera* and *Pseudophryne* and differences in composition are shown in Table 4.5. However, in Factors 4-6, only two measures are correlated to the same factors in *C. signifera* and *Pseudophryne*. In both *C. signifera* and *Pseudophryne*, Factor 1 comprised measures that describe the size and shape of black patches and the amount of contrasting edge on the ventral surfaces. Factor 2 was comprised of measures that describe size and shape of white patches. For Factor 3, strongly correlated measures describe patchiness of the patterns. Therefore, the following variables will be considered in discussion of the continuous variation in color patterns of both *C. signifera* and *Pseudophryne*: Proportion of White, Number of White Patches, Black Patch Size and Shape (Factor 1), White Patch Size and Shape (Factor 2) and Overall Patchiness (Factor 3).

Pattern description-Pattern characteristics that distinguish differences within *C.*

signifera and *Pseudophryne* color pattern are Proportion of White, Number of White Patches, and the first three factors from PCA; Black Patch Size and Shape (Factor 1) and White Patch Size and Shape (Factor 2), the Overall Patchiness (Factor 3). In order to represent the entire spectrum of apparent differences measured in color pattern, a subset of color patterns from *C. signifera* is illustrated in relationship to the two raw measures in Fig. 4.3, and the same subset of individuals is shown in relationship to each of the factors in Fig. 4.4. *Pseudophryne* measures are similar to those represented by BS012, BS015 and BS066.

Quantification of Proportion of White and Number of White Patches distinguishes overall differences in color pattern (Fig. 4.3a). High Proportion of White (> 0.06) values described individuals with few black patches (e.g., BS180) and included individuals that have solid white or gray venters (e.g., BS432), whereas low Proportion of White (< 0.02) described individuals with primarily black venters (e.g., BS012). Similarly, high Number of White Patches (> 40; Fig. 4.3b) described individuals with many small to medium sized patches, often with large black area (e.g., BS163). Low Number of White Patches described individuals that have few large white patches (< 20; e.g., BS180).

In contrast, PCA Factors distinguish fine-scale differences in overall patch measures, but only when considered simultaneously (Fig. 4.4). Black Patch Size and Shape scores greater than one represented individuals with a bold black-and-white pattern with overall large black patch area and either few large white patches or many small white patches (e.g., BS066, BS163). Intermediate and low Black Patch Size and Shape scores (e.g., < 1) made up approximately 85% of the dataset and represented a range of patterns (e.g., BS199, BS237, BS546). Many individuals with a large amount of

white area had low Black Patch Size and Shape scores below zero (e.g., BS143, BS199). Counterintuitively, other individuals with low to intermediate scores had large black patch area with either many white patches or instead, white patches with extensive perimeter (e.g., Fig 4.5a: BS012, BS237). The contribution of the Contrasting Edges measure to this factor apparently confounded the effect of Average Black Patch Area. Contrasting Edges is a ratio between the average black patch perimeter and average white patch perimeter (Table 4.3, 4.5). Individuals with large black patch area still had small Black Patch Size and Shape values because few white patches with extensive perimeter forced the ratio to become very small. Thus, low scores did not allow discrimination among more than 85% of the patterns in the dataset. High White Patch Size and Shape scores (> 1) described individuals with large white patches and low values (< 1) described individuals with large black patches (e.g., Fig 4.5b; BS180, BS438). High Overall Patchiness scores (> 1) described white individuals with several black patches (e.g., Fig 4.5c: BS438), whereas low Overall Patchiness (< 1) scores represented individuals that had black patterns with many white patches (e.g., Fig 4.5c: BS163).

When factors are considered simultaneously, three color pattern trends emerge. First, individuals with overall large black area had high Black Patch Size and Shape and Overall Patchiness scores, but low to medium White Patch Size and Shape scores (BS012). Second, individuals with large white area and few small black patches had low Black Patch Size and Shape and Overall Patchiness scores, but high White Patch Size and Shape scores (e.g., BS143). Third, when individuals had many medium or large black patches, Black Patch Size and Shape scores were low, but White Patch Size and

Shape and Overall Patchiness were high (e.g., BS180, BS438).

Within-site and regional variation-Although the aim of this study was not to quantify site-related differences among patterns, general trends are apparent based on standard box plots of within-site variation (Interquartile range; Fig. 4.5, 4.6). In *C. signifera*, within-site variation differed among the raw measures, factors and sites (Fig. 4.5, 4.6). For Proportion of White (Fig. 4.5a), the median varied among sites, and within-site variance was large. Sites with very low interquartile ranges are comprised of fewer than four individuals and variance at those sites is likely underestimated. Regionally, medians were lower in populations from eastern New South Wales and eastern Victoria and higher in Victoria, Tasmania and South Australia sites. For Number of White Patches (Fig. 4.5b), medians were more similar among sites. A few sites (e.g., Bunyip (Site 60), Warnambool (Site 66)) have very high numbers of white patches. Individuals from these sites have many small white flecks and therefore had higher medians (e.g., BS546, Fig. 4.3b). Within-site variation differed among sites, but neither within-site variation nor the medians appeared to differ regionally. For Black Patch Size and Shape (Fig. 4.6a), medians varied among some sites, and within-site variation was markedly higher in some sites. Regionally, high medians and large interquartile ranges were found in eastern New South Wales sites. For White Patch Size and Shape (Fig. 4.6b), medians were similar among most sites, though a few sites had slightly higher medians. Within-site variation was high only in sites that had small interquartile range in Black Patch Size and Shape. Regionally, highest variation in White Patch Size and Shape was found in populations in central Victoria and Tasmania. For Overall Patchiness (Fig. 4.6c), medians vary among

most sites. Within-site variation also varied substantially among sites. Regionally, eastern New South Wales and some sites located west of the Great Dividing Range had the highest medians. In addition, there are some differences in interquartile range among central Victoria and South Australia sites.

In *Pseudophryne*, overall variance was less than in *C. signifera* for Proportion of White ($\sigma^2_{C.\ signifera}$=0.06, $\sigma^2_{Pseudophryne}$= 0.003; Fig. 4.7), and, following the removal of a single individual (see below), for Number of White Patches ($\sigma^2_{C.\ signifera}$=289.44, $\sigma^2_{Pseudophryne}$= 258.48). In Ulladulla, New South Wales (Site 15; Fig. 4.8), the large variance (interquartile range) among individuals is likely due to a single individual with several small white patches. Much of the overall low variance observed in the *Pseudophryne* dataset may be due to the overall low number of samples and sites used in the dataset (Table 4.2). However, samples were approximately the same size in two sites, Cann River, Victoria (Site 21) and Kalaru, New South Wales (Site 50). When variance is compared between the species at these sites, *C. signifera* has higher variance in Number of White Patches (Cann River: $\sigma^2_{C.\ signifera}$=228.19, $\sigma^2_{Pseudophryne}$= 38.67, Kalaru: $\sigma^2_{C.\ signifera}$=532.95, $\sigma^2_{Pseudophryne}$= 167.90) and in Proportion of White (Cann River: $\sigma^2_{C.\ signifera}$=0.04, $\sigma^2_{Pseudophryne}$= 0.003, Kalaru: $\sigma^2_{C.\ signifera}$=0.04, $\sigma^2_{Pseudophryne}$= 0.001). This suggests that the difference in variance between the species is not only due to sample size. Within-sites, variance in *Pseudophryne* was low on Proportion of White and on all factors. A single difference in medians was apparent among sites (Fig. 4.8). In Cann River, Victoria (Site 21) the median for Number of White Patches and White Patch Size and Shape was higher than in other sites. For Black Patch Size and Shape and Overall Patchiness,

medians and within-site variance (interquartile range) did not differ among sites (Fig. 4.9).

Outliers identified in the box plots (Fig. 4.5, 4.6) represent extremes of color pattern or anomalies in factor composition where the measures summarized by a factor conflict strongly with one another. For example, BS163 (Fig. 4.4) represents an extreme value and has an exceptionally high score for Black Patch Size and Shape (Factor 1) because, on average, it has many small white patches that have small perimeter. Most black mottled individuals lack these additional white blotches. The ratio of contrasting edges is strongly influenced by the overall perimeter of white patches. As a result, both the average black patch area and contrasting edges are high for BS163.

Mimicry between C. signifera *and* Pseudophryne

Pearson correlation coefficients and significance of bivariate correlations between each the color pattern measures and first three PCA factors are shown in Table 4.6. In total, seven of the 29 measures were significant (Number of Black Patches: $r = 0.819$, $p = 0.045$, Total White Perimeter: $r = 0.812$, $p = 0.047$, White Equivalent Diameter: $r = 0.980$, $p = 0.002$, Black Fill Area: $r = 0.980$, $p = 0.002$, White Fill Area: $r = 0.983$, $p = 0.013$, White Major Axis: $r = 0.983$, $p = 0.001$, White Patch Area: $r = 0.980$, $p = 0.002$). After correcting for multiple tests ($p \leq 0.0016$), only a single measure (White Patch Major Axis) remained statistically significant ($p = 0.0013$) suggesting that the overall phenotype is not correlated between *C. signifera* and *Pseudophryne* populations.

Randomization tests revealed that differences between means of *C. signifera* and *Pseudophryne* were significantly smaller than allopatric populations for Proportion of White

(U'=4.77, p< 0.005) and Number of Black Patches (U'= 5.34, p< 0.005).

Phylogenetic signal in C. signifera *color pattern measures*

Table 4.7 summarizes the results of PHYSIG_LL analyses. The different color pattern measures exhibit differing levels of phylogenetic signal. For both raw measures and all three factors, K values were much smaller than one indicating that closely related individuals resemble each other less than expected if the traits evolved under Brownian Motion (BM) on the same phylogeny. Of all tested measures, Proportion of White exhibited the highest phylogenetic signal (K = 0.00025) and the randomization test demonstrated that the distribution of tip values is significantly different from random (p = 0.007). White patch number is nearly significant and had a slightly smaller K value than Proportion of White (K = 0.00021, p = 0.064). However, none of the factors had statistically significant phylogenetic signal, even though Black Patch Size and Shape had higher K than Number of White Patches. For all factors, the log likelihood (lnL) of a star phylogeny was much greater (less negative) indicating that the star phylogeny fits the data better than the observed phylogeny. This result is comparable to MSE_{Star} values being smaller than MSE_{Tree} (Blomberg *et al.* 2003).

Phylogenetic simulations

The aim of the simulations performed in this study was to test whether the observed variation in color pattern could be attributed to the process of random genetic drift along the phylogeny. A strong correlation between a trait and the phylogenetic

relationships are identified by high values of the ratio MSE_0/MSE ($p < 0.001$). Simulation results are summarized in Table 4.8. Gradual and speciational simulations differed in how well the phylogeny explained the pattern of trait variance. First, simulated datasets generated under the BMg model (bounded and unbounded) always had significantly higher MSE_0/MSE and therefore the phylogeny explained simulated trait variance better than the respective observed datasets. Under the BMs model, MSE_0/MSE for most traits was not significantly different between the observed and simulated datasets (Table 4.8). Only for White Patch Size and Shape was MSE_0/MSE significantly greater in the simulated datasets. Therefore, phylogeny explained the variance significantly better in the simulated datasets for this trait.

4.4 Discussion

Phylogenetic analysis and phylogeographic patterns

Crinia signifera is monophyletic with three ancient geographically associated lineages and several sub-clades comparable to those found in Symula *et al.* (2008; Fig. 2.2, 4.3). The addition of sites did not clarify relationships among the major haplotype clades, but extended the range of clade A and sub-clade C3 (Fig. 4.2). In eastern Victoria (Sites 53-56), clade A encompasses areas south and east of the Great Dividing Range (Fig. 4.2b,c), and is parapatric with sub-clade C3. Extension of clade A northward to Mallacoota (Site 53, Fig. 4.2) and westward to Drouin (Site 58) and Welshpool (Site 56, Fig. 4.2) does not conflict with geographical limits of clades in other species (Chapple *et al.* 2005, Nicholls and Austin 2005, Rockman *et al.* 2001, Donnellan *et al.* 1999). However,

the extent of sampling in these studies is not identical. A new haplotype sub-clade, C6 (bpp = 0.99), was identified to the west of the Great Dividing Range that included samples from Mansfield (Site 57) and Seymour (Site 25), Victoria suggesting that investigation of sites within the Great Dividing Range may provide valuable insight into historical processes that shaped phylogeographic patterns in southeastern Australia.

Several sites were identified where sympatric individuals belong to divergent clades or sub-clades (Mallacoota (Site 53), Drouin (Site 58), Seymour (Site 25), Hamilton (Site 29), Portland (Site 30)). In all instances, the clades to which these individuals belonged were deeply divergent and parapatric (Fig. 4.2b). Thus, because these individuals belong to divergent mtDNA haplotype clades and because individuals that share haplotypes are limited to geographically neighboring sites, this observation is unlikely to be a result of incomplete lineage sorting, but rather due to mitochondrial introgression (McGuire *et al.* 2007). As a result, hybridization may occur in the contact zones between the major clades and sub-clades of *C. signifera*, implying the potential lack of pre-zygotic barriers among clades. Although other studies of similarly distributed studies have not found equivalent evidence for introgression (Chapple *et al.* 2005, Nicholls and Austin 2005, Rockman *et al.* 2001, Donnellan *et al.* 1999), this is unlikely to be a characteristic unique to phylogenetic relationships among *C. signifera*. Instead, this is probably because fewer individuals per site tend to be sampled in species with large distributions. Few additional phylogeographic inferences can be drawn from the analysis of a single mtDNA marker, and are beyond the scope of this study.

Advertisement call differences have been used to infer historical processes that

have led to population-level divergence in southeast Australia (Littlejohn 2005). In frogs, males produce advertisement calls to attract potential mates and to avoid mating with heterospecifics (Duellman and Trueb 1986, Wells 1977). When intraspecific variation arises in advertisement calls, sexual selection can lead to divergence among traits, generate pre-zygotic reproductive isolation and promote genetic divergence among lineages (Verrell 1999, Lande 1981). In *C. signifera*, observed differences in advertisement call are hypothesized to be the product of adaptation to habitat differences that arose as the product of Pleistocene climatic fluctuations (Littlejohn 2005, 1964). Symula *et al.* (2008) examined one hypothesis of geographic relationships among clades based on advertisement call data and demonstrated that advertisement call similarity between Tasmania and mainland populations (Mallacoota (Site 53) and Boydtown (Site 51)) likely reflects the retention of ancestral call characteristics and not phylogenetic history. However, in the present study, haplotypes from Mallacoota can be found in either clade A or B. It is possible that the advertisement calls from these two mainland sites (Littlejohn 2005) were collected from individuals with clade B haplotypes. Therefore, the similarity in advertisement calls between these mainland sites may be a product of phylogenetic history.

Introgression between clade A and B implies a lack of pre-zygotic isolation between the clades and suggests females do not recognize differences that may occur between individuals in haplotype clades A and B. Surprisingly, in Mallacoota (Site 53) at the contact zone between haplotype clades A and B, members of a single amplectant pair belonged to different clades. Inferences that can be drawn from this observation are

limited because courtship between these individuals was not observed. However, the observation supports that females do not always discriminate between males from different clades, and supports the absence of pre-zygotic barriers between clades A and B. It is entirely possible that there are not differences between calls in clade A and B, facilitating hybridization between the clades. This seems unlikely because geographic differences in advertisement call occur among sites that belong to less divergent sub-clades within clade C (Symula *et al.* 2008, Littlejohn 2005, 1964). Instances of introgression were also identified between sub-clades within clade C with known call differences (Fig. 1.2, 4.2). Thus, the presence of multiple instances of introgression among clades and sub-clades where there are known advertisement call variants provides an ideal situation to comparatively test the role of pre-zygotic isolation in the maintenance of genetically distinct lineages. Certainly, the phylogenetic evidence and patterns of advertisement call data warrant further investigation into how cryptic lineages remain essentially isolated on the landscape in the absence of pre-zygotic barriers.

Color pattern quantification

Based upon color pattern quantification, three major features vary in *C. signifera* color pattern. First, individuals can lack patches altogether (e.g., Fig. 1.1d-f). These individuals tend to have a large proportion of white (> 0.6; Fig. 4.3a) or large numbers of small white patches (> 40; Fig. 4.3b). Typically, these individuals have low Black Patch Size and Shape and Overall Patchiness (< 1; Fig. 4.4a, b), but high White Patch Size and Shape (> 1; Fig. 4.4c). Second, individuals can be black-and-white with a low proportion

of white (e.g., Fig. 1.1a). These patterns have small white area partitioned into few white patches (Fig. 4.3) and generally, score high on Black Patch Size and Shape (> 1; Fig. 4.4a). Third, individuals can be black-and-white with a high proportion of white (e.g., Fig. 1.1b-c). In these patterns, both the Proportion of White and Number of White Patches are medium to low. Also in these patterns, Black Patch Size and Shape scores are low (< 1) and White Patch Size and Shape and Overall Patchiness are high (> 1).

Most differences in pattern are apparent based solely upon the Proportion of White and Number of White Patches (Fig. 4.3) and color pattern attributes described by the PCA factor scores should be interpreted with caution. Simultaneous consideration of the first three factors does clearly identify the three major pattern variants. However, fine-scale differences captured by the factors often skew factor scores. For example, due to factor composition, some individuals have unexpected factor scores (e.g., BS014, Fig. 4.4). Using a strict interpretation of Black Patch Size and Shape, individuals with low scores should have low black patch area interrupted with many white patches and very low contrasting edges (Fig. 4.4). However, the largely black pattern in BS014 has the lowest Black Patch Size and Shape score. In BS014, white patches have extensive perimeter and therefore are confounded by the contribution of the contrasting edges measure (Table 4.3, 4.5). Therefore, unexpected factor scores may capture unique attributes of individual color patterns. In another instance, the exceptionally different *Pseudophryne* from Ulladulla (Site 15) was not notably different for Proportion of White, Number of White Patches, but was outstanding when White Patch Size and Shape was measured. Thus, it is possible that variance accounted for by these factors was strongly

influenced by fine-scale individual differences. At least in *Pseudophryne*, color-patterns vary to the extent that ventral patterns have been used for individual identification (Mitchell 2005, Cogger 2000). Thus, differences accounted for by factors do not necessarily have significant evolutionary implications. Modes of ventral pattern inheritance could provide insight into factor interpretation, but genetic mechanisms have not yet been examined.

Color pattern in *C. signifera* and *Pseudophryne* are proposed to be visual components associated with the playing dead behavior (Williams *et al.* 2000) and therefore depend on the perception of a predator (Chittka and Osorio 2007, Endler 1978). Avian predators can discriminate fine-scale features that may not be detectable by the human eye (Osorio *et al.* 1999). In the study of predation on clay replicas of *C. signifera* (Chapter 3), efforts were made to minimize differences among replicas, but fine-scale differences were evident among black-and-white individual patterns. Regardless, individuals that had any black on the ventral surface were avoided more often in some habitats. Therefore, the more significant characteristic used by predators may be proportion of black or white rather than those represented by the principal components. Therefore, though principal components were examined relative to phylogenetic relationships, biological inferences on the role of the pattern characteristics quantified by the principal components are difficult to draw relative to predator avoidance of color pattern.

Within-site and regional variation are also apparent in *C. signifera*. Notably, medians differ among some sites for most of the measured features (Fig. 4.3, 4.4). However, even though medians differ, in nearly all populations, individuals that lack bold black-and-white color pattern (e.g., BS219 or higher, Fig. 4.3a) occur in most populations.

Unexpectedly, regional differences are also apparent among sites. First, individuals with largely black patterns are concentrated in eastern New South Wales and eastern Victoria and are distributed beyond borders of the major clades (Fig. 4.5-14, 4.9). Second, individuals that lack bold black-and-white color pattern are found in nearly all populations. Although not quantified here, the frequency of individuals that lack black-and-white color pattern are more common in central Victoria and South Australia.

Ecological and geographical features that could potentially influence within-site and region-specific variation outside of genetic drift are not explicitly addressed in this study. However, in comparison to *C. signifera* where largely black patterns were found in northern populations, in sympatric Australian *Liopholis* skinks, frequencies of individuals with a higher proportion of black increased in southern populations (Chapple *et al.* 2008). Furthermore, in the region where individuals with low proportions of white were most common in *C. signifera*, *L. whitii* lacks the black morphs altogether. In one study, these geographical differences in squamate color patterns are attributed to geographical differences in predation pressures (Forsman and Shine 1995). A second comparative study of all Australian reptiles found that polymorphic species exploit a wider variety of habitats and hypothesized that polymorphic coloration is maintained due to differential predator avoidance among habitats (Forsman and Åberg 2008). Similarly, Symula (Chapter 3) demonstrated that the advantage to bearing black-and-white color pattern varies among habitats in *C. signifera*, but whether predators respond differently to proportion of black has not yet been tested. Examination of *C. signifera* relative to geography and other ecological factors may provide insight into potential differences in

selective environments, but are beyond the scope of this study.

Mimicry between C. signifera *and* Pseudophryne

As proposed by Williams *et al.* (2000), mimicry may explain the combination of shared black-and-white ventral coloration and defensive behaviors in *C. signifera* and *Pseudophryne*. Bivariate correlations revealed significant relationships in some pattern characteristics (Table 4.6) between the species. Whole frog measures Total Black Area ($r = 0.819$, $p = 0.045$) and Total White Perimeter ($r = 0.812$, $p = 0,047$) were significantly correlated. Furthermore, randomization tests indicate that Proportion of White ($U' = 4.77$, $p < 0.005$) and Number of Black Patches ($U' = 5.34$, $p < 0.005$) differed significantly less in sites were *Pseudophryne* was present. Although, overall, the color patterns are not significantly correlated (Bonferroni $p = 0.00165$), these results suggest that color pattern between the two species is similar. It was previously shown (Chapter 3) that *C. signifera* color pattern, deters predators in some habitats when there is black in the pattern (e.g., BS180). Thus, the apparent similarity in color patterns between sympatric populations suggests that *Pseudophryne* would afford similar protection from predators. Together, these results suggest that the black-and-white color patterns are potentially similar due to mimicry and the shared advantage of avoiding predation.

There are at least two apparent differences between *Pseudophryne* and *C. signifera*. First, *Pseudophryne* always bears bold black-and-white ventral coloration (Cogger 2000), whereas *C. signifera* populations can be composed of black-and-white individuals (e.g., BS012, BS180) or individuals with solid white, grey or flecked patterns (e.g., Fig. 4.5;

BS432, BS143). Second, in this study, *Pseudophryne* all have black-and-white venters with a low proportion of white (Fig. 4.5). In *C. signifera*, individuals had black-and-white patterns with similarly low proportion of white, but also had individuals with black-and-white patterns with high proportion of white (e.g., BS237). Field guides that include sympatric *Pseudophryne* depict individuals with large white patches (Robinson 2002, Cogger 2000, Barker *et al.* 1995). Similarly, museum collections of *Pseudophryne* have representative individuals with higher proportion of white. However, these color patterns were not observed in the field (Table 4.2) even though sampled localities were similar to those in museum collections. Other surveys have found individual *Pseudophryne* with low proportion of white syntopic with individuals with high proportion of white (e.g., http://museumvictoria.com.au/bioinformatics/frog/images/dendlive5.htm) supporting that *Pseudophryne* color pattern variation is drastically underestimated (Fig. 4.6, 4.7). Despite this underestimation of pattern variation in *Pseudophryne*, the randomization tests demonstrated that the two species are similar when they are found in syntopy. Therefore, similarity in color pattern in syntopic *C. signifera* and *Pseudophryne* populations support that that *C. signifera* is a mimic of *Pseudophyrne*.

This study does not address the color in the pattern and there are potential differences in both black and white color between species. Both black color differences (e.g., BS180, BS237) and white differences are apparent among *C. signifera* individuals (e.g., BS143, BS432). These color differences are apparent in the field (Fig. 1.2), but are not captured by the method of pattern measurement used here. Measurements of *Pseudophryne* from Ulladulla suggest that the colors only reflect in the visual spectrum, but

measurements were not taken for *C. signifera*. Quantification of these differences could be critical in assessing whether predators discriminate species-specific color characteristics (Endler 1978).

Not all color pattern measures are correlated between *C. signifera* and *Pseudophryne* (Table 4.6). While this may be an artifact of the types of measures quantified here, it implies that these species are not perfect model and mimic. Numerous examples of imperfect mimics exist, with an array of proposed mechanisms that explain how the imperfection still results in protection from predators (Rowe *et al.* 2003, Holloway *et al.* 2001). The color patterns are proposed to be the visual component of an anti-predator display (Williams *et al.* 2000). Therefore, the effectiveness of the display and mimicry relies on the visual systems and behavior of the predators (Endler 1990). How similar the model and mimic have to be to afford protection depends on the predator's ability to perceive differences and how they search for prey (e.g., Osorio *et al.*1999). For example, predators often generalize signals such that they ignore fine-scale differences in stimuli (color patterns), but extend their avoidance to very different color patterns (See review in Ghirlanda and Enquist 2003). Generalization in avoidance behavior is well studied in birds (e.g., Darst and Cummings 2006, Osorio *et al.* 1999), but as demonstrated in the clay replica experiment (Chapter 3), birds are not the primary predators on these frogs. Evidence demonstrating generalization of color pattern in mammals is not available, but mammals generalize other stimuli (Ghirlanda and Enquist 2003). Demonstration that mammalian predator avoidance is independent of these differences would further support the hypothesis of mimicry between *C. signifera* and *Pseduophryne*.

Sites where *C. signifera* and *Pseudophryne* were defined as allopatric were those where *Pseudophryne* was not found simultaneously with *C. signifera*. Despite multiple attempts, it was not possible to collect *Pseudophryne* at each *C. signifera* collection site. While drought conditions contributed to collections of *Pseudophryne*, some biological factors also limit detection. First, *C. signifera* is much more flexible in breeding habitats and will breed in any area where there is pooling water (Lauck 2005, Lemckert 2005a,b). *Pseudophryne* requires terrestrial nesting sites in habitats that are likely to be subjected to flooding (Mitchell 2005). While the two species often are found syntopically, *Pseudophryne* does not occur in all habitats exploited by *C. signifera*. Second, *C. signifera* will call year-round (Cogger 2000) making it more conspicuous whereas *Pseudophryne* breeds only during a short period in the winter (Mitchell 2005). The combination of habitat-specificity and shorter breeding season implies that relative to *C. signifera*, *Pseudophryne* is rare.

The lower relative abundance of *Pseudophryne* in contrast to *C. signifera* has implications for the hypothesis for mimicry. Classical predictions of Batesian mimicry indicate that the protection afforded to a mimetic species should break down in the absence of a model (e.g., Pfennig *et al.* 2007) or when the mimic is more common than the model (e.g., Mallet and Joron 1999). This prediction is supported in theoretical and laboratory studies (Rowland *et al.* 2007, Lindstrom *et al.* 2001). However, recent studies on natural populations suggest that rarity of the model species may not necessarily eliminate mimicry (Ries and Mullen 2008, Darst and Cummings 2006), but rather limit the distribution of putative mimics. Therefore, under the hypothesis of mimicry, the frequency of bold black-and-white coloration in *C. signifera* may be directly associated with

whether or not *Pseudophryne* is rare. For example, in geographical regions where *Pseudophryne* has undergone recent declines (e.g., *P. semimarmorata*, Central Victoria), most populations of *C. signifera* lack black-and-white mottling. Additionally, the maintenance of *C. signifera* without bold black-and-white coloration within populations could be influenced by the limited of areas of syntopy with *Pseudophryne*.

Phylogenetic signal, genetic drift and color pattern variation

In all of the measured variables, phylogenetic signal (K) was low and was only significant for Proportion of White and Number of White Patches. It is not surprising that Factors 1-3 did not have significant phylogenetic signal, because the characteristics quantified by these values are not apparent when considered independently and because it is possible that the factors measure individual-specific differences that are unlikely to be captured by the mtDNA marker. Revell *et al.* (2008) investigated the properties of K under several simulated condition and showed that low values of K could be attributed to multiple different evolutionary processes including high rates of evolution, strong stabilizing selection and punctuated, divergent selection. Thus, when K is low, the ability to infer evolutionary processes acting on traits is limited (Revell *et al.* 2008). Furthermore, any error in phylogeny reconstruction (Blomberg *et al.* 2003) or measurement in the trait (Revell *et al.* 2008) may artificially lower K.

In the absence of strong phylogenetic signal, inferences about trait evolution are better assessed using simulations (Ives *et al.* 2007, Garland *et al.* 1993) or by other model testing approaches (Lee *et al.* 2006, Butler and King 2004). The simulations performed in

this study were performed to test whether the mechanism of genetic drift along the phylogeny could explain variance in color pattern traits. In this study, the process of genetic drift was simulated under two different evolutionary models, gradual Brownian motion (BMg) and speciational Brownian motion (BMs). Combined, the simulation results suggest that Brownian motion does not amply describe the variation observed in either Proportion of White or Number of White Patches in *C. signifera* (Table 4.8). Thus, though there is evidence for phylogenetic signal in some of the measured traits, the hypothesis that variation in color pattern is a result of genetic drift can be rejected.

Generally, the results from simulations of Black Patch Size and Shape (Factor 1) and White Patch Size and Shape (Factor 2) reject the gradual BM model, but are inconsistent with rejecting or failing to reject speciational BM (Table 4.8). As addressed previously, the aspects of color patterns accounted for by these factors are difficult to explain unless the factors are considered simultaneously. Furthermore, inferring expectations of how these traits might evolve along a phylogeny are not intuitive because they appear to incorporate individual-specific differences. Therefore, these traits are not discussed further in light of genetic drift.

Based on the simulations, it is hard to reject that genetic drift under speciational Brownian motion (BMs) does not explain variation in *C. signifera* color pattern (Table 4.8). In both bounded and unbounded simulations, there is no significant difference between the simulated and observed datasets (e.g., Proportion of White $p = 0.237$ BMBs, $p = 0.324$ BMBu). In general, it is challenging to draw evolutionary inferences from speciational models because they are heavily biased by taxon sampling and lineage

extinction (Ackerly 2000). For example, accurate interpretation of this model requires that all branching events and lineages were sampled (Martins and Garland 1991). Therefore, relative to this *C. signifera* dataset, there are three potential sources of bias in the *C. signifera* dataset. Clade A is the older, sister lineage to the remainder of *C. signifera* (Symula *et al.* 2008), and numerous extinction events have likely occurred in clade A that cannot be represented genetically or with color pattern. Therefore, variation in clade A should be underrepresented in simulated datasets, and instead will be concentrated in the larger clades. Second, the geographical distributions of the clades and sub-clades are drastically different in size. Therefore, even if all historical lineages were represented, clade A (n = 30) would have disproportionately fewer branching events than either clade B (n = 75) or C (n = 140), again biasing the extent of simulated variation in clade A. Third, though this dataset consists of the most extensive range and most densely sampled phylogenetic analysis of southeastern Australia, there are still underrepresented geographic samples (e.g., the Great Dividing Range, western New South Wales, Queensland). As such, the failure to reject the speciational model may be a result of bias introduced by characteristics of the *C. signifera* datasets.

Addressing these biases is problematic. Ackerly (2000) suggested that using sub-samples might overcome the artificial inflation of variance. Thus, one potential way to deal with the biases is to generate equivalently sized sub-samples among clades or sub-clades. However, this does overcome the bias due to random lineage extinction (Ackerly and Nyffeler 2004, Martins and Garland 1991). Additionally, at some level, the genetic divergence in the mtDNA marker no longer represents organism-level or even

population-level phylogeny, but rather, the divergence is representative of organismal generations. At this level, branching events are not equivalent to speciation events. How to establish this level relative to branch lengths is not entirely clear, but one possibility is to effectively assign a hard polytomy to parts of the tree by reducing extremely short branch lengths to zero and then, examine whether the model still fits the data.

Demonstration that the pattern of variation in color pattern is discordant with that predicted by the phylogeny suggests the possibility that another mechanism maintains variation in color pattern. A simple way that the two color patterns could remain in the population is if the black-and-white color pattern is heterozygous. As a result, even under strong selection like that identified in Chapter 3, disadvantageous color patterns will remain in a population. Alternatively, natural selection can generate variation in color pattern through either diversifying or stabilizing selection. When two phenotypes are equally advantageous, diversifying selection can generate polymorphic or variable populations. It has been demonstrated that the black-and-white color pattern is advantageous in some populations (Chapter 3). In the absence of selection in favor of the white pattern, the black-and-white pattern should become fixed in the population. However, *C. signifera* populations commonly have both color patterns in populations (Fig. 4.7). In the study using clay models, there were differences in proportion of attacks on black-and-white between two habitat types (Fig. 3.2). Since only two habitats were examined and *C. signifera* exploits many habitat types, it is possible that the white pattern is advantageous in another habitat type. Thus, diversifying selection could generate the variability seen in *C. signifera*.

The process of stabilizing selection results in low variation centered on a given optimum (Felsenstein 1988). This process can be modeled on a phylogeny using an Ornstein-Uhlenbeck process (Butler and King 2004). Presently, the only biologically motivated optimum for color pattern in *C. signifera* is defined by the hypothesis of mimicry (Williams *et al.* 2000). If *C. signifera* is a mimic of the different color patterns in the toxic *Pseudophryne*, *C. signifera* color pattern variation should resemble that of the sympatric *Pseudophryne*. Under the hypothesis of mimicry, the color pattern of *Pseudophryne* could represent an optimal value for the color pattern in *C. signifera*. Programs are available to simulate traits under this model and test for stabilizing selection (Butler and King 2004, Martins 2004, Blomberg *et al.* 2003, Garland *et al.* 1999). However, it is unclear how the optimum trait value would be set for *C. signifera*. It is possible to estimate the OU model parameters from the present *C. signifera* dataset, but this estimate will not necessarily be relevant to the hypothesis of mimicry because they would be based on *C. signifera,* not *Pseudophryne* (Ives *et al.* 2007, Butler and King 2004, Blomberg *et al.* 2003). Another difficulty of implementing models of stabilizing selection to test the hypothesis of mimicry is the lack of adequate representation of variability in *Pseudophryne* color pattern (above). For example, *P. semimarmorata* lacks black-and-white coloration on the throat and instead has bright orange on the limbs. In this study, estimation of color pattern variation for sympatric *Pseudophryne* species is limited to five sampling sites for only two species that are found in a very small portion of the *C. signifera*'s distribution. Several *Pseudophryne* species are present that are sympatric with limited regions of the *C. signifera* distribution (Cogger 2000) and ventral color pattern can vary among these species. Therefore, a different

optimum would need to be specified for each species distribution and *Pseudophryne* color pattern (Butler and King 2004), but is not possible using this dataset. These types of model-based approaches would enhance understanding the interaction of mimicry and phylogenetic history on the evolution of *C. signifera* color pattern.

The results presented in this study illustrate variation in color pattern in *C. signifera* and suggest that natural selection through mimicry may influence whether populations maintain black-and-white color patterns. Several characteristics of color pattern in *C. signifera* and *Pseudophryne* are strongly correlated and color pattern in *C. signifera* is much more similar to *Pseudophryne* when the species are found syntopically. This supports the hypothesis that the two species are involved in a mimetic relationship. Color pattern is not strongly correlated with phylogenetic relationships indicating that color pattern variation in *C. signifera* is unlikely to have been shaped solely by neutral processes like genetic drift. Combined, these two aspects of the study provide motivation to design alternative experiments designed to test specific aspects of the hypothesis of mimicry and to develop methods that model the expected evolution of color pattern along the phylogeny when under selection.

Table 4.1. Collection localities and individual identification numbers for *C. signifera*. Sample sites, GPS coordinates, and museums where specimens were deposited for phylogenetic analysis and color pattern quantification are also shown. All samples from Table 1 are included. Sites are sorted into two groups. First, individuals from localities and site numbers (1-47) assigned in Symula *et al.* 2008 added for phylogenetic analysis are arranged from north to south along the east coast and then east to west along the southern part of the distribution. Second, localities and site numbers (48-66) from the 2007 field season are listed north to south along the east coast and east to west along the southern part of the distribution. Individuals for which color pattern could not be quantified and which were pruned from phylogenetic trees are indicated with a †. Site numbers in the left column correspond to localities on the maps in Fig. 2.1a, 5 and 9. Latitude and longitude are in decimal degrees. States are abbreviated as follows: NSW = New South Wales, VIC = Victoria, SA = South Australia, TAS = Tasmania. Museums used for voucher deposition are abbreviated as follows: South Australia Museum = SAM, Museum Victoria = MV, Australian National Wildlife Collection = ANWC, Australian Museum = AM, Queen Victoria Museum = QVM.

Site	Individual		Locality	State	Latitude/ Longitude	Museum	Genbank
1	BS050-051, BS053-054, BS056-059	N = 8	Evans Head	NSW	-29.09 153.39	AM	
2	ABTC25425†	N = 1	Glenn Innes	NSW	-29.71 151.75	AM	
3	ABTC12334†	N = 1	Armidale	NSW	-30.22 151.67	AM	
4	BS040-042, BS044, BS046-048	N = 7	Coffs Harbour	NSW	-30.32 153.11	AM	
5	BS035	N = 1	Port Macquarie	NSW	-31.50 152.90	AM	
6	BS031-033	N = 3	Clarencetown	NSW	-32.57 151.77	AM	
7	BS011, BS012, BS014, BS016, BS018-020	N = 7	Cooranbong	NSW	-33.13 151.35	AM	
8	BS152, BS154†, BS156-158, BS160-161	N = 7	Macquarie Woods	NSW	-33.41 149.31	AM	
9	BS021-027	N = 7	Coogee	NSW	-33.93 151.26	AM	
10	ABTC17627†	N = 1	Heathcote	NSW	-34.07 151.02	AM	
11	BS162-163	N = 2	Kangaroo Valley	NSW	-34.74 150.54	AM	
12	ABTC12884†-12885†	N = 2	Wagga Wagga	NSW	-35.13 148.23	AM	
14	BS235-242	N = 8	Canberra	ACT	-35.24 149.11	ANWC	
15	BS060, BS063-066	N = 5	Ulladulla	NSW	-35.35 150.45	AM	
18	BS164-168, BS170-172, BS453, BS455	N = 8	Kianga	NSW	-36.20 150.13	AM	
19	BS067-071†, BS072-076	N = 10	Eden	NSW	-37.05 149.90	AM	
21	BS173-174, BS175†-176, BS178-180, BS182	N = 4	Cann River	VIC	-37.56 149.15	MV	
22	BS183-184	N = 2	Bairnsdale	VIC	-37.67 147.56	MV	
23	ABTC12882†-12883†	N = 2	Granya	VIC	-36.10 147.32	MV	
24	BS088†-093, BS095	N = 7	Lilydale	VIC	-37.78 145.36	MV	
25	BS185-189, BS193-194	N = 7	Seymour	VIC	-37.56 145.14	MV	
26	BS001, BS005, BS007-010	N = 6	Bundoora	VIC	-37.72 145.05	MV	
27	BS195-196	N = 2	Maryborough	VIC	-37.07 143.73	MV	
28	197†-202, BS204-206	N = 9	Stawell	VIC	-37.07 142.76	MV	
29	BS141†-146, BS148	N = 7	Hamilton	VIC	-37.70 141.91	MV	
30	BS131-140	N = 10	Portland	VIC	-38.37 141.61	MV	

Table 4.1. *Continued*

Site	Individual		Locality	State	Latitude/ Longitude	Museum	Genbank
31	ABTC37438	N = 1	Mount Gambier	SA	-38.05 140.94	SAM	
33	BS212-219, BS221	N = 9	Naracoorte	SA	-37.10 140.79	SAM	
34	BS227-233	N = 7	Mary Seymour Conservation Park	SA	-37.16 140.62	SAM	
35	ABTC37700†-37701†	N = 2	Padathaway	SA	-36.69 140.48	SAM	
36	ABTC58307†	N = 1	Gum Lagoon Conservation Park	SA	-36.27 140.02	SAM	
37	ABTC58814†	N = 1	Milang	SA	-35.40 139.97	SAM	
38	ABTC36237†	N = 1	Kingston	SA	-36.82 139.85	SAM	
39	BS096-098, BS102-103	N = 5	Adelaide	SA	-35.06 138.75	SAM	
40	BS116-BS120, BS122-129	N = 13	Clare	SA	-33.84 138.62	SAM	
41	BS106-110, BS112-115	N = 19	Crystal Brook	SA	-33.33 138.24	SAM	
42	ABTC33253	N = 1	Second Valley	SA	-35.52 138.22	SAM	
44	BS433-435†, BS436-442	N = 10	Sheffield	TAS	-41.39 146.33	QVM	
45	BS423-432	N = 10	Epping	TAS	-41.78 147.32	QVM	
46	BS413-414†, BS415-417, BS420-422	N = 8	Wielangta	TAS	-42.66 147.89	QVM	
48	BS443, BS445, BS447-448, BS450-452	N = 7	Batemans Bay	NSW	-35.66 150.28	AM	
49	BS459-467	N = 9	Quaama	NSW	-36.47 149.87	AM	
50	BS470†-477	N = 8	Kalaru	NSW	-36.74 149.94	AM	
51	BS482-484, BS486-490	N = 7	Boydtown	NSW	-37.11 149.87	AM	
52	BS502-507, BS509-511	N = 9	Timbillica	NSW	-37.38 149.70	AM	
53	BS492-499, BS501	N = 10	Mallacoota	VIC	-37.55 149.73	MV	
54	BS516-BS524	N = 9	Nowa Nowa	VIC	-37.74 148.04	MV	
55	BS355-357, BS359, BS361	N = 5	Tyers	VIC	-38.14 146.53	MV	
56	BS365-367†, BS368-374	N = 10	Welshpool	VIC	-38.67 146.44	MV	
57	BS555-558, BS560-562, BS564	N = 8	Mansfield	VIC	-37.05 146.08	MV	
58	BS385-394†	N = 10	Drouin	VIC	-38.14 145.88	MV	
59	BS375-382, BS384	N = 9	Korumburra	VIC	-38.44 145.83	MV	
60	BS345-346†, BS347-348, BS350	N = 5	Bunyip	VIC	-38.06 145.71	MV	
61	BS335-341†, BS342-343	N = 9	Beaconsfield	VIC	-38.03 145.43	MV	
62	BS395-398, BS400-404	N = 9	Waurn Ponds	VIC	-38.20 144.30	MV	
63	BS526-533, BS535	N = 9	Ballarat	VIC	-37.55 143.89	MV	
64	BS536-544	N = 9	Colac	VIC	-38.27 143.63	MV	
65	BS405-412	N = 8	Cape Otway	VIC	-38.76 143.49	MV	
66	BS545-549, BS551-554	N = 9	Warnambool	VIC	-38.36 142.51	MV	

Table 4.2. Collection localities and individual identification numbers for *Pseudophryne*. Number of photographs GPS data, number of photographs and museum deposition information are also shown. Individual numbers refer to those animals collected for voucher specimens at each site. Site numbers refer to localities on Figure 4.1 and are indicated with a star next to points on the map. N refers to number of photographs that were used for digital photograph analyses. Not all photographed individuals were kept as voucher specimens. Museums used for voucher deposition are abbreviated as follows: South Australia Museum = SAM, Museum Victoria = MV, Australian Museum = AM. Tissues were all deposited in the SAM.

Site	Individual		Locality	State	Latitude/ Longitude	Museum
15	BS067-BS078	N = 10	Ulladulla	NSW	-35.35 150.45	AM
21	BS514-BS515	N = 4	Cann River	VIC	-37.56 149.15	MV
50	BS478-BS479	N = 6	Kalaru	NSW	-36.74 149.94	MV
51	BS480-BS481	N = 3	Boydtown	NSW	-37.11 149.87	MV
52	BS512-BS513	N = 2	Timbillica	NSW	-37.38 149.70	MV

Table 4.3. Titles and descriptions of measures used to quantify black-and-white pattern on the ventral surfaces of *C. signifera* and *Pseudophryne*. All measures listed under Patch Description are calculated as the mean of all measured patches on an individual. MatLab commands used to obtain these measures are listed in parentheses after descriptions of the measures.

Category	Measurements	Description
I. Whole frog		
	Contrasting Edges	Ratio of the average black blotch perimeter and the average white blotch perimeter.
	Patch Number (black)	Total number of black patches (numObjects).
	Pattern Continuity (black)	The difference between the number of black regions on the ventral surface and the holes (white areas) in the regions (bweuler).
	Pattern Continuity (white)	The difference between the number of white regions on the ventral surface and the holes (black areas) in those regions (bweuler).
	Proportion of White	Ratio of total white area to total measured area.
	Patch Number (white)	Total number of white patches (numObjects).
	Total Perimeter (white)	Sum of the perimeters of all white patches on an individual.
	Total Area (black)	Sum of the area (cm^2) of all black pixels (bwarea).
	Total Area (white)	Sum of the area (cm^2) of all white pixels (bwarea)
II. Patches		
	Eccentricity (black)	Average measure of how circular or stretched black patches are. Values closer to 0 are more circular and values closer to 1 are more oblong (regionprops, 'Eccentricity').
	Eccentricity (white)	Average measure of how circular or stretched white patches are. Values closer to 0 are more circular and values closer to 1 are more oblong (regionprops, 'Eccentricity').
	Equivalent Diameter (black)	Diameter of circle with same area as the black patches (regionprops, 'EquivDiameter').
	Equivalent Diameter (white)	Diameter of circle with same area as the white patches (regionprops, 'EquivDiameter').
	Euler Number (black)	Average measure of how many holes are in each black patch (regionprops, 'EulerNumber').
	Euler Number (white)	Average measure of how many holes are in each white patch (regionprops, 'EulerNumber').
	Fill Area (black)	Average of black area of patches with holes in patches filled (regionprops, 'FilledArea').
	Fill Area (white)	Average of white area of patches with holes in patches filled (regionprops, 'FilledArea').
	Major Axis (black)	Average of major axis estimated from an ellipse with the same second moments as the black patches (regionprops, 'MajorAxisLength').
	Major Axis (white)	Average of major axis estimated from an ellipse with the same second moments as the white patches (regionprops, 'MajorAxisLength').
	Minor Axis (black)	Average of minor axis length estimated from an ellipse with the same second moments as the black patches (regionprops, 'MinorAxisLength').
	Minor Axis (white)	Average of minor axis length estimated from an ellipse with the same second moments as the white patches (regionprops, 'MinorAxisLength').
	Orientation (black)	Average orientation (degrees) of each black patch (regionprops, 'Orientation').

Table 4.3. *continued*

Category	Measurements	Description
II. Patches		
	Orientation (white)	Average orientation (degrees) of each white patch (regionprops, 'Orientation').
	Patch Area (black)	Average area of black patches scaled to total ventral surface area (regionprops, 'Area').
	Patch Area (white)	Average area of white patches scaled to total ventral surface area (regionprops, 'Area').
	Solidity (black)	Average proportion of black pixels that fill the smallest convex polygon that can encompass each patch (regionprops, 'Solidity').
	Solidity (white)	Average proportion of white pixels that fill the smallest convex polygon that can encompass each patch (regionprops, 'Solidity').
	Squareness (black)	Average proportion of black pixels that fill the smallest rectangle that can surround the patch. Values closer to 1 are more rectangular (regionprops, 'Extent').
	Squareness (white)	Average proportion of white pixels that fill the smallest rectangle that can surround the patch. Values closer to 1 are more rectangular (regionprops, 'Extent').

Table 4.4. Summary of variance explained by Principal Components Analysis (PCA). Results for factors from Varimax (orthogonal) rotation are shown for all factors with eigenvalues greater than one. Total variance for factors determined to be significant based on the scree plot are also presented.

Crinia signifera		*Pseudophryne bibronii/Pseudophryne dendyi*	
Factor (Rotated Principal Components)	% Variance Explained (Rotated)	Factor (Rotated Principal Components)	% Variance Explained (Rotated)
1	21.517	1	34.933
2	19.704	2	29.080
3	10.241	3	10.738
4	7.697	4	7.261
5	7.449	5	5.795
6	7.233	6	3.526
7	6.251	-	-
8	3.687	-	-
Total Explained variance (Eigenvalues > 1)	83.760	Total Explained variance (Eigenvalues > 1)	91.33
Total explained variance (Scree plot (Factors 1-3))	59.140	Total explained variance (Scree plot (Factors 1-3))	74.751

Table 4.5. Factors extracted in Principal Component Analysis (PCA) and the variables correlated with each factor. Patch measures have the associated color (black/white) in parentheses following the variable name. Underlined variables are those that differ between the *C. signifera* and *Pseudophryne* dataset.

Crinia signifera		*Pseudophryne*	
Factor	Variables	Factor	Variables
1-Black area and shape	Contrasting edges	1-Black area and shape	Contrasting edges
	Patch area (black)		Patch area (black)
	Euler number (black)		Euler number (black)
	Eccentricity (black)		Eccentricity (black)
	Major axis (black)		Major axis (black)
	Minor axis (black)		Minor axis (black)
	Fill area (black)		Fill area (black)
	Equivalent diameter (black)		Equivalent diameter (black)
			Number of patches (black)
			Squareness (black)
			Solidity (black)
2-White area and shape	Patch area (white)	2-White area and shape	Patch area (white)
	Major axis (white)		Major axis (white)
	Minor axis (white)		Minor axis (white)
	Fill area (white)		Fill area (white)
	Equivalent diameter (white)		Equivalent diameter (white)
	Euler number (white)		Solidity (white)
			Eccentricity (white)
3-Overall patchiness	Pattern continuity (black)	3-Overall patchiness	Pattern continuity
	Pattern continuity (white)		Pattern continuity
	Number of patches (black)		Number of patches (white)
4-	Solidity (black)	4-	Total area (white)
	Squareness (black)		Total area (black)
5-	Squareness (white)	5-	Orientation (white)
	Solidity (white)		Proportion of white
6-	Number of patches (white)	6-	Orientation (black)
	Total perimeter (white)		
7-	Total area (white)	-	-
8-	Orientation (black)	-	-

Table 4.6. Summary of bivariate correlations of color pattern measurements between *C. signifera* and *Pseudophryne*. Comparisons were made between five sites. A single * indicates significance at $\alpha \leq 0.05$. Two * indicate significance following Bonferroni correction with $\alpha \leq 0.00165$.

	Measurements	**Pearson Correlation**	**p-value**
I. Whole frog			
	Contrasting edges	0.611	0.137
	Number of patches (black)	0.819	0.045*
	Pattern continuity (black)	0.663	0.111
	Pattern continuity (white)	0.235	0.352
	Proportion of white	-0.089	0.443
	Number of patches (white)	0.641	0.122
	Total perimeter (white)	0.812	0.047*
	Total area (black)	-0.190	0.488
	Total area (white)	-0.502	0.195
II. Patches			
	Eccentricity (black)	-0.100	0.437
	Eccentricity (white)	-0.763	0.067
	Equivalent diameter (black)	0.685	0.101
	Equivalent diameter (white)	0.980	0.002*
	Euler number (black)	0.428	0.236
	Euler number (white)	0.694	0.097
	Fill area (black)	0.980	0.002*
	Fill area (white)	0.923	0.013*
	Major Axis (black)	0.668	0.109
	Major Axis (white)	0.983	0.001**
	Minor Axis (black)	0.769	0.064
	Minor Axis (white)	0.769	0.064
	Orientation (black)	-0.498	0.200
	Orientation (white)	0.451	0.223
	Patch Area (black)	0.592	0.146
	Patch Area (white)	0.980	0.002*
	Solidity (black)	-0.339	0.289
	Solidity (white)	0.140	0.411
	Squareness (black)	-0.596	0.145
	Squareness (white)	-0.493	0.200

Table 4.7. Summary of tests for phylogenetic signal. Estimated values for phylogenetic signal as performed in PHYSIG_LL for each Proportion of White, Number of White Patches and the first three PCA factors with eigenvalues greater than one. MSE_0 represents mean squared error estimated using the phylogenetically correct mean. MSE_{Star} represents the mean squared error estimated from a star phylogeny. MSE_{Tree} represents the mean squared error estimated from the best GARLI tree. K indicates the level of phylogenetic signal estimated from the best GARLI tree. K* represents a measure of phylogenetic signal estimated from contemporaneous tips and is reported as a comparison to other studies. Log likelihoods for a star phylogeny and the best GARLI tree are represented as lnL_{Star} and $lnL_{Observed}$, respectively. The p-value shown was calculated following 1000 permutation tests.

Variable (Measure)	**MSE_0**	**MSE_{Star}**	**MSE_{Tree}**	**Observed MSE_0/MSE**	**Expected MSE_0/MSE**	**K (Obs./Exp.)**	**K***	**lnL_{Star}**	**$lnL_{Observed}$**	**p-value**
Proportion of white	0.075	0.057	16.687	0.0045	17.506	0.00026	0.00024	2.731	-693.25	0.007
White Patch number	242.670	197.429	65929.209	0.0037	17.506	0.00021	0.00021	-994.598	-1706.44	0.064
Factors										
1. Black area and shape	0.852	0.747	219.655	0.0038	17.506	0.00022	0.00024	-311.365	-1007.67	0.196
2. White area and shape	0.814	0.789	6008.801	0.0001	17.506	0.000008	0.000009	-318.118	-1413.01	0.890
3. Patchiness	0.856	0.851	2333.348	0.0004	17.506	0.00002	0.00036	-327.382	-1297.13	0.588

Table 4.8. Summary of color pattern simulations under Brownian motion (BM) models of trait evolution. Observed values are listed for each of the four traits examined. Black Patch Size and Shape and White Patch Size and Shape are shown as Factor 1 and Factor 2, respectively. Test statistics were compared using the null distribution generated from 1000 datasets for each model of trait evolution. Phylogenetic variance MSE_0/MSE was used to test whether the null model fits the phylogenetic pattern of MSE_0 better than the observed. Null and alternate hypotheses are given for each of the test statistics. BMBg represents bounded, gradual BM simulations. BMUg represents gradual, unbounded BM simulations. BMBs and BMUs represent bounded and unbounded simulations, respectively. The * indicates significance in favor of H_A. Non-significant p-values are otherwise reported as the proportion of simulated datasets that are greater than the observed test statistic.

Test	**Hypotheses**	**Model**	**Observed Values**				**p-values**			
			Proportion of White	White Patch Number	Factor 1	Factor 2	Proportion of White	White Patch Number	Factor 1	Factor 2
Phylogenetic covariance	H_0: $MSE_0/MSE_{Sim}=MSE_0/MSE_{Obs}$ H_A: $MSE_0/MSE_{Sim}>MSE_0/MSE_{Obs}$	BMBg	0.0037	0.0045	0.0039	0.0001	< 0.001*	< 0.001*	<0.001*	<0.001*
		BMUg	0.0037	0.0045	0.0039	0.0001	< 0.001*	< 0.001*	< 0.001*	< 0.001*
		BMBs	0.0037	0.0045	0.0039	0.0001	0.237	0.287	0.261	< 0.001*
		BMUs	0.0037	0.0045	0.0039	0.0001	0.324	0.393	0.369	< 0.001*

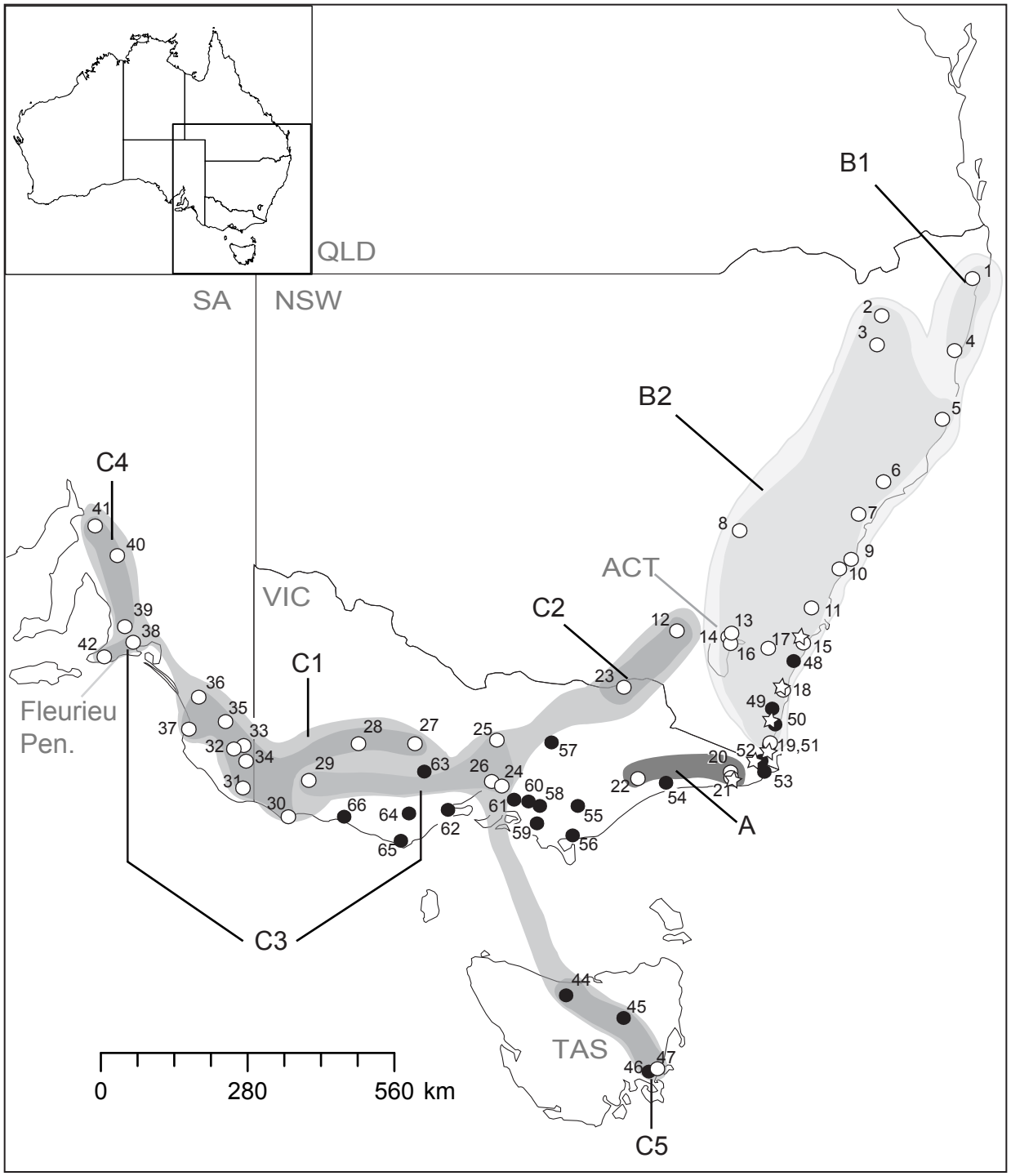

Figure 4.1. Geographic localities for collection sites of *C. signifera* and *Pseudophryne*. Localities represented by circles are sites where *C. signifera* were collected. Closed circles indicate sites from Symula *et al.* (2008) that were collected in 2004 and open circles indicate localities collected in 2007. Samples from Tasmania were collected in 2007, but included in Symula *et al.* (2008) analyses. Stars indicate localities where *Pseudophryne* were collected. Shading represents clades identified in Symula *et al.* (2008) relative to new sampling localities.

Figure 4.2. The best maximum likelihood tree of *C. signifera* , geographic distribution of clades and sub-clades and areas of introgression. The overall topology and branch lengths are shown for the best maximum likelihood tree estimated by GARLI 0.951 with Bayesian posterior probabilities shown for nodal support. Black-filled dots represent posterior probabilities (bpp) > 0.95 and white-filled dots represent bpp > 0.90. Each clade is expanded to show all sequenced individuals in the tree. Individuals that represented redundant haplotypes are separated by a comma and shown on a single tip except for in the two most common haplotypes. One haplotype is represented by BS471 (Clade B2) and includes individuals: Kalaru, NSW (Site 50): BS471, BS474; Eden, NSW (Site 19): BS067, BS068, BS069, BS070, BS071, BS073, BS074, BS076; Boydtown, NSW (Site 51): BS482, BS484, BS486, BS489, BS490; Timbilica, NSW (Site 52): BS504, BS506; Mallacoota, VIC (Site 53): BS497. The second haplotype is represented by BS545 (Clade C3) and includes individuals: Waurn Ponds (Site 61): BS401, BS404; Colac, VIC (Site 64): BS541; Warnambool, VIC (Site 66): BS545, BS546, BS551, BS552; Cape Otway, VIC (Site 68): BS405, BS406, BS408, BS411, BS412. Locations of the clades and sub-clades are shown relative to geographic sampling localities. Shading corresponds to shading on the phylogeny. States are abbreviated as follows: New South Wales (NSW), Victoria (VIC), Tasmania (TAS), South Australia (SA), Queensland (QLD). The square outline within the map illustrates the region of the map expanded to show areas of apparent introgression. Dotted lines and arrows leading from a sampling locality indicate to which clade individuals from that site belong. Arrows are not drawn to indicate gene flow or dispersal, but only to clarify potential clade membership.

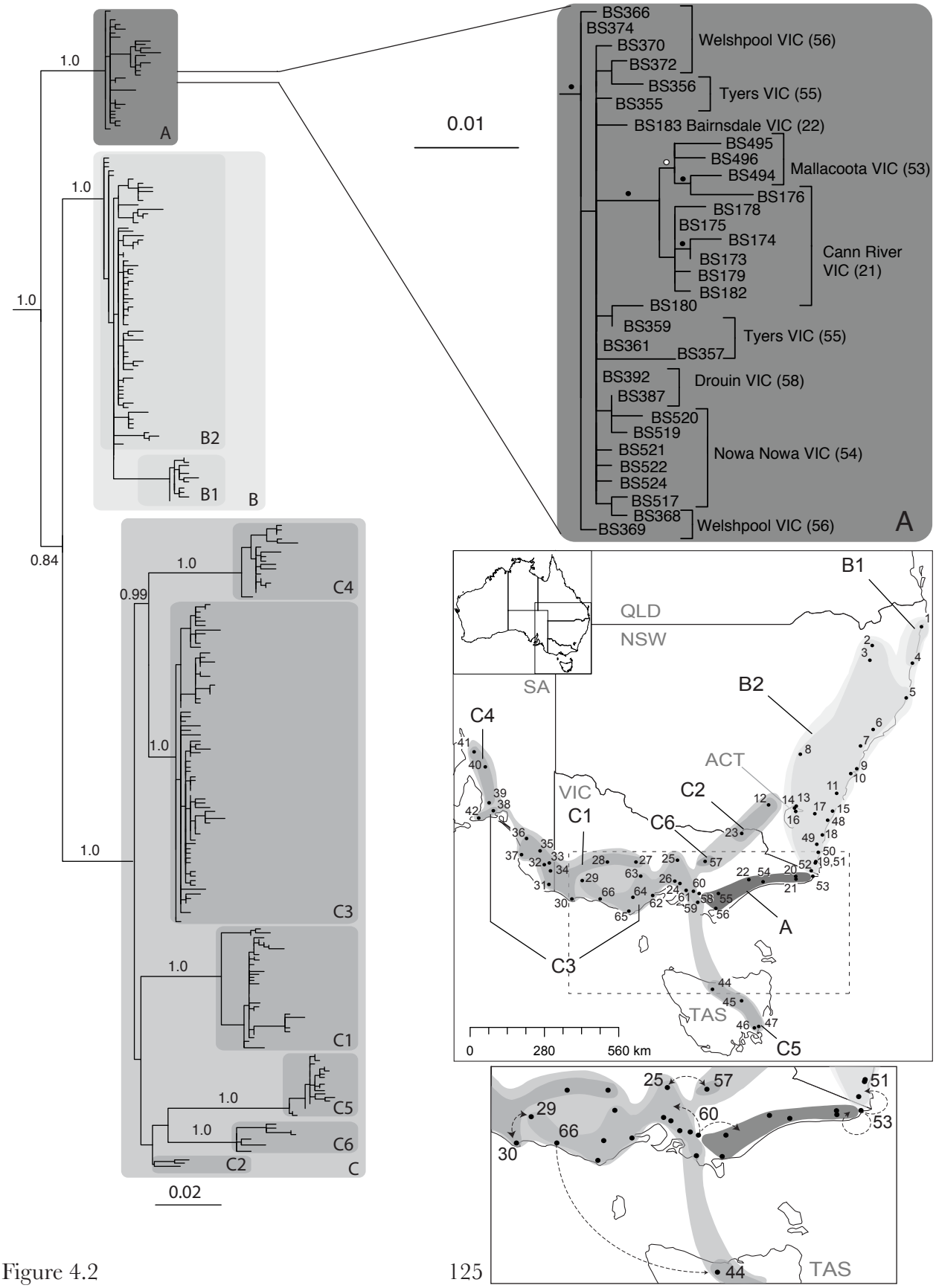
A
B
B2
B1
C
C4
C3
C1
C5
C6
C2
1.0
0.84
0.99
0.02
0.01
BS366
BS374
BS370
BS372
BS356
BS355
BS183 Bairnsdale VIC (22)
BS495
BS496
BS494
BS176
BS178
BS175
BS174
BS173
BS179
BS182
BS180
BS359
BS361
BS357
BS392
BS387
BS520
BS519
BS521
BS522
BS524
BS517
BS368
BS369
Welshpool VIC (56)
Tyers VIC (55)
Mallacoota VIC (53)
Cann River VIC (21)
Drouin VIC (58)
Nowa Nowa VIC (54)
QLD
NSW
SA
VIC
ACT
TAS
0
280
560 km
25
57
51
29
60
53
66
30
44

Figure 4.2

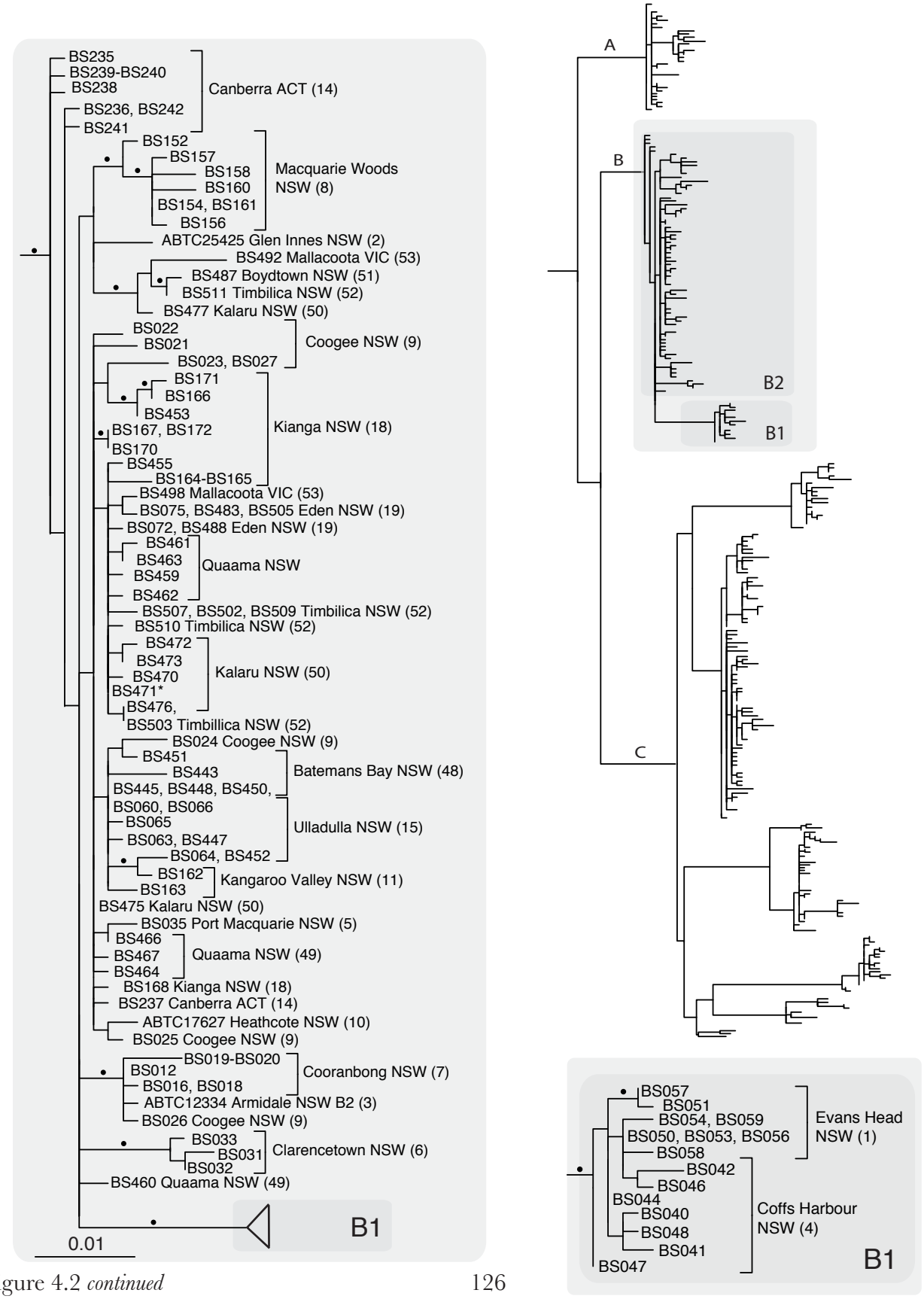

Figure 4.2 *continued*

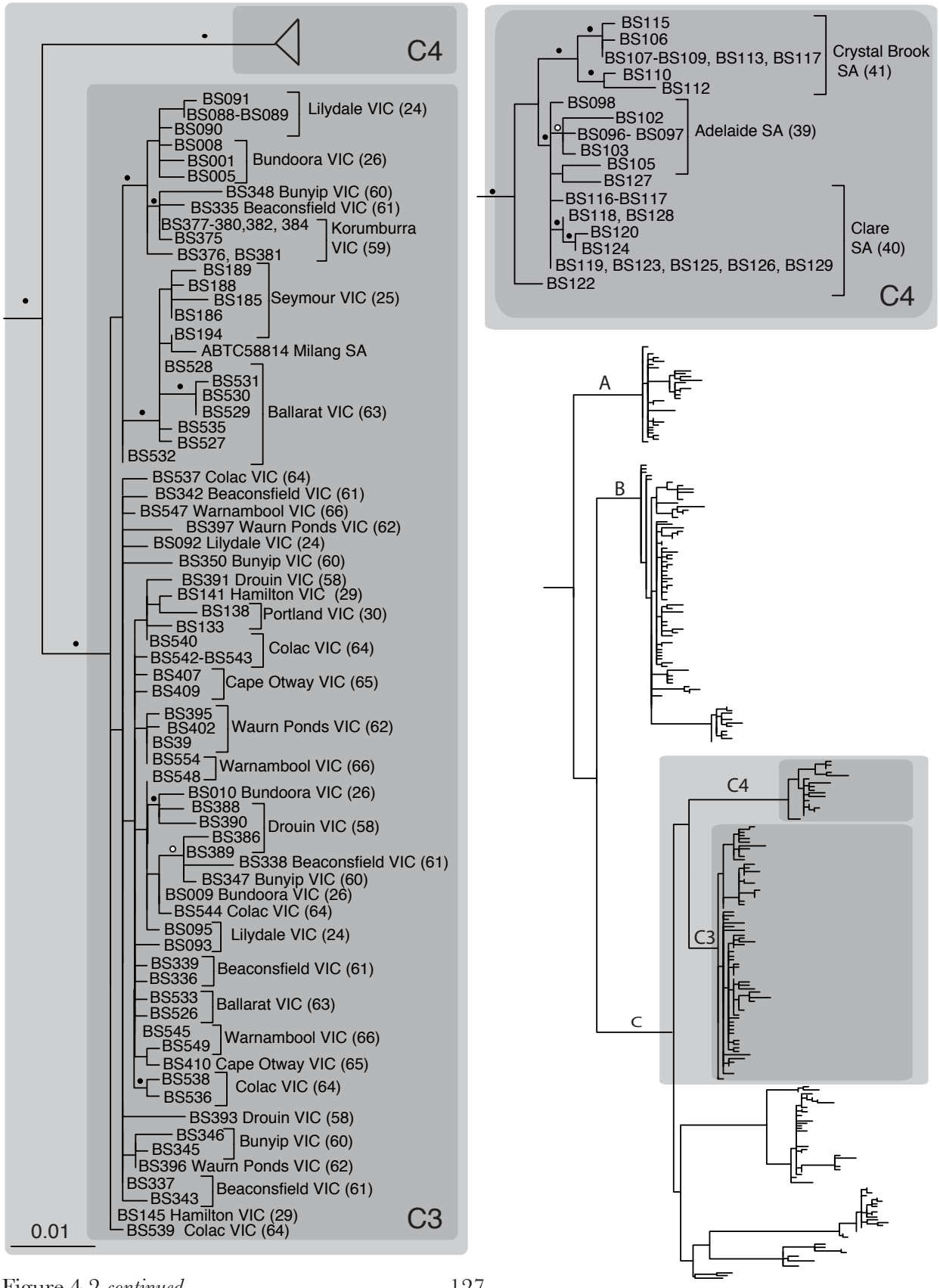

Figure 4.2 *continued*

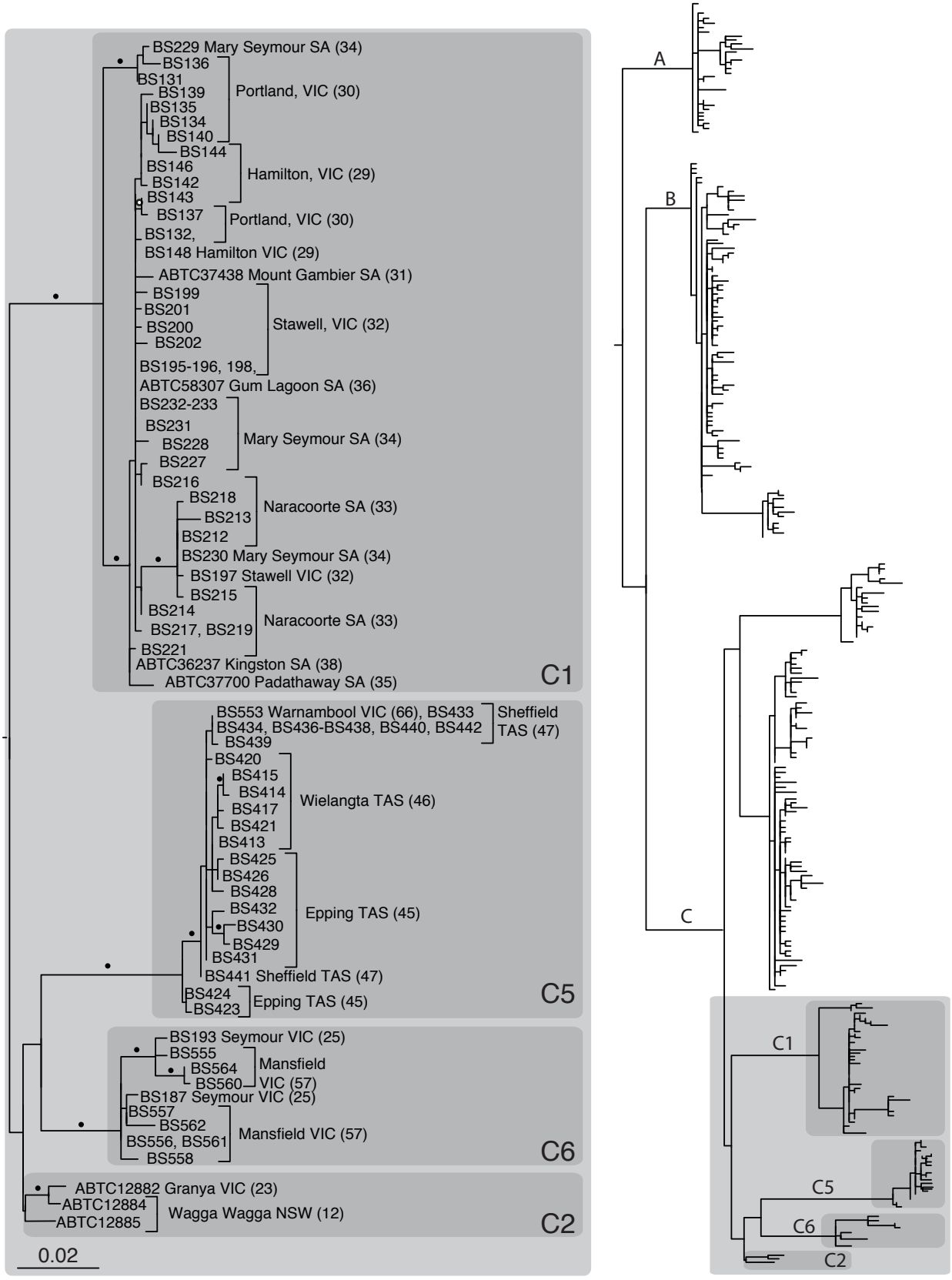

Figure 4.2 *continued*

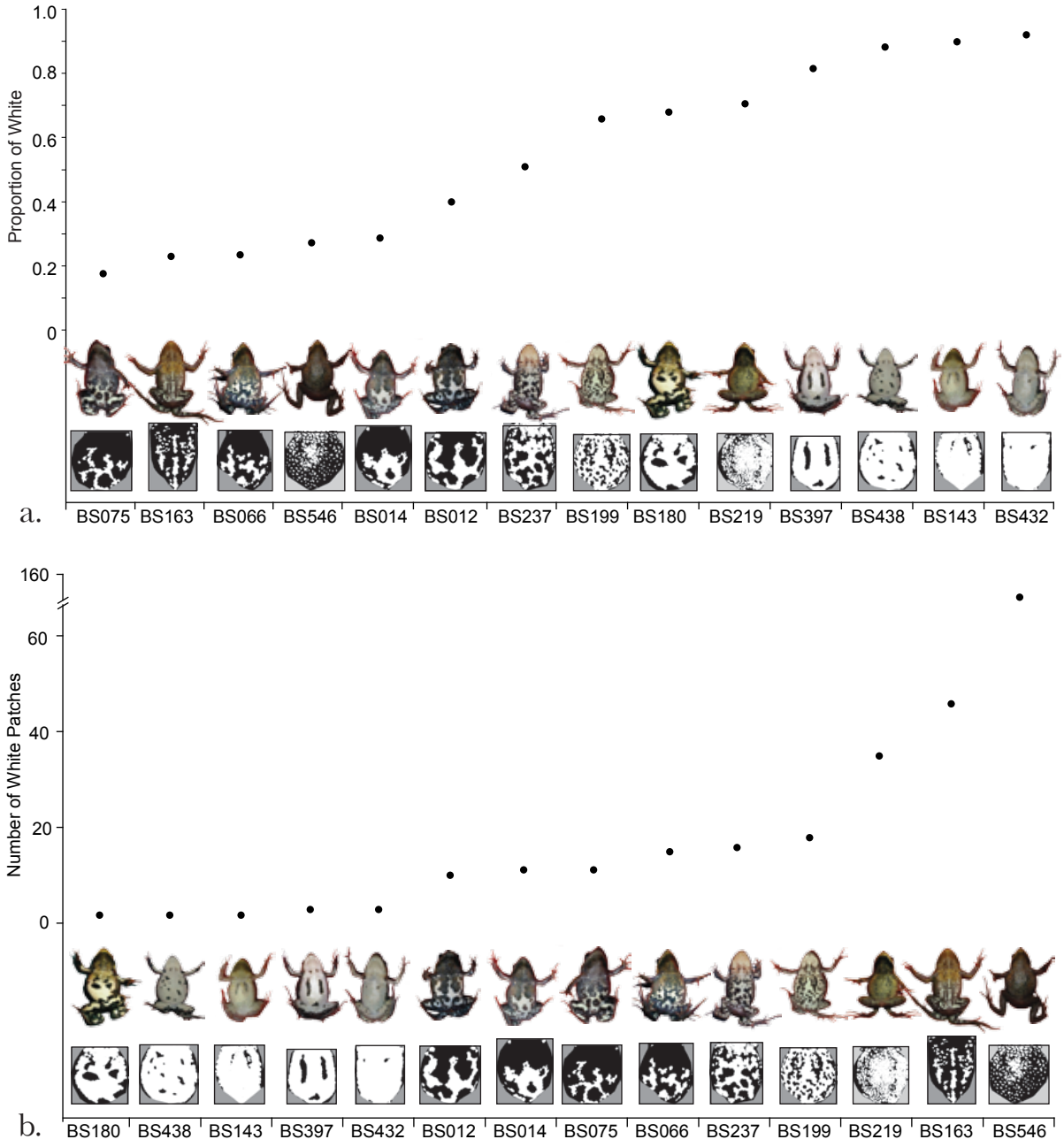

Figure 4.3. A sample of *C. signifera* color pattern variation for two traits: (a.) Proportion of White and (b.) Number of White Patches. Below the images of frogs, samples of binary images that result from automated conversion in MatLab are illustrated in order to show how varying degrees of white or gray are similarly categorized. Note that frogs are not shown in the same order between measures.

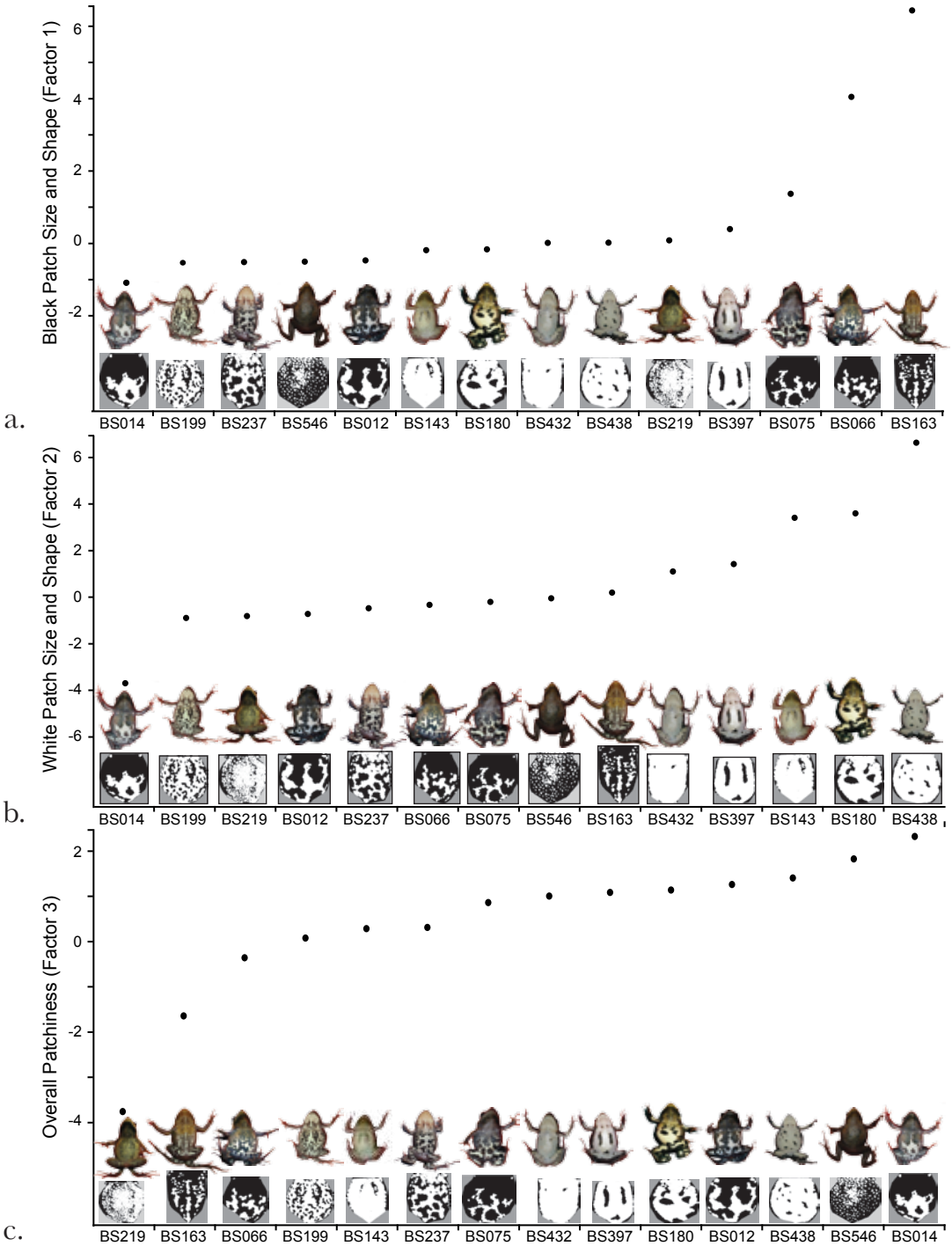

Figure 4.4. A sample of *C. signifera* color patterns relative to variation in each of the first three rotated PCA factors: (a.) Size and Shape of Black Patches (Factor 1), (b.) Size and Shape of White Patches (Factor 2), (c.) Overall Patchiness (Factor 3). Below the images of frogs, samples of binary images that result from automated conversion in MatLab are illustrated in order to show how varying degrees of white or gray are similarly categorized. Note that frogs are not shown in the same order among factors and that the scale of variance differs among factors.

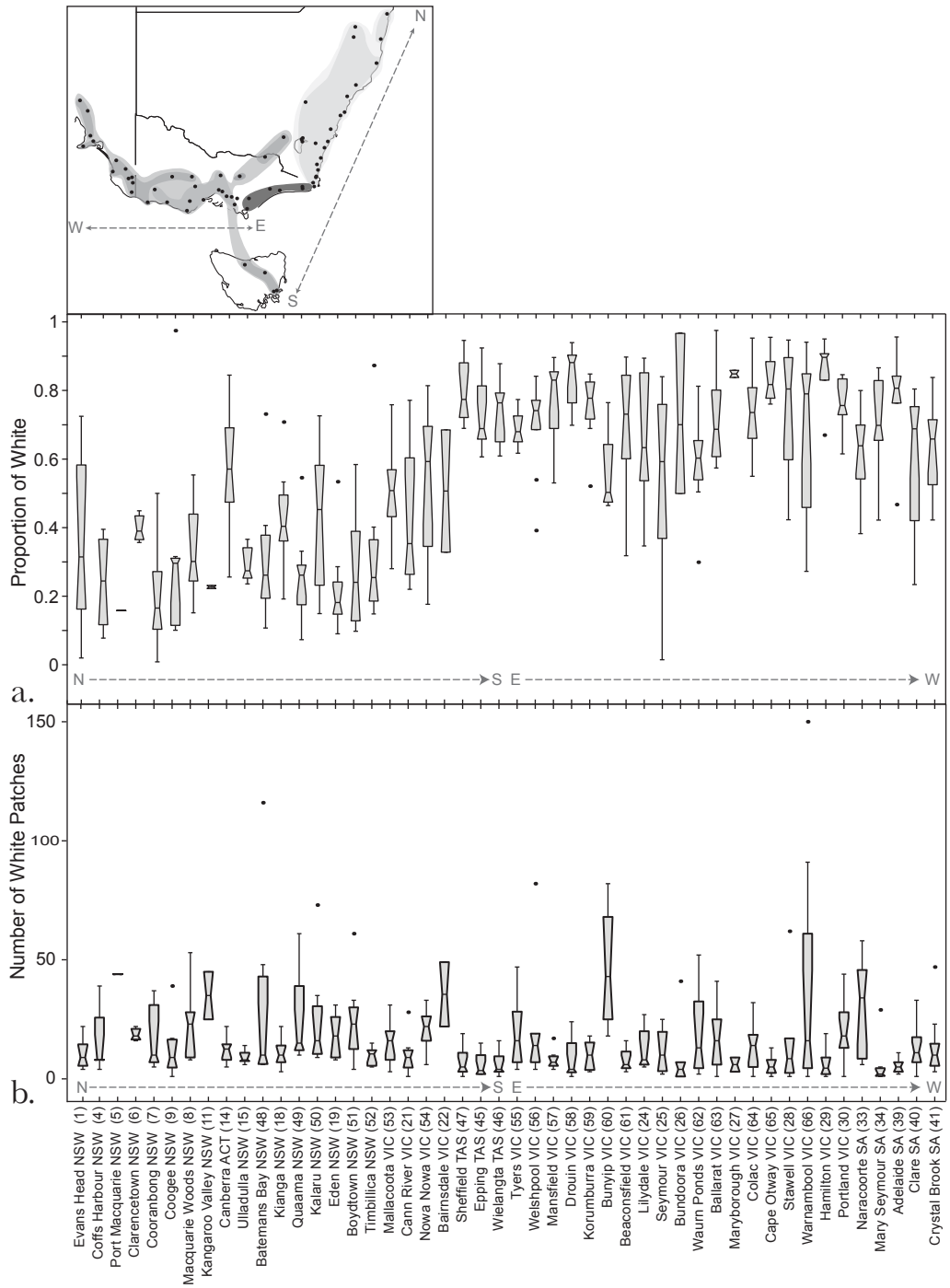

Figure 4.5. Within- and among-site variation of color patterns in *C. signifera* represented by box plots: (a.) Proportion of White and (b.) Number of White Patches. Boxes represent the first inter-quartile range, lines across the middle of the box represent the median and the whiskers represent the third interquartile range. Outliers (dots) are those points that lie beyond one and a half times the interquartile range. Notches in the boxes represent median variability. Sites listed along the x-axis are arranged from north to south along the east coast of Australia and east to west along the south as illustrated on the map above the graphs. Site numbers are shown in Fig. 4.1.

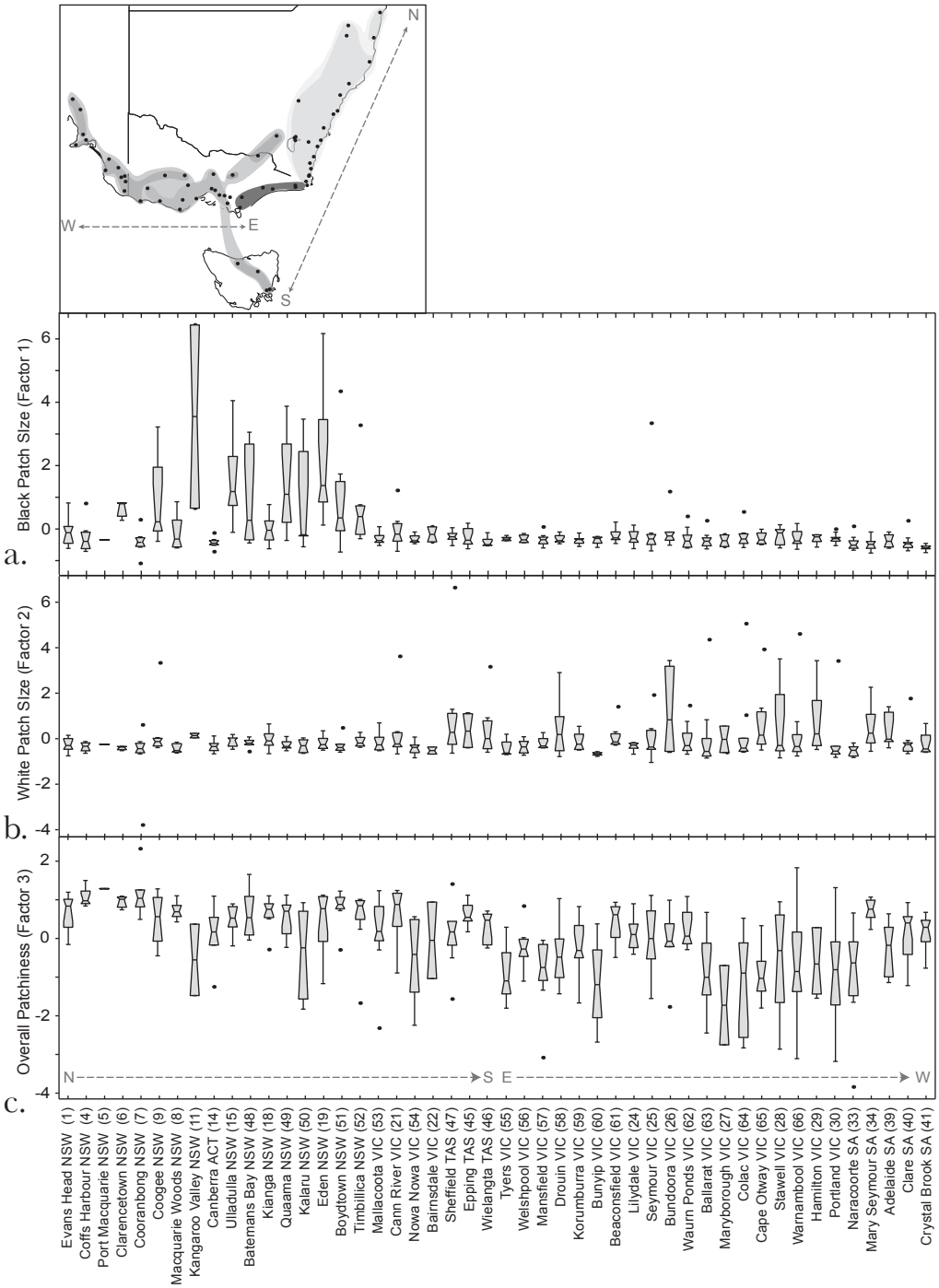

Figure 4.6. Within- and among-site variation of color patterns in *C. signifera* represented by box plots for each of the three rotated PCA factors: (a.) Size and Shape of Black Patches, (b.) Size and Shape of White Patches, (c.) Overall Patchiness. Note that the scale of variance differs among factors. Boxes represent the first inter-quartile range, lines across the middle of the box represent the median and the whiskers represent the third interquartile range. Outliers are those points that lie beyond one and a half times the interquartile range. Notches in the boxes represent median variability. Sites listed along the x-axis are arranged from north to south along the east coast of Australia and east to west along the south as illustrated on the map above the graphs. Site numbers are shown in Fig. 4.1.

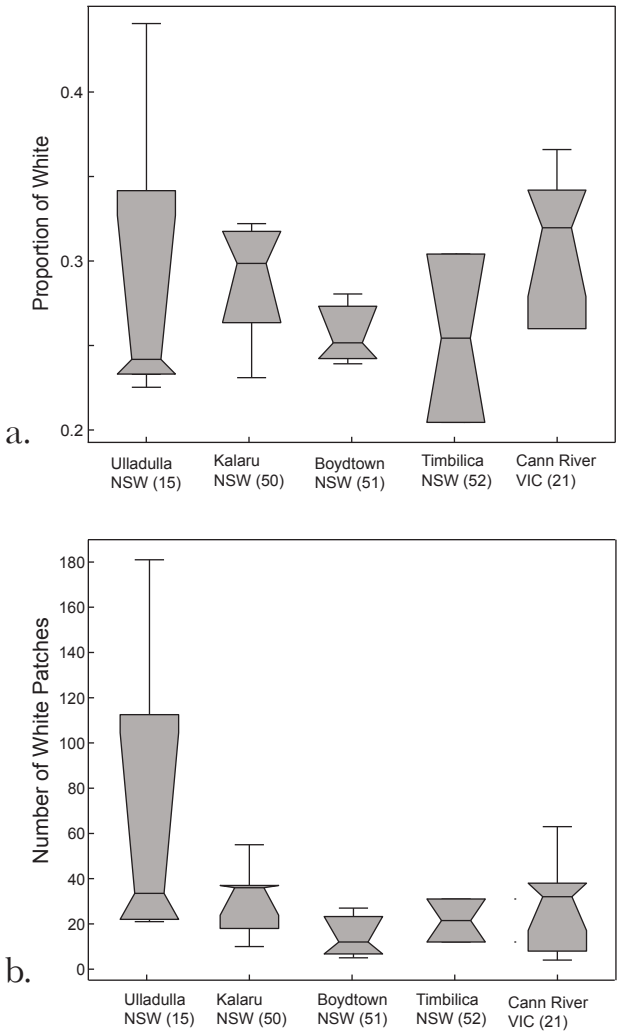

Figure 4.7. Within- and among-site variation of color patterns in *Pseudophryne* represented by box plots: (a.) Proportion of White and (b.) Number of White Patches. Boxes represent the first inter-quartile range, lines across the middle of the box represent the median of the trait and the whiskers represent the third interquartile range. Outliers are those points that lie beyond one and a half times the interquartile range. Notches in the boxes represent variability of the median. Sites are arranged from north to south along the east coast of Australia on the x-axis and site numbers correspond to those on Fig. 4.1 (stars) and in Table 4.2.

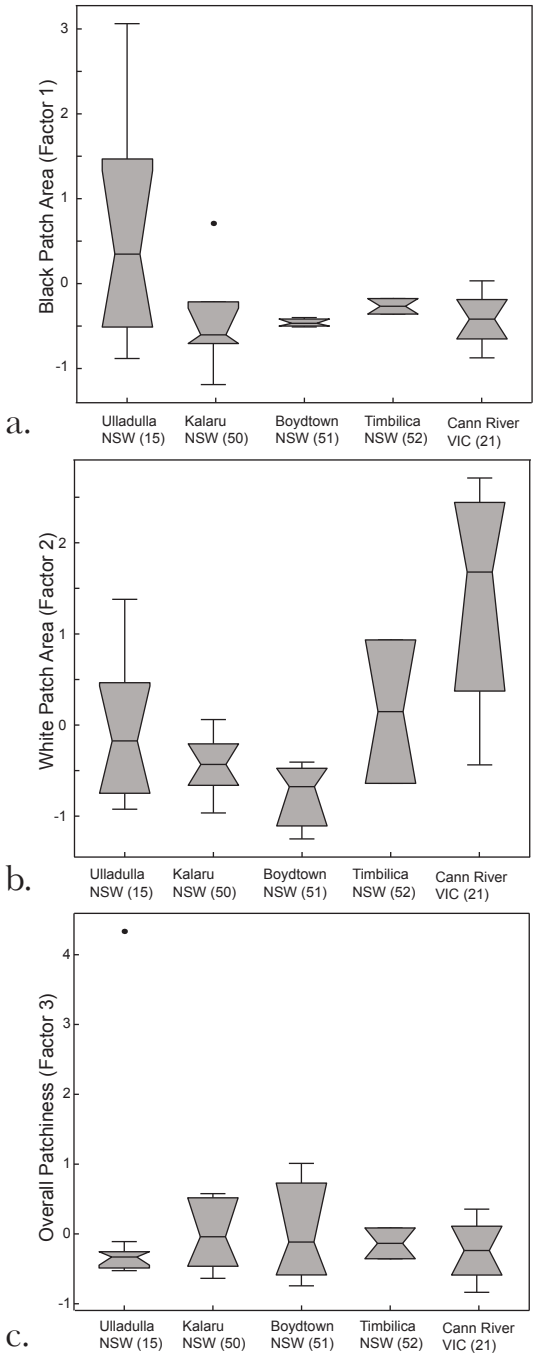

Figure 4.8. Within- and among-site variation of color pattern variation in *Pseudophryne* represented by Box plots for each of the three rotated PCA factors: (a.) Size and Shape of Black Patches, (b.) Size and Shape of White Patches, (c.) Overall Patchiness. Boxes represent the first inter-quartile range, lines across the middle of the box represent the median of the trait and the whiskers represent the third interquartile range. Outliers are those points that lie beyond one and a half times the interquartile range. Notches in the boxes represent median variability. Sites are arranged from north to south along the east coast of Australia on the x-axis along with site numbers shown on Fig. 4.1 (stars) and in Table 4.2. Note that the scale of variance differs among the graphs.

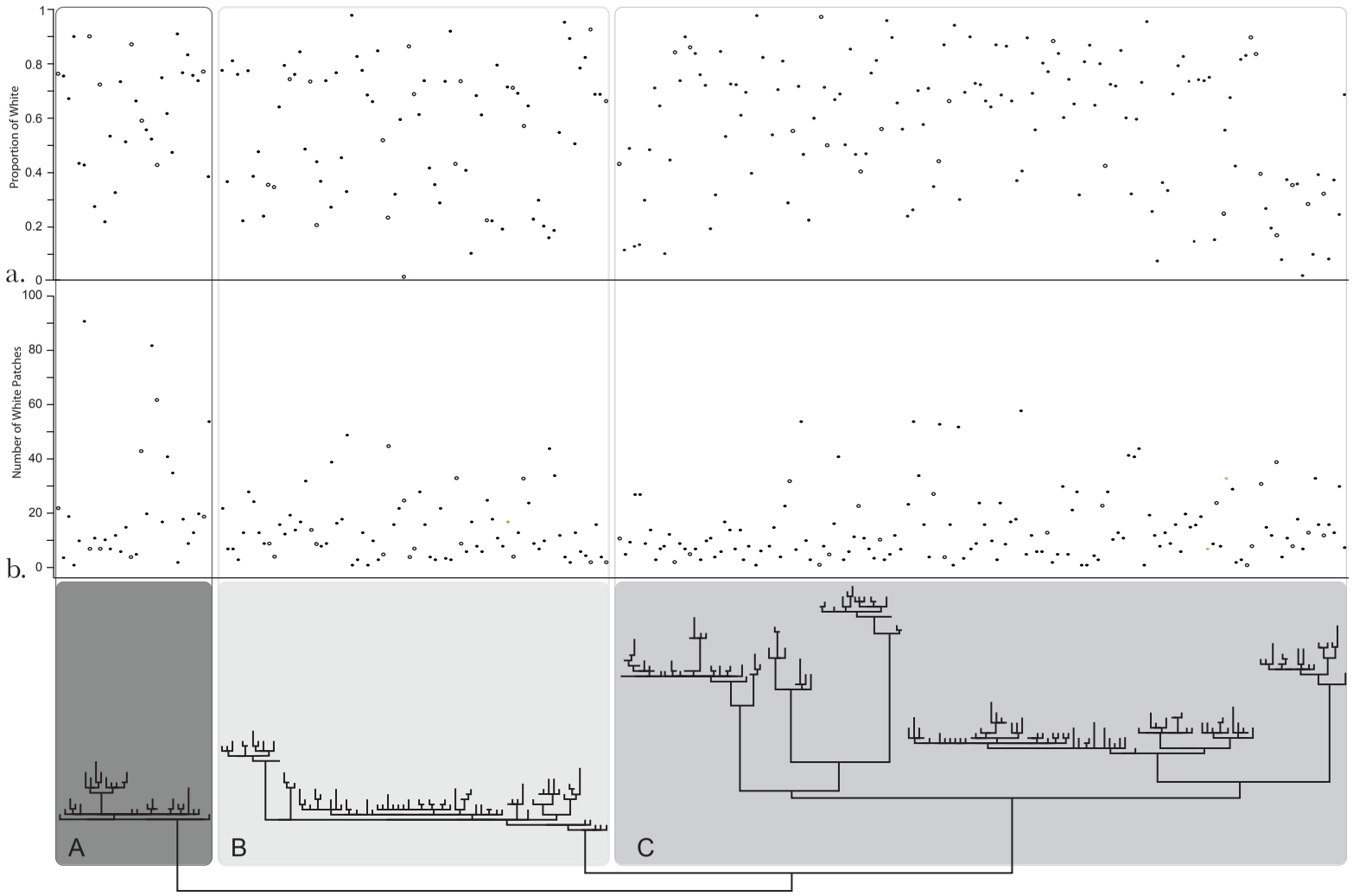

Figure 4.9. Color pattern variation observed in *C signifera* relative to phylogenetic relationships for (a.) Proportion of White and (b.) Number of White Patches. Closed circles represent individual measures. Open circles represent means of multiple individuals represented by a single tip (redundant haplotypes). The illustrated tree is the best ML tree estimated by GARLI with branch lengths used in phylogenetic simulations, and shading correspond to that in Fig. 4.2.

References

Ackerly, D. D. 2000. Taxon sampling, correlated evolution, and independent contrasts. *Evolution*, 54:1480-1492.

Ackerly, D.D., Nyffeler, R. 2004. Evolutionary diversification of continuous traits: phylogenetic tests and application to seed size in the California flora. *Evolutionary Ecology*, 18:249-272.

Allen, J.A., Weale, M.E. 2005. Anti-apostatic selection by wild birds on quasi-natural morphs of the land snail *Cepaea hortensis*: a generalised linear mixed models approach. *Oikos*, 108:335-343.

Balogh, A.C.V., Gamberale-Stille, G. Leimar, O. 2008. Learning and the mimicry spectrum: from quasi-Bates to super-Müller. *Animal Behaviour*, 76:1591-1599.

Barker, R.D., Vestjens, W.J.M. 1979. *The food of Australian birds, Volume 1 - Non-passerines*. CSIRO, Canberra.

Barker, J., Grigg, G.C., Tyler, M.J. 1995. *A Field Guide to Australian Frogs*. Surrey Beatty and Sons, Chipping Norton.

Barrows, T.T., Stone, J.O., Fifield, L.K., Cresswell, R.G. 2002. The timing of the Last Glacial Maximum in Australia. *Quaternary Science Reviews*, 21:159-173.

Bates, H.W. 1862. Contributions to an insect fauna of the Amazon valley. Lepidoptera: Heliconidae. *Transactions of the Linnean Society of London*, 23:495-566.

Berry, L., Lill, A. 2003. Do predation rates on artificial nests accurately predict predation rates on natural nests? The effects of nest type, egg type and nest-site characteristics. *Emu*, 103:207-214.

Blacket, M.J., Cooper, S.J.B., Krajewski, C., Westerman, M. 2006. Systematics and evolution of the dasyurid marsupial genus *Sminthopis*: II. The Murina species group. *Journal of Mammalian Evolution*, 13:125-138.

Blanchard, F.N. 1929. Re-discovery of *Crinia tasmaniensis*: With notes on this and other Tasmanian frogs. *Proceedings of the Zoological Society of London*, 1910:627-634.

Blomberg, S.P., Garland, T., Jr. and Ives, A.R. 2003. Testing for phylogenetic signal in comparative data: Behavioral traits are more labile. *Evolution*, 57:717-745.

Bond, A.B., Kamil, A.C. 2002. Visual predators select for crypticity and polymorphism in virtual prey. *Nature*, 415:609-613.

Bond, A.B. 2007. The evolution of color polymorphism: Crypticity, searching images, and apostatic selection. *Annual Review of Ecology, Evolution and Systematics*, 38:489-514.

Boulton, R.L., Clarke, M.F. 2003. Do yellow-faced honeyeater (*Lichenostomus chrysops*) nests experience higher predation at forest edges? *Wildlife Research*, 10:119-125.

Bowler, J.M. 1982. Aridity in the late Tertiary and Quaternary of Australia. In: W.R. Barker and P.J.M. Greenslade (Ed.), *Evolution of the Flora and Fauna of Arid Australia*. Peacock Publications, Adelaide, pp. 35-45.

Brisson, J.A., DeToni, D.C., Duncan, I., Templeton, A.R. 2005. Abdominal pigmentation variation in *Drosophila polymorpha:* Geographic variation in the trait, and underlying phylogeography. *Evolution*, 59:1046-1059.

Brodie, E.D., III. 1993. Differential avoidance of coral snake banded patterns by free-ranging avian predators in Costa Rica. *Evolution*, 47:227-235.

Brower, J.Vz. 1960. Experimental studies of mimicry. IV. The reactions of starlings to different proportions of models and mimics. *American Naturalist*, 94:271-282.

Brower, A.V. 1996. Rapid morphological radiation among races of butterfly *Heliconius erato* inferred from patterns of mitochondrial DNA evolution. *Evolution*, 50:195-221.

Brown, J.M., Lemmon, A.R. 2007. The importance of data partitioning of the utility of Bayes factors in Bayesian phylogenetics. Systematic Biology, 56:643-655.

Brown, K.S., Benson, W.W. 1974. Adaptive polymorphism associated with multiple Müllerian mimicry in *Heliconius numata* (Lepid.: Nymph.). *Biotropica*, 6:205-28.

Bull, C.M. 1975. Parallel polymorphism in Australian frogs of the genus *Ranidella*. *Heredity*, 35:273-278.

Bull, C.M. 1977. Back pattern polymorphism and tadpole growth rate in two western Australian frogs. *Australian Journal of Zoology*, 25:243-248.

Butler, M. A., King, A. A. 2004. Phylogenetic comparative analysis: A modeling approach for adaptive evolution. *American Naturalist*, 164:683–695.

Cain, A.J. 1973. Visual selection by tone of Cepaea nemoralis. *Journal of Choncology*, 23:333-336.

Cannatella, D.C., Hillis, D.M., Chippindale, P.T., Weigt, L., Rand, A.S., Ryan, M.J. 1998. Phylogeny of frogs of the *Physalaemus pustulosus* species group, with an examination of data incongruence. *Systematic Biology*, 47:311-335.

Chapple, D.G., Keogh, J.S. 2004. Parallel adaptive radiation in arid and temperate Australia: molecular phylogeography and systematics of the *Egernia whitii* (Lacertilia: Scincidae) species group. *Biological Journal of the Linnean Society*, 83:157-173.

Chapple, D.G., Keogh, J.S., Hutchinson, M.N. 2005. Substantial genetic substructuring in southeastern and alpine Australia revealed by molecular phylogeography of the *Egernia whitii* (Lacertilia: Scincidae) species group. Molecular Ecology, 14:1279-1292.

Chapple, D.G., Hutchinson, M.N., Maryan, B., Plivelich, M., Moore, J.A., Keogh, J.S. 2008. Evolution and maintenance of colour pattern polymorphism in *Liopholis* (Squamata:Scincidae). *Australian Journal of Zoology*, 56:103-115.

Charlesworth, D., Charlesworth, B. 1975. Theoretical genetics of Batesian mimicry. I. Single Locus Model. *Journal of Theoretical Biology*, 55:283-303.

Chittka, L., Osorio, D. 2007. Cognitive dimensions of predator responses to imperfect mimicry. *PLOS Biology*, 5:2754-2758.

Cogger, H. G. 2000. *Reptiles and Amphibians of Australia, Sixth edition*. Ralph Curtis Books, Florida.

Colhoun, E.A., Hannan, D., Kiernan, K. 1996. Late Wisconsin glaciation of Tasmania. Papers and Proceedings of the Royal Society of Tasmania, 130:33-45.

Cook, L.M. 1986. Polymorphic snails on varied backgrounds. *Biological Journal of the Linnean Society*, 29:89-99.

Cott, H.B. 1940. *Adaptive Coloration in Animals*. Methuen and Co., Ltd., London.

Croshaw, D.A. 2005. Cryptic behavior is independent of dorsal color polymorphism in juvenile northern leopard frogs (*Rana pipiens*). *Journal of Herpetology*, 39:125-129.

Daly, J.W., Highet, R.J., Myers, C.W. 1984. Occurrence of skin alkaloids in nondendrobatid frogs from Brazil (Bufonidae), Australia (Myobatrachidae) and Madagascar (Mantellinae). *Toxicon*, 22:905-919.

Daly, J.W., Garraffo, H.M., Pannell, L.K., Spande, T.F. 1990. Alkaloids from Australian frogs (Myobatrachidae): Pseudophrynamines and pumiliotoxins.

Journal of Natural Products, 53:407-421.

Daly, J.W. 1995. The chemistry of poisons in amphibian skin. *Proceedings of the National Academy of Science, USA*, 92:9-13.

Darst, C.R., Cannatella, D.C. 2004. Novel relationships among hyloid frogs inferred from 12S and 16S mitochondrial DNA sequences. *Molecular Phylogenetics and Evolution*, 31:462-475.

Darst, C.R., Cummings, M.E. 2006. Predator learning favours mimicry of a less toxic model in poison frogs. *Nature*, 440:208-211.

Desmarchelier, J.M., Goede, A., Ayliffe, L.K., McCulloch, M.T., Moriarty, K. 2000. Stable isotope record and its palaeoenvironmental interpretation for a late Middle Pleistocene speleotherm from Victoria Fossil Cave, Naracoorte, South Australia. *Quaternary Science Reviews*, 19:763-774.

Dickinson, J.A., Wallace, M.W., Holdgate, G.R., Gallagher, S.J., Thomas, L. 2002. Origin and timing of the Miocene-Pliocene unconformity in southeast Australia. *Journal of Sedimentary Research*, 72:288-303.

Dolman, G., Moritz, C. 2006. A multilocus perspective on refugial isolation and divergence in rainforest skinks (*Carlia*). *Evolution*, 60:573-582.

Donnellan, S.C., McGuigan, K., Knowles, R., Mahony, M., Moritz, C. 1999. Genetic evidence for species boundaries in frogs of the *Litoria citropa* species-group (Anura: Hylidae). *Australian Journal of Zoology*, 47:275-293.

Duellman, W.E., Trueb, L. 1986. Biology of Amphibians. The Johns Hopkins University Press, Baltimore, MD, USA.

Edwards, D.L., Roberts, J.D., Keogh, J.S. 2007. Impact of Plio-Pleistocene arid cycling on the population history of a southwestern Australian frog. *Molecular Ecology*, 16:2782-2796.

Endler, J.A. 1978. A predator's view of animal color patterns. *Evolutionary Biology*, 11:319-364.

Endler, J.A. 1990. On the measurement and classification of color in studies of animal color patterns. *Biological Journal of the Linnean Society*, 41:315-352.

Endler, J.A. 1993. The color of light in forests and its implications. *Ecological Monographs*, 63:1-27.

Erspamer, V., Falconieri-Erspamer, G., Mazzanti, G., Endean, R. 1984. Active peptides in the skins of one hundred amphibian species from Australia and Papua New Guinea. *Comparative Biochemistry and Physiology*, 77C:99-108.

Evans, B.J., Kelley, D. B., Tinsley, R.C., Melnick, D.J., Cannatella, D.C. 2004. A mitochondrial DNA phylogeny of African clawed frogs: phylogeography and implications for polyploid evolution. *Molecular Phylogenetics and Evolution*, 33:197-213.

Felsenstein, J. 1985. Phylogenies and the comparative method. *The American Naturalist*, 125:1-15.

Felsenstein, J. 1988. Phylogenies and quantitative characters. *Annual Review of Ecology and Systematics*, 19:445-471.

Fisher, R.A. 1927. On some objections to mimicry theory: statistical and genetic. *Transactions of the Royal Entomological Society of London*, 75:269-278.

Ford, E.B. 1975. *Ecological Genetics*. Chapman and Hall, London.

Forsman, A., Shine, R. 1995. The adaptive significance of colour pattern polymorphism in the Australian scincid lizard *Lampropholis delicata*. *Biological Journal of the Linnean Society* 55, 273-291.

Forsman, A., Ahnesjö,, J. Caear, S., Karlsson, M.K. 2008. A model of ecological and evolutionary consequences of color polymorphism. *Ecology*, 88:34-40.

Forsman, A., Åberg, V. 2008. Associations of variable coloration with niche breadth and conservation status among Australian reptiles. *Ecology*, 89:1201-1207.

Franks, D.W., Oxford, G.S. 2009. The evolution of exuberant visible polymorphisms. Evolution, Accepted Article; doi:10.111/j.1558-5646.2009.00748.

Fulton, G.R., Ford, H.A. 2003. Quail eggs, modelling clay eggs, imprints and small mammals in an Australian woodland. *Emu*, 103:255-258.

Galeotti, P., Rubolini, D., Dunn, P.O., Fasola, M. 2003. Colour polymorphism in birds: causes and functions. *Journal of Evolutionary Biology*, 16:635-646.

Gallagher, S.J., Greenwood, D.R., Taylor, D., Smith, A.J., Wallace, M.W., Holdgate, G.R. 2003. The Pliocene climatic and environmental evolution of southeastern Australia: evidence from the marine and terrestrial realm. *Palaeogeography, Palaeoclimatology, Palaeoecology*, 193, 349-382.

Garland, T., Jr., Dickerman, A.W., Janis, C.M. and Jones, J.A. 1993. Phylogenetic analysis of covariance by computer simulation. *Systematic Biology*, 42:265-292.

Garland, T., Jr., Midford, P.E., Ives, A.R. 1999. An introduction to phylogenetically based statistical methods, with a new method for confidence intervals on ancestral values. *American Zoologist*, 39:374-388.

Garrick, R.C., Sands, C.J., Rowell, D.M., Hillis, D.M., Sunnucks, P. 2007. Catchments catch all: long-term population history of a giant springtail from the southeast Australian highlands - a multigene approach. Molecular Ecology, 16:1865-1882.

Ghirlanda, S, Enquist, M. 2003. A century of generalization. *Animal Behaviour*, 66: 15-36.

Goebel, A.M., Donnelly, J.M., Atz, M.E. 1999. PCR primers and amplification methods for 12S ribosomal DNA, the control region, cytochrome oxidase I, and cytochrome b in bufonids and other frogs, an overview of PCR primers which have amplified DNA in amphibians successfully. *Molecular Phylogenetics and Evolution*, 11:163-199.

Graham, C.H., Moritz, C., Williams, S.E. 2006. Habitat history improves prediction of biodiversity in rainforest fauna. *Proceedings of the National Academy of Sciences USA*, 103:632-636.

Gray, S.M., McKinnon, J.S. 2006. Linking color polymorphism maintenance and speciation. Trends in Ecology and Evolution, 22:72-79.

Hanlon, R.T., Chiao, C.C., Mathger, L.M., Barbsa, A., Buresch, K.C., Chubb, C. 2009. Cephalopod dynamic camoflauge: bridging the continuum between background matching and disruptive coloration. *Philosophical Transactions of the Royal Society of London, B, Biological Sciences*, 364: 429-437.

Hedrick, P.W. 2006. Genetic polymorphism in heterogeneous environments: The age of genomics. *Annual Review of Ecology, Evolution and Systematics*, 37:67-93.

Hewitt, G.M. 2004. Genetic consequences of climatic oscillations in the Quaternary. *Philosophical Transactions of the Royal Society of London, B, Biological Sciences*, 359:183-195.

Heyer, R.W., Daugherty, C.H., Maxson, L.R. 1982. Systematic Resolution of the genera of the *Crinia* complex (Amphibia: Anura: Myobatrachidae). *Proceedings of the Biological Society of Washington*, 95:423- 427.

Higgins, P.J., Davies, S.J.J.F. 1996. *Handbook of Australian, New Zealand and Antarctic Birds,*

Volume 3, Snipe to Pigeons. Oxford University Press, New York.

Hoffman, E. A., Blouin, M.S. 2000. A review of colour and pattern polymorphisms in anurans. *Biological Journal of the Linnean Society*, 70:633-665.

Hoffman, E.A., Schueler, F.W., Jones, A.C., Blouin, M.S. 2006. An analysis of selection on a colour polymorphism in the northern leopard frog. *Molecular Ecology*, 15:2627-2641.

Holdgate, G.R., Wallace, M.W., Gallagher, S.J., Smith, A.J., Keene, J.B., Moore, D., Shafik, S. 2003. Plio-Pleistocene tectonics and eustasy in the Gippsland basin, southeast Australia: evidence from magnetic imagery and marine geological data. *Australian Journal of Earth Science*, 50:403– 426.

Holloway, G., Gilbert, F., Brandt, A. 2001. The relationship between mimetic imperfection and phenotypic variation in insect colour patterns. *Proceedings of the Royal Society of London, Series B*, 269:411-416.

Hope, G.S. 1994. Quaternary Vegetation. In: R.S. Hill (Ed.), *History of Australian Vegetation*. Cambridge University Press, New York, pp. 368-389.

Hope, G., Kershaw, A.P., van der Kaars, S., Xiangjun, S., Liew, P.M., Heusser, L.E., Takahara, H., McGlone, M., Miyoshi, N., Moss, P.T. 2004. History of vegetation and habitat change in the Austral-Asian region. *Quaternary International*, 118-119:103-126.

Houlden, R.B., Costello, B.H., Sharkey, D., Fowler, E.V., Melzer, A., Ellis, W., Carrick, F., Baverstock, P.R., Elphinstone, M.S. 1999. Phylogeographic differentiation in the mitochondrial control region in the koala, *Phascolarctos cinereus* (Goldfuss 1817). Molecular Ecology, 8:999-1011.

Hugall, A., Moritz, C. Moussalli, A., Stanisic, J. 2002. Reconciling paleodistribution models and comparative phylogeography in the Wet Tropics rainfores land snail *Gnarosophia bellendenkerensis* (Brazier 1875). *Proceedings of the National Academy of Science USA*, 99:6112-6117.

Ives, A.R., Midford, P.E., Garland, T., Jr. 2007. Within-species variation and measurement error in phylogenetic comparative methods. *Systematic Biology*, 56:252-270.

James, C. H., Moritz, C. 2000. Intraspecific phylogeography in the sedge frog *Littoria fallax* (Hylidae) indicates pre-Pleistocene vicariance in open forest species from eastern Australia. *Molecular Ecology*, 9:349-358.

Jiggins, C.D., Naisbit, R.E., Coe, R.L., Mallet, J.M. 2001. Reproductive isolation caused by mimicry. *Nature*, 411:302-305.

Jones, J.S., Leith, B.H., Rawlyings, P. 1977. Polymorphism in *Cepaea*: A problem with too many solutions? *Annual Review of Ecology and Systematics*, 8:109-143.

Joron, M., Iwasa, Y. 2005. The evolution of a Müllerian mimic in a spatially distributed community. *Journal of Theoretical Biology*, 237:87-103.

Kapan, D.D. 2001. Three-butterfly system provides a field test of müllerian mimicry. *Nature*, 409:338-340.

Keogh, J.S., Scott, I.A.W., Hayes, C. 2005. Rapid and repeated origin of insular gigantism and dwarfism in Australian tiger snakes. *Evolution*, 59:226-233.

Kershaw, A.P., D'Costa, D.M., McEwen Mason, J.R.C., Wagstaff, B.E. 1991. Palynological evidence for quaternary vegetation and environments of mainland southeastern Australia. *Quaternary Science Reviews*, 10:391-404.

Kime, N.M., Rand, A.S., Kapfer, M., Ryan, M.J. 1998. Consistency of female choice in the túngara frog: a permissive preference for complex characters. Animal Behaviour, 55:641–649.

Kuchta, S.R. 2005. Experimental support for aposematic coloration in the salamander *Ensatina escholtzii xanthoptica*: Implications for mimicry of pacific newts. *Copeia*, 2005:265-271.

Lamar, W.W., Wild, E.R. 1995. Comments on the natural history of *Lithodytes lineatus* (Anura: Leptodactylidae), with a description of the tadpole. *Herpetological Natural History*, 3:135-142.

Lambeck, K., Chappell, J. 2001. Sea level change through the last glacial cycle. *Science*, 292:679-686.

Lande, R. 1981. Models of speciation by sexual selection on polygenic traits. *Proceedings of the National Academy of Science, U.S.A.*, 78:3721-3725.

Lauck, B. 2005. Life history of the frog *Crinia signifera* in Tasmania, Australia. *Australian Journal of Zoology*, 53:21-27.

Lee, C., Mooers, A.O., Blay, S., Singh, A., Oakley, T.H. 2006. CoMET: A Mesquite package for comparison of continuous models of character evolution on phylogenies. *Evolutionary Bioinformatics Online*, 2:193-196.

Lemckert, F. 2005a. Body size of male common eastern froglets *Crinia signifera* does not appear to influence mating success during explosive mating events. *Acta Zoologica Sinica*, 51:232-236.

Lemckert, F. 2005b. Population structure, individual growth and survival of an Australian frog *Crinia signifera* at a pond. *Acta Zoologica Sinica*, 41:393-400.

Lemmon, E.M., Lemmon, A.R., Cannatella, D.C. 2007. Geological and climatic forces driving speciation in the continentally distributed trilling chorus frogs (*Pseudacris*). *Evolution*, 61:2086-2103.

Leys, R., Watts, C.H.S., Cooper, S.J.B., Humphreys, W.F. 2003. Evolution of subterranean diving beetles (Coleoptera: Dyctidae Hydorporini, Bidessini) in the arid zone of Australia. *Evolution*, 57:2819-2834.

Lindström, L., R. V. Alatalo, A. Lyytinen, and J. Mappes. 2001. Predator experience on cryptic prey affects the survival of conspicuous aposematic prey. *Proceedings of the Royal Society of London, B Biological Sciences*, 268:357-361.

Littlejohn, M.J. 1958. A new species of frog of the genus *Crinia* Tschudi from south-eastern Australia. *Proceedings of the Linnean Society of NSW*, 83:222-223.

Littlejohn, M.J. 1959. Call differentiation in a complex of seven species of *Crinia* (Anura: Leptodactylidae). *Evolution*, 13:452-468.

Littlejohn, M.J. 1964. Geographic isolation and mating call differentiation in *Crinia signifera*. *Evolution*, 18:262-266.

Littlejohn, M.J., Martin, A.A. 1965. A new species of *Crinia* (Anura: Leptodactylidae) from South Australia. *Copeia*, 1965:319-324.

Littlejohn, M.J. 1967. Patterns of zoogeography and speciation in south-eastern Australian Amphibia. In: Weatherly, A.H. (Ed.), *Australian Inland Waters and Their Fauna*. Australian National University Press, Canberra, pp. 150-174.

Littlejohn, M.J., Roberts, J.D., Watson, G.F., Davies, M. 1993. Family Myobatrachidae. In: Glasby, C.J., Ross, G.J.B., Beesley, P.L. (Eds.), *Fauna of Australia, Vol. 2A Amphibia and Reptilia*. Australian Government Publishing Service, Canberra, pp. 1-46.

Littlejohn, M.J., Wright, J.R. 1997. Structure of the acoustic signals of *Crinia glauerti* (Anura: Myobatrachidae) from south-western Australia, and comparison with those of *C. signifera* from South Australia. *Transactions of the Royal Society of South Australia*, 121:103-117.

Littlejohn, M.J. 2003. *Frogs of Tasmania, Second edition*. University of Tasmania, Hobart, Tasmania.

Littlejohn, M.J. 2005. Geographic variation in advertisement calls of *Crinia signifera* (Anura: Myobatrachidae) in the Bass Strait area of south-eastern Australia. *Australian Journal of Zoology*, 53:221-228.

Loveridge, A. Australian Amphibia in the Museum of Comparative Zoology, Cambridge, Massachusetts. *Bulletin of the Museum of Comparative Zoology*, 78:1-60.

Lowe, K.W. 1978. Foraging strategies of the Royal Spoonbill (*Platalea regia*), the Sacred Ibis (*Threskiornis aethiopica*) and the White-faced Heron (*Ardea novaehollandiae*) in Westernport Bay. Unpublished research report, Department of Zoology, University of Melbourne.

Maan, M. E., Cumming, M.E. 2008. Female preferences for aposematic signal components in a polymorphic poison frog. *Evolution*, 62:2334-2345.

MacNally, R.C. 1985. Habitat and Microhabitat distributions in relation to ecological overlap in two species of *Ranidella* (Anura). *Australian Journal of Zoology*, 33:329-338.

Maddison, D.R., Maddison, W.P. 2004. MacClade4: analysis of phylogeny and character evolution, Ver. 4.08. Sinauer Associates, Sunderland, MA.

Main, A.R. 1957. Studies in Australian Amphibia I: Genus *Crinia* Tschudi in south-western Australia and some species from south-eastern Australia. *Australian Journal of Zoology*, 5:30-55.

Main, A.R. 1961. *Crinia insignifera* on Rottnest Island. *Journal of the Royal Society of Western Australia*, 48:60-64.

Main, A.R. 1965. The inheritance of dorsal pattern in *Crinia* species (Anura: Leptodactylidae). *Journal of the Royal Society of Western Australia*, 48:60-64.

Main, A.R. 1968. Ecology, systematics and evolution of Australian frogs. *Ecological Research*, 5:37-86.

Mallet, J. 1993. Speciation, raciation, and color pattern evolution in *Heliconius* butterflies: evidence from hybrid zones. In *Hybrid Zones and the Evolutionary Process*, ed. Harrison, R.G., pp. 226-60. Oxford University Press, New York.

Mallet, J., Joron, M. 1999. Evolution of diversity in warning color and mimicry: Polymorphisms, shifting balance, and speciation. *Annual Review of Ecology and Systematics*, 30:201-233.

Manríquez, K.C., Pardo, L.M., Wells, R.J.D., Palma, A.T. 2008. Crypsis in *Paraxanthus barbiger* (Decapoda: Brachyura): Mechanisms against visual predators. *Journal of Crustacean Biology*, 28:473-479.

Marchant, S., Higgins, P.J. 1990a. *Handbook of Australian, New Zealand and Antarctic Birds, Volume 1, Part A Ratites to Petrels.* Oxford University Press, Melbourne.

Marchant, S., Higgins, P.J. 1990b. *Handbook of Australian, New Zealand and Antarctic Birds, Volume 1, Part B Australian Pelicans to Ducks.* Oxford University Press, Melbourne.

Marchant, S., Higgins, P.J. 1993. *Handbook of Australian, New Zealand and Antarctic Birds, Volume 2, Raptors to Lapwings.* Oxford University Press, New York.

Markgraf, V., McGlone, M., Hope, G. 1995. Neogene paleoenvironmental and paleoclimatic change in southern temperate ecosystems-a southern perspective. *Trends in Ecology and Evolution*, 10:143-147.

Martins, E.P. and Garland, T.G., Jr. 1991. Phylogenetic analyses of the correlated evolution of continuous characters: A simulation study. *Evolution*, 45:534-557.

Martins, E. P. 2004. COMPARE, version 4.6b. Computer programs for the statistical analysis of comparative data. Distributed by the author at http://compare.bio.indiana.edu/. Department of Biology, Indiana University, Bloomington IN.

Maselli, V.M., Brinkworth, C.S., Bowie, J.H., Tyler, M.J. 2004. Host-defence skin peptides of the Australian common froglet *Crinia signifera*: sequence determination using positive and negative ion electrospray mass spectra. *Rapid Communications in Mass Spectrometry*, 18:2155-2161.

Matthews, A., Dickman, C.R., Major, R.E. 1999. The influence of fragment size and edge on nest predation in urban bushland. *Ecography*, 22:349-356.

McGuigan, K., McDonald, K., Parris, K., Moritz, C. 1998. Mitochondrial DNA diversity and historical biogeography of a wet forest-restricted frog (*Litoria pearsoniana*) from mid-east Australia. *Molecular Ecology*, 7:175-186.

McGuire, J.A., Linkem, C.W., Koo M.S. Hutchison, D.W., Lappin, A.K., Orange, D.I., Lemos-Espinal, J., Riddle, B.R., Jaeger, J.R. 2007. Mitochondrial Introgression and incomplete lineage sorthing through space and time: Phylogenetics of crotaphytid lizards. *Evolution*, 61:2879-2897.

McKenzie, G.M. 2002. The late Quaternary vegetation history of the south-central highlands of Victoria, Australia. II. Sites below 900m. *Austral Ecology*, 27:32-54.

McKenzie, G.M., Kershaw, A.P. 2004. A Holocene pollen record from cool temperate rainforest, Aire crossing, the Otway region of Victoria, Australia. *Review of Palaeobotany Palynology*, 132:281-290.

Merilata, S. 2001. Habitat heterogeneity, predation and gene flow: colour polymorphism in the isopod, *Idotea baltica. Evolutionary Ecology*, 15:103-116.

Merilata, S. 2006. Frequency-dependent and maintenance of prey polymorphism. *Journal of Evolutionary Biology*,19:2022-2030.

Milstead, W.W., Rand, A.S., Stewart, M. 1974. Polymorphism in cricket frogs: an hypothesis. *Evolution*, 28:489–491.

Mitchell, N.J. 2005. Nest swapping in an Australian toadlet (*Pseudophryne bibroni*): do males respond to chemical signals? *Herpetological Review*, 36:19-21.

Moore, J.A. 1954. Geographic and genetic isolation in Australian Amphibia. *American Naturalist*, 88:65- 74.

Müller, F. 1879. *Ithuna* and *Thyridia*: a remarkable case of mimicry in butterflies. *Proceedings of the Entomological Society of London*, 1879:20-29.

Nicholls, J.A., Austin, J.J. 2005. Phylogeography of an east Australian wet-forest bird, the satin bowerbird (*Ptilonorhynchus violaceus*), derived from mtDNA, and its relationship to morphology. *Molecular Ecology*,14:1485-1496.

Odendaal, F.J. and Bull, C.M. 1982. A parapatric boundary between *Ranidella signifera* and *R. riparia* (Anura: Leptodactylidae) in South Australia) Australian Journal of Zoology, 163:93-103.

Odendaal, F.J., Bull, C.M., Telford, S.R. 1986. Influence of the acoustic environment on the distribution of the frog *Ranidella riparia. Animal Behaviour*, 34:1836-1843.

Olendorf, R., Rodd, H., Punzalan, D., Houde, A.E., Hunt, C., Reznick, D., Hughes, K.A. 2006. Frequency-dependent survival in natural guppy populations. *Nature*, 441:633-636.

Osorio, D., Miklosi, A., Gonda, Zs. 1999. Visual ecology and perception of coloration patterns by domestic chicks. *Evolutionary Ecology*, 13:673-689.

Parker, H.W. 1940. The Australasian frogs of the family Leptodactylidae. *Novitates Zoologicae*, 42:1-107.

Pasteur, G. 1982. A classificatory review of mimicry systems. *Annual Review of Entomology*, 15:43-74.

Pfennig, D.W., Harcombe, W.R., Pfennig, K.S. 2001. Frequency-dependent Batesian mimicry. *Nature*, 410:322.

Pfennig, D.W., Harper, G.R.,Jr., Brumo, A.F., Harcombe, W.R., Pfennig, K.S. 2007. Population differences in predation on Batesian mimics in allopatry with their model: selection against mimics is strongest when they are common. *Behavioral Ecological Sociobiology*,61:505-511.

Phifer-Rixey, M., Heckman, M., Trussell, G.C., Schmidt, P.S. 2008. Maintenance of clinal variation for shell colour phenotype in the periwinkle, *Littorina obtusata*. *Journal of Evolutionary Biology*, 21:966-978.

Piper, S.D., Catterall, C.P. 2004. Effects of edge type and nest height on predation of artificial nests within subtropical Australian eucalypt forests. *Forest Ecology and Management*, 203:361-372.

Posada, D., Crandall, K.A. 1998. Modeltest: testing the model of DNA substitution. *Bioinformatics*, 14:817–818.

Poulton, E.B. 1890. *The Colors of Animals: Their Meaning and Use, Especially Considered in the Case of Insects*. D. Appleton and Co., New York.

Punzalan, D., Rodd, F.H., Hughes, K.A. 2005. Perceptual processes and the maintenance of polymorphism through frequency-dependent predation. *Evolutionary Ecology*, 19:303-320.

Read, K., Keogh, J.S., Scott, I.A.W., Roberts, J.D., Doughty, P. 2001. Molecular phylogeny of the Australian frog genera *Crinia*, *Geocrinia*, and allied taxa (Anura: Myobatrachidae). *Molecular Phylogenetics and Evolution*, 21:294-308.

Revell, L.J., Harmon, L.J., Collar, D.C. 2008. Phylogenetic signal, evolutionary process and rate. *Systematic Biology*, 57:591-601.

Ries, L., Mullen, S.P. 2008. A rare model limits the distribution of its more common mimic: A twist on frequency-dependent Batesian mimicry. *Evolution*, 62:1798-

1803.

Robinson, M. 2002. *A Field Guide to Frogs of Australia.* Australian Museum/Reed New Holland: Sydney.

Rockman, M.V., Rowell, D.M., Tait, N.N. 2001. Phylogenetics of *Planipapillus*, Lawn-headed onychophorans of the Australian Alps, based on nuclear and mitochondrial gene sequences. *Molecular Phylogenetics and Evolution*, 21:103-116.

Ronquist, F., Huelsenbeck, J.P. 2003. MRBAYES 3: Bayesian phylogenetic inference under mixed models. *Bioinformatics*, 19:1572-1574.

Rowe, C., Lindström, L., Lyytinen, A. 2003. *Proceedings of the Royal Society of London, B Biological Sciences*, 271:407-413.

Rowell, D.M. 1990. Fixed fusion heterozygosity in *Delena cancerides* Walck (Araneae: Sparassidae): an alternative to speciation by monobrachial fusion. *Genetica*, 80:139-157.

Rowland H.M., Ihalainen E., Lindstrom, L., Mappes, J., Speed, M.P. 2007. Co- mimics have a mutualistic relationship despite unequal defences. *Nature*, 448:64-67.

Sanderson, M.J. 2003. r8s: inferring absolute rates of molecular evolution and divergence times in the absence of a molecular clock. *Bioinformatics*, 19:301-302.

Santos, J.C., Coloma, L., Cannatella, D.C. 2003. Multiple, recurring origins of aposematism and diet specialization in poison frogs. *Proceedings of the National Academy of Sciences*, 100:12792-12797.

Saporito, R.A., Zuercher, R. Roberts, M., Gerow, K.G., Donnelly, M.A. 2007. Experimental evidence for aposematism in the dendrobatid poison frog *Oophaga pumilio*. *Copeia*, 2007:1006-1011.

Schaefer, H.C., Vences, M., Veith, M. 2002. Molecular phylogeny of Malagasy poison frogs, genus *Mantella* (Anura: Mantellidae). *Organisms, Diversity and Evolution*, 2:97-105.

Schäuble, C.S., Moritz, C. 2001. Comparative phylogeography of two open forest frogs from eastern Australia. *Biological Journal of the Linnean Society*, 74:157-170.

Schneider, C.J., Cunningham, M., Moritz, C. 1998. Comparative phylogeography and the history of endemic vertebrates in the Wet Tropics rainforests of Australia. *Molecular Ecology*, 7:487-498.

Servedio, M. 2000. The effects of predator learning, forgetting, and recognition errors on the evolution of warning coloration. *Evolution*, 54:751-763.

Sherratt, T. 2006. Spatial mosaic formation through frequency-dependent selection in Mullerian mimicry complexes. *Journal of Theoretical Biology*, 240:165-174.

Shine, R. 1977. Habitats, diets, and sympatry in snakes: A study from Australia. *Canadian Journal of Zoology*, 55:1118-1128.

Smith, B.P., Tyler, M.J., Kaneko, T., Garraffo, H.M., Spande, T.F., Daly, J.W. 2002. Evidence for biosynthesis of pseudophrynamine alkaloids by an Australian myobatrachid frog (*Pseudophryne*) and for sequestration of dietary pumiliotoxins. *Journal of Natural Products*, 65:439-447.

Sokal, R. R., Rohlf, F. J. 1995. *Biometry: the Principles and Practice of Statistics in Biological Research, 2nd edition.* W. H. Freeman and Co., San Francisco.

Speed, M.P., Turner, J.R.G. 1999. Learning and memory in mimicry: II. Do we understand the mimicry spectrum? *Biological Journal of the Linnean Society*, 67:281-312.

Speed, M.P. 2000. Warning signals, receiver psychology and predator memory. *Animal Behaviour*, 60:269-278.

Stevens, M., Parraga, A., Cuthill, I.C., Partridge, J.C., Troscianko, T.S. 2007. Using digital photography to study animal coloration. *Biological Journal of the Linnean Society*, 90:211-237.

Strahan, R. 1995. *Mammals of Australia.* Smithsonian Institution Press, USA.

Straughan, I.R., Main, A.R. 1966. Speciation and polymorphism in the genus *Crinia* Tschudi in Queensland. *Proceedings of the Royal Society of Queensland*, 78:11-28.

Storz, JF. 2002. Contrasting patterns of divergence in quantitative traits and neutral DNA markers: analysis of clinal variation. *Molecular Ecology*, 13:789-809.

Summers, K., Symula, R., Clough, M., Cronin, T. 1999. Visual mate choice in poison frogs. *Proceedings of the Royal Society of London B Biological Sciences*, 266:2141-2145.

Sunnucks, P., Blacket, M.J., Taylor, J.M., Sands, C.J., Ciavaglia, S.A., Garrick, R.C., Tait, N.N., Rowell, D.M., Pavlova, A. 2006. A tale of two flatties: different responses of two terrestrial flatworms to past environmental climatic fluctuations at Tallaganda in montane south-eastern Australia. *Molecular Ecology*, 15:4513-4531.

Svádová, K., Exnerova, A., Stys, P., Landova, E., Valenta, J., Fucikova, A., Socha, R. 2009. Role of different colours of aposematic insects in learning, memory and generalization of naive bird predators. *Animal Behaviour*, 77:327-336.

Swofford, D.L. 2003. PAUP* Phylogenetic Analysis Using Parsimony (*and Other Methods). Version 4. Sinauer Associates, Sunderland, Massachusetts.

Symula, R., Schulte, R., Summers, K. 2001. Molecular phylogenetic evidence for a mimetic radiation in Peruvian poison frogs supports a Müllerian mimicry hypothesis. *Proceedings of the Royal Society of London, Series B*, 268: 2415-2421.

Symula, R., Keogh, J.S., Cannatella, D.C. 2008. Ancient phylogeographic divergence in southeastern Australia among populations of the widespread common froglet, *Crinia signifera*. *Molecular Phylogenetics and Evolution*, 47:469-480.

Tabachnick, B.G., Fidell, L.S. 2007. *Using Multivariate Statistics, Fifth Edition*. Pearson Education, Inc.:Boston, MA.

Triggs, B. 2004. *Tracks, Scats and Other Traces: A field guide to Australian Mammals*. Oxford University Press, USA.

Verrell, P.A. 1999. Geographic variation in sexual behavior: sex, signals and speciation. In: Foster, S.A., Endler, J.A. (Eds.). *Geographical Variation in Behavior*. Oxford University Press, Oxford, pp. 262-286.

Villafuerte, R., Negro, J.J. 1998. Digital imaging for colour measurement in ecological research. *Ecology Letters*, 1: 151-154.

Wells, K.D. 1977. The social behavior of anuran amphibians. *Animal Behaviour,* 25:666-693.

Wells, K.D. 2007. *The Ecology and Behavior of Amphibians*. The University of Chicago Press, Chicago.

Wente, W.H., Phillips, J.B. 2003. Fixed green and brown color morphs and a novel color-changing morph of the pacific tree frog, *Hyla regilla*. *American Naturalist*, 162:461-473.

Wiens, J.J. 2003. Missing data, incomplete taxa and phylogenetic accuracy. *Systematic Biology*, 52:528-538.

Williams, C.R., Brodie, E.D., Jr., Tyler, M.J., Walker, S.J. 2000. Antipredator mechanisms of Australian frogs. *Journal of Herpetology*, 34:431-443.

Williams, N.J., Harle, K.J., Gale, S.J., Heijnis, H. 2006. The vegetation history of the last glacial-interglacial cycle in eastern New South Wales, Australia. *Journal of Quaternary Science*, 21:735-750.

Williamson, I., Bull, C.M. 1996. Population ecology of the Australian Frog *Crinia signifera*: Adults and juveniles. *Wildlife Research*, 23:249-265.

Wollenberg, K.C., Lotters, S., Mora-Ferrer, C., Veith, M. 2008. Disentangling composite colour patterns in a poison frog species. *Biological Journal of the Linnean Society*, 93:433-444.

Wong, B.B.M., Keogh, J.S. and McGlashan, D.J. 2004. Current and historical patterns of drainage connectivity in eastern Australia inferred from population genetic structuring in a widespread freshwater fish *Pseudomugil signifer* (Psudomugilidae). *Molecular Ecology*, 13: 391- 401.

Woolbright, L.L., Stewart, M.M. 2008. Spatial and temporal variation in color pattern morphology in the tropical frog, *Eleutherodactylus coqui*. *Copeia*, 2008:431-437.

Wüster, W., Allum, C.S.E., Bjargadóttir, I.B., Bailey, K.L., Dawson, K.J., Guenioui, J., Lewis, J., McGurk, J., Moore, A.G., Niskanen, M., Pollard, C.P. 2004. Do aposematism and Batesian mimicry require bright colours? A test, using European viper markings. *Proceedings of the Royal Society of London, B*, 2004:2495-2499.

Zar, J.H. 1999. *Biostatistical Analysis, Fourth edition*. Prentice Hall Books, NJ.

VITA

Rebecca E. Symula graduated from C. A. Bouton Jr.-Sr. High School in Voorheesville, New York in 1993. She attended Susquehanna University in Selinsgrove, Pennsylvania and received the degree of Bachelor of Science in May 1997. Then in August 1998, she started in the Biology Graduate Program at East Carolina University in Greenville, North Carolina under the supervision of Dr. Kyle G. Summers. She received the degree of Master of Science in Biology in December 2001. In the summer of 2002, she entered the Ecology, Evolution and Behavior (EEB) program in the Section of Integrative Biology at the University of Texas at Austin.